CHEMICAL AND BIOLOGICAL INVESTIGATION OF THE STEM OF *DICHAPETALUM CRASSIFOLIUM*

THIS THESIS IS SUBMITTED TO THE UNIVERSITY OF GHANA, LEGON, IN PARTIAL FULFILMENT OF THE REQUIREMENT FOR THE AWARD OF MASTER OF PHILOSOPHY DEGREE IN CHEMISTRY

BY

HENRY AKWAFFO ONYAME

[10246376]

DEPARTMENT OF CHEMISTRY,

UNIVERSITY OF GHANA.

JUNE, 2015

DEDICATION

TO THE GLORY OF ALMIGHTY GOD AND ONYAME FAMILY

DECLARATION

This is to certify that this thesis is the result of research undertaken by Henry Akwaffo Onyame toward the award of a Master of Philosophy Degree in Chemistry in the Department of Chemistry, University of Ghana. It has not been presented for a degree in this University or any other University.

.....

Henry Akwaffo Onyame

(Candidate)

…….....

Dr. Dorcas Osei-Safo

(Supervisor)

……

Dr. Mary Anti Chama

(Supervisor)

ACKNOWLEDGMENTS

I am most grateful to God for bringing me this far. With profound gratitude I would to want to appreciate the invaluable contribution of my supervisors; Dr. Dorcas Osei-Safo and Dr. Mary Anti Chama for their helpful suggestions and constructive criticisms throughout this work. Special appreciation goes to Prof. Ivan Addae-Mensah whose involvement led to the successful completion of this work. I would want to thank Prof. Reiner Waibel and coworkers of the University of Erlangen for obtaining the NMR data of the isolates.

I am grateful to my family, my parents and especially my immediate sister, Mrs. Elizabeth Kumashie and family for their financial assistance throughout this program. My sincere gratitude also goes to my pastor and wife, Rev. Samuel Akoto and Mrs. Eleanor Akoto for their prayers, encouragement, love and assistance throughout my life.

I am very grateful to Mr. J. J. Harrison of the Chemistry Department for his advice and being a source of inspiration throughout my stay in this University. My heartfelt gratitude goes to Mr. Godwin A. Dziwornu also of the Chemistry Department without whose priceless assistance this work would not have been completed.

I acknowledge the following individuals from Food and Drugs Authority; Mr. Ernest Afesey, Mr. Eric Kakari-Boateng, Mr. Nicholas Amoah Owusu and Mr. Isaac Adom for their assistance in obtaining IR spectra of my isolates.

Special appreciation also goes to the following staff of Noguchi Memorial Institute for Medical Research; Mr. Joseph Otchere, Mrs. Yvonne Ashong, Mr. Joseph Quatey and especially to Mr.

Edmund Dumashie for their assistance for the work done on the anti-schistosomiasis biological studies.

I appreciate the assistance I received from the technical staff of the Chemistry Department, especially Mr. Bob Essien and also to the secretarial staff.

I owe special appreciation to my colleagues; Claudine Fleischer, Fredrick Kumah, Roland Kofi Gyampoh, Shadrach Quanoo, Ehud Ashiawo and the rest of the staff of the Chemistry Department.

I want to thank my wonderful brother, Mr. Gilbert Boafo and his family, Pastor Gabriel Dela, all the Adult Bible Class facilitators and the I. C. G. C. Wisdom Temple Choir for their support and love.

To all others whose names I have not mentioned, I am grateful to you all and God Almighty bless you.

ABSTRACT

In the present study, the stem of *Dichapetalum crassifolium* was investigated for its phytochemical constituents and their biological properties. The petroleum ether extract yielded friedelan-3-one, friedelan-3β-ol and a mixture of friedelan-3-one and friedelan-3β-ol. The ethyl acetate extract yielded pomolic acid, dichapetalin M and maslinic acid as well as the friedelins and a mixture of β-sitosterol and stigmasterol. No solid was isolated from the methanol extract. These compounds were identified and characterized using comparative thin-layer chromatography, comparative melting point, mixed melting point, IR, ^{1}H and ^{13}C NMR spectroscopy.

In the light of recent investigations suggesting that the dichapetalins and some other triterpenoids have a broad spectrum of biological activities coupled with the urgent need of potential anti-schistosomal agents, the crude extracts as well as three isolates; friedelan-3-one, β-sitosterol/stigmasterol and dichapetalin M were screened for their potential egg hatch inhibition activity against *Schistosoma mansoni* and *Schistosoma haematobium*. The petroleum ether, ethyl acetate and methanol crude extracts gave IC_{50} values of 443.7 ± 0.04, 638.0 ± 0.08 and 893.7 ± 0.08 µg/ml respectively. Among the tested isolates, friedelan-3-one, β-sitosterol/stigmasterol and dichapetalin M gave IC_{50} values of 378.1 ± 0.23, 177.9 ± 0.10 and 191.0 ± 0.12 µg/ml respectively. The observed egg hatch inhibition activity of the most active isolates, the mixture of β-sitosterol/stigmasterol and dichapetalin M, were however found to be about 11 and 12-fold respectively less potent compared to that of the standard drug, praziquantel (IC_{50} = 15.47 ± 0.06 µg/ml), used in the study.

This study constitutes the first report of the chemical and biological investigation of this member of the family Dichapetalaceae. Among the compounds isolated, maslinic acid is reported for the first time from the plant family.

TABLE OF CONTENT

Page

DEDICATION ii

DECLARATION iii

ACKNOWLEDGMENTS iv

ABSTRACT vi

TABLE OF CONTENT viii

LIST OF TABLES xii

LIST OF SCHEMES xiv

LIST OF FIGURES xv

CHAPTER ONE

Introduction

1.1 Description of *Dichapetalum Crassifolium* 1

1.2 The Dichapetalins as Potential Natural Anti-Cancer Agents 2

1.3 Schistosomiasis 5

1.4 Aim and Objectives 6

CHAPTER TWO

Literature Review

2.1 Ethnobotanical Uses of Some Selected *Dichapetalum* Species 7

2.2 Earlier Investigation into Some Toxic *Dichapetalum* Species and their Chemical Composition 9

2.3 The Dichapetalins and Their Biological Activities 12

2.3.1 Structural differences among the Dichapetalins 12

2.3.2 Biological Activities of the Dichapetalins 22

2.4 Dichapetalins from Other Sources and their Biological Activities 28

2.5 Other Compounds Isolated From Previously Investigated *Dichapetalum* Species 31

2.6 Schistosomiasis: A Major Neglected Parasitic Disease in Ghana 35

2.6.1 Control of Schistosomiasis 37

2.6.2 Drugs for Treating Schistosomiasis 37

2.6.3 Natural Products as Potential Source for the Control of Schistosomiasis 39

CHAPTER THREE

Present Investigation

3.1 Summary 43

3.2 Investigation of the Extracts from the stem of *D. crassifolium* 44

3.2.1 Phytochemical Screening of the PE, EA and MeOH crude extracts 44

3.2.2 Investigation of the (PE) Extract 45

3.2.2.1 Isolation and identification of friedelan-3-one, DCS-P1 46

3.2.2.2 Isolation and identification of friedelan-3β-ol, DCS-P2 49

3.2.2.3 Isolation of a mixture of friedelan-3-one and friedelan-3β-ol, DCS-P1P2 51

3.3 Investigation of the Ethyl acetate (EA) Extract 51

3.3.1 Purification and identification of friedelan-3-one, DCS-E1 54

3.3.2 Purification and identification of friedelan-3β-ol, DCS-E2 54

3.3.3 Purification and identification of a mixture of friedelan-3-one and friedelan-3β-ol, DCS-E1E2 and DCS-E3. 55

3.3.4 Purification and identification of a mixture of β-sitosterol and stigmasterol, DCS-E4 55

3.3.5 Purification of DCS-E5 and DCS-E6 (identified as pomolic acid) 58

3.3.6 Purification and identification of dichapetalin M, DCS-E7 66

3.3.7 Purification and identification of Maslinic Acid, DCS-E8 69

3.3.8 Purification and isolation of DCS-E9, DCS-E10 and DCS-E11 75

3.4 *In Vitro* Screening of the Crude Extracts, Friedelan-3-one, β-Sitosterol/stigmasterol and dichapetalin M For Anti-Schistosomal Activity 76

3.5 Conclusion 83

3.6 Recommendation 84

CHAPTER FOUR

Experimental

4.1 Collection and Preparation of Plant Material 86

4.2 General Experimental Procedure 86

4.3 Chemicals and reagents 87

4.4 Solvent Extraction of the Plant Material 89

4.4.1 Extraction with Petroleum ether (40-60^{o}C) 89
4.4.2 Extraction with Ethyl acetate 90

4.4.3 Methanol Extraction 90

4.5 Phytochemical Screening test procedure 90

4.6 Investigation of the Extracts 92

4.6.1 Petroleum ether (40-60^{o}C) extract 92

4.6.2 Ethyl acetate (EA) extract 93

4.7 *In Vitro* Screening of Crude Extracts and some Solid Isolates

for anti-schistosomal Activity 96

4.7.1 Schistosome Egg recovery and Concentration from infested

urine sample by the modified Kotze *et al* Method 96

4.7.2 In vitro screening of test compounds against schistosome eggs using

the 96-well plate Egg-Hatch Assay 97

APPENDIX I: IR data of isolates 99

APPENDIX II: ^{1}H and ^{13}C NMR data of isolates 112

APPENDIX III: Ethical Clearance 128

REFERENCES 129

List of Tables

		Page
Table 2.1	Ethnobotanical uses of selected Dichapetalum species	7
Table 2.2	Occurrence of the dichapetalins in investigated Dichapetalum species	13
Table 2.3	Cytotoxicity of dichapetalin A against some cancer cell lines	23
Table 2.4	Chemosensitivities of some dichapetalins on HCT116 and WM 266-4 cancer cell lines	25
Table 2.5	Potential anti-schistosomal drugs from plants (and natural product derived) sources	40
Table 3.1	Phytochemical screening test results on the crude extract of *Dichapetalum crassifolium*	44
Table 3.2	IR frequencies of DCS-P1 compared to that of Friedelan-3-one	47
Table 3.3	Comparison of IR data of DCS-P2 with that of Friedelan-3β-ol	50
Table 3.4	Infrared data of DCS-E4 compared to that of a reference sample	56
Table 3.5	IR data for DCS-E5 and pomolic acid, DCS-E6	58
Table 3.6	Comparison of ^{13}C Chemical shifts of DCS-E6 (pomolic acid) with reference data	60
Table 3.7	Infrared data of DCS-E7 compared to that of dichapetalin M	66
Table 3.8	Comparison of ^{1}H and ^{13}C NMR data of DCS-E7 (dichapetalin M) with literature data	68
Table 3.9	^{1}H and ^{13}C chemical shifts of DCS-E8 (Maslinic acid) and reference data	73

Table 3.10A %EHI recorded for the duplicate test at different concentrations of extracts, pure compounds and standard, praziquantel. 78

Table 3.10B *In vitro* average %EHI values at different concentrations of extract, pure compounds and praziquantel. Data are Mean ± S. E. M 79

Table 3.10C *In vitro* half maximal inhibitory concentration (IC_{50}) of test compounds 82

List of Schemes

		Page
Scheme 1	The lethal synthetic pathway for the inhibition of Kreb's Cycle	10
Scheme 2	Metabolic blocking of citric acid cycle by fluoroacetic acid	11
Scheme 3	Investigation of PE Extract	45
Scheme 4	Summary of work carried out on Ethyl Acetate extract	53
Scheme 5	Biosynthetic pathways of sterols required for normal plant development	57

List of Figures

		Page
Figure 1	Dichapetalins with methyl ester side chain	15
Figure 2	Dichapetalins with 5-membered lactone and allyl alcohol side chain	17
Figure 3	Dichapetalins with spiroketal side chain	19
Figure 4	Dichapetalins with lactol side chain	21
Figure 5	Structural differences between dichapetalins and acutissimatriterpenes	29
Figure 6	Dichapetalin-type triterpenoids isolated from *Phyllanthus acutissima*	30
Figure 7	Other compounds isolated from Dichapetalum species	33
Figure 8	Life cycle of *Schistosoma* species	36
Figure 9	Schistosomiasis drugs	38
Figure 10	Potential anti-schistosomal drugs	42
Figure 11a-c	Expanded ^{1}H NMR of DCS-E6	62-64
Figure 12	Expanded ^{1}H NMR of DCS-E8	72
Figure 13	Graph of % Maximum Inhibition vrs Log [Crude Extract]	81
Figure 14	Graph of % Maximum Inhibition vrs Log [Test compounds]	81

CHAPTER ONE

INTRODUCTION

1.1 Description of *Dichapetalum Crassifolium*

Dichapetalum crassifolium Chodat (synonym: *Dichapetalum crassifolium* var. *integrum* Breteler) belongs to the family Dichapetalaceae[1]. Dichapetalaceae consists of angiosperms and comprises three genera; *Dichapetalum*, *Stephanopodium* and *Tapura*[2]. *Dichapetalum* Thouars is the major genus with 124 species out of which 86 are found in Africa, 19 in Asia and the rest in South America. *Dichapetalum* species are small tropical trees, shrubs or sometimes climbing plants, with leaves alternate, simple and individual, as well as small flowers and a nut or drupe[3].

The main centre of distribution of *Dichapetalum* in Africa is Central Africa, comprising Cameroun, Gabon, Equatorial Guinea, Republic of Congo, Democratic Republic of Congo, Central African Republic and the northern part of Angola[4]. *D. crassifolium* is distributed in West and Central Africa, Western Tanzania and Northern Zambia and thrives in rain forest at altitudes of 0-1700m[1]. In Ghana, *D. crassifolium* can be found in the Central, Western and Ashanti regions[4].

D. crassifolium is a large liana that can grow up to a height of 40m or more and could grow to a diameter of 5cm at the base. The lower parts of the stem may grow roots, the stem and branches have lenticels which are large and prominent. The leaves are lamina, usually grooved on both surfaces or hairless on either surface with elliptic to obovate shaped blades. The petioles may grow to 1-16mm long, the midrib of the leaves may be flat or rose above, more prominent beneath with 3-7 major lateral nerves on each side[1,5].

The plant has pedunculate inflorescence with up to 50 flowers. The flowers are often grouped on a short, leafless axillary shoot, and the developed flowers have 4-6mm long petals and stamens

and 4-7mm long pistils. The peduncle is free from the petiole, 10-12mm long with small bracts and bracteoles which are less than 1mm long. The pedicel grows up to 5mm long with obtuse-truncate shaped calyx and erect sepals which group at the base. The sepals are 2.5-3mm in long. The petals are erect, entire or emarginated at the apex, narrowly oblong-obovate and 2.5-6mm long.

Young fruits are seen on *D. crassifolium* in the middle of June and November. The grown fruits may be 1-3 lobed and 1-3 seeded. The 1-seeded fruits are ellipsoid to obovoid shaped, laterally compressed, 15-25mm long, 10-20mm broad, 10-18mm thick, obtuse at the apex and orange colored at maturity. The 2-3 seeded fruits develop deep cleft apically and laterally. The exocarp of the fruit is firm, 1-2mm thick with juicy mesocarp that is somewhat fibrous and adhered to the endocarp. The endocarp is bony, 1-2mm thick and strongly grooved outside but is hairy in the immature state. The seeds are subellipsoid, laterally compressed and 10mm long with brownish, smooth, glossy and strongly veined seedcoat[1,5].

To the best of my knowledge, no ethnobotanical use has been recorded for *D. crassifolium* and there has not yet been any chemical investigation of the plant.

1.2 The Dichapetalins as Potential Natural Anti-Cancer Agents.

While earlier investigations into *Dichapetalum* species focused on the more toxic species, current investigations have and continue to concentrate on the entire chemical constituents of the less toxic ones including investigation of their biological activities. The presence of fluorinated compounds, mainly monofluoroacetate and fluorocarboxylic acids have been implicated in the toxicity of the *Dichapetalum* species[6,7,8].

Currently, there is increasing research into these *Dichapetalum* species due to the discovery of the novel phenylpyranotriterpenoid compounds named dichapetalins from the less toxic species[9,10]. The Dichapetalins constitute a small family of secondary metabolites of mixed biosynthesis in which a 2-phenylpyrano moiety is annulated to a dammarane-triterpene skeleton. The basic structure of a dichapetalin is biogenetically characterized by the addition of a C_6-C_2 unit, which probably might be derived from the shikimmic pathway to a 13, 30-cyclodammarane-type skeleton. The dichapetalin derivatives are distinguished by the nature of the side chain at C_{-17}[9].

In 1995, Achenbach[10] and co-workers were the first to discover the first member of the group, dichapetalin A from the roots of *D. madagascariense* Poir and a year later they established its absolute configuration by X-ray crystallographic measurement[11]. Dichapetalin A was found to present strong anti-cancer activity against L1210 murine leukemia ($EC_{90} = 1.7 \times 10^{-10}$ M) but four fold less efficient towards KB carcinoma cells and murine bone marrow cells stimulated with GM-CSF (granulocyte-macrophage colony-stimulating factor) *in vitro*. In 1996, Achenbach and co-workers isolated seven other new dichapetalins, B - H but they exhibited poor or no cytotoxic activities. A recollection of the plant led to the isolation of dichapetalin M in 2008, which in a brine shrimp lethality test was found to be (LC_{50} = 0.011µg/ml) 28-fold more potent than dichapetalin A (LC_{50} = 0.31µg/ml). In the same test, dichapetalin C was active to some extent but dichapetalins D and F were inactive[12,13].

Fang[14] *et al* in 1994 isolated 2 new dichapetalins, I and J in addition to A from the stem bark of *D. gelonioides* collected from the Philippines. A recollection of the plant in 2003 and subsequent chemical investigation led to the isolation of 2 other new members, dichapetalins K and L which were not isolated in the first collection. Dichapetalins K and L showed broad activity towards the

human ovarian cancer cell line SW626 while dichapetalins A, I and J exhibited selective and cytotoxic activities (EC_{50} = 0.2 - 0.5 µg/ml) against the same cell lines.

Tuchinda[15] and co-workers have isolated five new dichapetalin-type triterpenoids from the aerial parts of *Phyllanthus acutissima* called acutissimatriterpenes A-E. The C_{-17} side chain and the presence or otherwise of a methylenedioxy unit in the phenylpyrano moiety distinguishes the acutissimatriterpenes from the dichapetalins. After testing the acutissimatriterpenes against a panel of six cancer cell lines namely, P-388 murine lymphocyte leukemia, KB human nasopharyngeal carcinoma, Col-2 human colon cancer, MCF-7 human breast cancer, Lu-1 human lung cancer and ASK rat glioma, acutissimatriterpenes A and B were found to be active active against murine lymphocyte leukemia giving EC_{50} = 0.4 and 0.5µg/ml respectively whereas acutissimatriterpene E showed significant activity against murine lymphocyte leukemia (EC_{50} = 0.005µg/ml) and moderate activity against human breast cancer (EC_{50} = 1.1µg/ml) and human lung cancer (EC_{50} = 3.1µg/ml). Acutissimatriterpenes C and D showed insignificant activities (EC_{50} > 5µg/ml) against all the cancer lines tested[15].

The structures of the dichapetalins and acutissimatriterpenes are showed on pages 15-21 and 29-30 respectively.

Towards the end of 2013, Long[16] and co-workers isolated 6 new dichapetalins from *D. mombuttense*, *D. leucosia*, *D. zenkeri*, *D. eickii* and *D. ruhlandii* namely dichapetalins N–S, in addition to the previously isolated dichapetalins A, B, C, I, L and M and determined their structures based on spectroscopic methods. The cytotoxic and anti-proliferative profile of these dichapetalins against the human colorectal carcinoma HCT116 and human melanoma WM 266-4 cancer cell lines showed dichapetalin P to be more potent by 74-fold than dichapetalin A on WM 266-4 cells.

Dichapetalin M so far has recorded the highest cytotoxic activity recording EC_{50} values of 0.007 and 0.05µg/ml on HCT1116 and WM 266-4 cell lines respectively.[16]

Chemical investigation of the root of *D. filicaule* led to the isolation of the most recent member of the group, dichapetalins X, in addition to dichapetalin A[17]. The anthelminthic activities of dichapetalin A and X were found to be 162.4 and 523.2 µg/ml respectively[17].

Jing[18] and co-workers have isolated 14 new dichapetalins from the stem and leaves of *D. gelonioides*. From the different biological studies carried out by Jing *et al*, the dichapetalins showed antifeedant, nematicidal, antifungal, nitric oxide and anticholinestrase inhibitory activities, indicating the wide range of biological activities that the dichapetalins could exhibit.

1.3 Schistosomiasis

Schistosomiasis, also known as bilharzia, bilharziosis or snail fever is a chronic parasitic disease caused by blood-dwelling fluke worms of the genus *Schistosoma* and is endemic in Africa, Asia and South America[19]. According to WHO, schistosomiasis is the second most prevalent tropical disease and it affects more than 200 million people worldwide[20]. In sub-Saharan Africa, the disease is said to cause the death of over 280, 000 people annually, and in Ghana, schistosomiasis is wide-spread in all the regions with overall prevalence estimated between 54.6-80%[21,22]. The disease therefore remains a considerable public health problem in these endemic regions.

Currently, praziquantel is the only drug of choice for the control of schistosomiasis infection and resistance of some *Schistosoma* species to praziquantel has already been reported[23]. The classical strategy of alternating treatments to avoid the development of resistance is very crucial and so more recently there has been a growing interest in the scientific community to search for extracts and novel compounds from different plant sources with bioactivities to treat schistosomiasis

infection.[24,25,26]. While many plant species from various families have been screened for their possible antischistosomal potencies, there has not been any report as regards members of the family Dichapetalaceae.

1.4 Aim and Objectives

This current investigation was carried out as part of ongoing research into the less toxic species of the genus *Dichapetalum* aimed at isolating the phytochemicals present, with special focus on the dichapetalins and their biological properties. The species under study was *D. crassifolium*, whose phytoconstituents and their antischistosomal properties were investigated.

The objectives were achieved as follows:

I. Soxhlet extraction of the compounds present in the stem of *D. crassifolium.*
II. Isolation and purification of the compounds by column chromatography and other separation and purification methods.
III. Characterization of the pure isolates using spectroscopic methods.
IV. Anti-schistosomiasis studies on both crude and some isolated compounds.

CHAPTER TWO

LITERATURE REVIEW

2.1 Ethnobotanical Uses of Some Selected *Dichapetalum* Species

In spite of rapid development in methods of organic synthesis in synthetic laboratories, medicinal plants continue to play significant roles in modern medicine due to their inherent distinct chemical and biological properties. In nature, plants are able to synthesize complex molecules from simple ones through highly specific reactions that they use for defense and communication. These complex compounds play significant roles not only as medicinal and pharmaceutical agents but as leads for synthetic optimization. Most species of *Dichapetalum* have been reported to have folkloric uses among which have been summarized in Table 2.1 below.

TABLE 2.1: Ethnobotanical uses of selected *Dichapetalum* Species

***Dichapetalum* Species**	**Ethnobotanical Use**
D. cymosum[26,27]	Contains fluoroacetic acid which could be useful in anti-HIV infective therapy.
D. braunii Engl.[7]	Grounded leaves for sore treatment
D. barteri[8]	Rodenticide
D. barbatum[28]	For treating wounds, possess antimicrobial activities.

D. gelonioides[18,29,30]	Leaves for treating amenorrhea, used as coolant in treating mouth ulcers, raticide and rodenticide.
D. rhodesium[31]	Tonic for infants, used as contraceptive and birth inducer.
D. thunbergh[32]	Has an herbal and homeopathic property.
D.macrocarpum, D. mossambicense and *D. venenatum*[33]	Used as arrow poisons
D. madagascariense[6]	Treatment of jaundice, urethritis, bacterial infections and viral hepatitis. Fruit pulp is edible, plant wood is used for domestic purposes.
D. toxicarium[34]	Treating swellings, coughs, rheumatism, urethritis and chronic sores, used as rodenticide, sneeze powder for restoring consciousness. Fruit pulp is edible.
D. pallidum[35]	Used for treating dysentery and diarrhea.

Most of the *Dichapetalum* species have been reported to be toxic to livestock and humans including *D. toxicarium, D. deflexum, D. tomentosum, D. braunii, D. cymosum, D. madagascariense, D. heudelotii, D. michelsonii, D. ruhlandii and D. stulmanii*[31, 36]. The quest into their toxicity has received considerable attention from most researchers.

2.2 Earlier Investigation into Some Toxic *Dichapetalum* Species and their Chemical Composition

Fluorocarboxylic acids[6,7] have been reported to be responsible for toxicity in some *Dichapetalum* species. Fluoroacetic acid [**1**] was identified as the main toxic compound in *D. cymosum* by Marais in 1944. His research further showed that fluoroacetic acid was in the lipid fraction[27]. Some other fluorocarboxylic acids responsible for the toxicity of the species of the genus *Dichapetalum* are ω-fluoro-oleic acid [**8**], ω-fluoro-palmitic acid [**9**], ω-fluoro-capric acid [**10**], ω-fluoro-myristic acid [**11**] and *threo*-18-fluoro-9,10-dihydroxystearic acid [**12**][7,37]. Subsequent investigations showed that the African genus of the family Dichapetalaceae contains high levels of fluoroacetate which are in higher amounts in the roots and stem compared to the leaves[8].

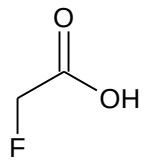

Fluoroacetic acid **[1]**

According to a South African report in 1996, *D. cymosum*[38] was implicated in the mortality of eight percent of cattle. It has been reported that a sheep dies after feeding on one or two leaves of the plant, while three or four leaves would kill an ox. Marais reported the LD_{50} of the fluoroacetate to be 0.5mg/kg in the plant[39].

The primary point of action of fluoroacetate as proved by Peters is its interference with the metabolism of pyruvate in general and more specifically with aconitase. In the citric acid cycle, one step involves the conversion of acetyl CoA [**2**] and oxaloacetic acid [**5**] to citric acid by the enzyme citric synthase[40].

Scheme 1: The lethal synthetic pathway for the inhibition of Kreb Cycle

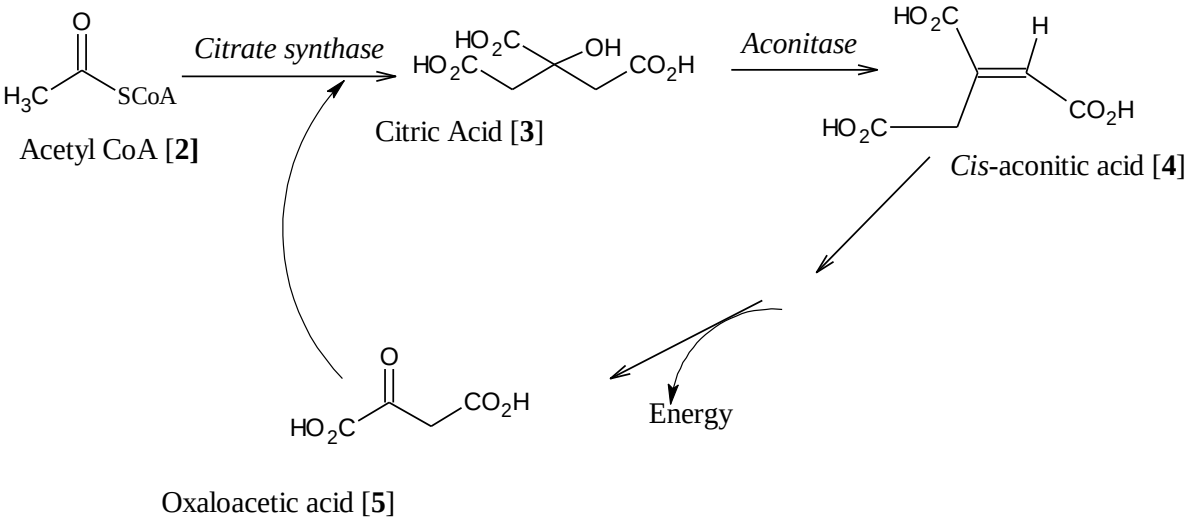

The citric acid [**3**] undergoes dehydration to produce aconitic acid [**4**] which undergo a series of metabolic reactions resulting in the release of energy from the cell. Oxaloacetic acid [**5**] is regenerated finally to enable the cycle to continue. Since all cells undergo the citric acid cycle, fluoroacetate is toxic to all cells by being activated to fluoroacetyl CoA [**6**] in the pathway responsible for generating metabolic energy[41,42] (Scheme 2). The fluoroacetyl CoA [**6**] competes with acetyl CoA for the enzyme citrate synthase which is then converted to 2R, 3R-fluorocitric acid [**7**][40].

The fluorocitric acid stereoisomer acts as a competitive inhibitor of the enzyme aconitase in the cycle, halting the regeneration of aconitic acid and in the process inhibits respiration and subsequently deprives the cell of energy. Kun and co-workers have suggested that fluorocitric acid binds irreversibly to the protein responsible for the transport of citrate into the mitochondria. Further accumulation of fluorocitrate results in calcium deficiency as a result of the formation of

Scheme 2 Metabolic blocking of the citric acid cycle by fluoroacetic acid

chelate with calcium ions in the serum of blood[43].

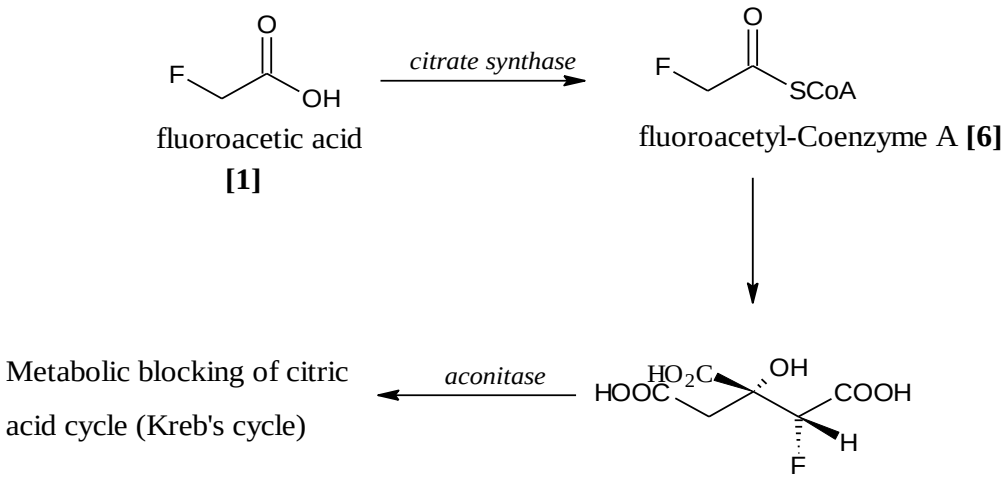

fluoroacetic acid **[1]**

fluoroacetyl-Coenzyme A **[6]**

2R, 3R- fluorocitric acid **[7]**

Though *D. barteri* and *D. toxicarium* also contain fluoroacetate, the main toxic carboxylic acid in *D. toxicarium* is ω-fluoro-oleic acid [**8**] since it constitutes the major component[7]. Furthermore, whereas fluoroacetate was found to be concentrated in the leaves, ω-fluoro-oleic is reported to be concentrated in the seeds of *D. toxicarium*[7]. Other fluorocarboxylic acids isolated from the seeds of *D. toxicarium* are ω-fluoro-palmitic acid [**9**], ω-fluoro-capric acid [**10**], ω-fluoro-myristic acid [**11**] and *threo*-18-fluoro-9,10-dihydroxystearic acid [**12**][7].

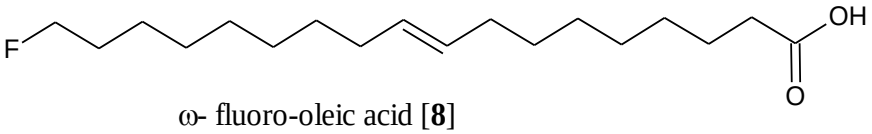

ω- fluoro-oleic acid [**8**]

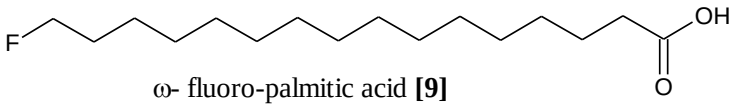

ω- fluoro-palmitic acid **[9]**

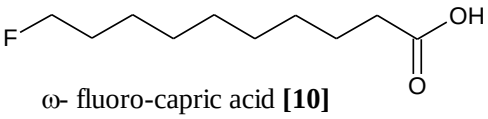

ω- fluoro-capric acid **[10]**

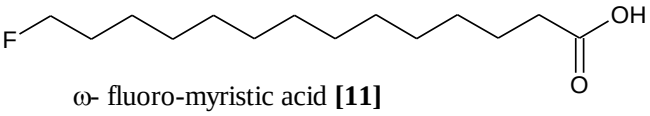

ω- fluoro-myristic acid **[11]**

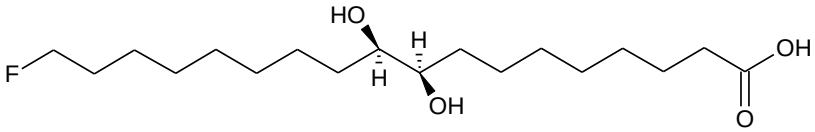

threo-18-fluoro-9,10 dihydroxystearic acid **[12]**

2.3 THE DICHAPETALINS AND THEIR BIOLOGICAL ACTIVITIES

2.3.1 Structural differences among the Dichapetalins

The dichapetalins constitute a small family of secondary metabolites of mixed biosynthesis in which a 2-phenylpyrano moeity is annulated to ring **A** of a dammarane-triterpene skeleton **[13]**. The basic structure of dichapetalin **[14]** is biogenetically characterized by the addition of a C_6-C_2 unit, which probably might be derived from the shikimmic acid pathway to a 13, 30-cyclodammarane skeleton[9].

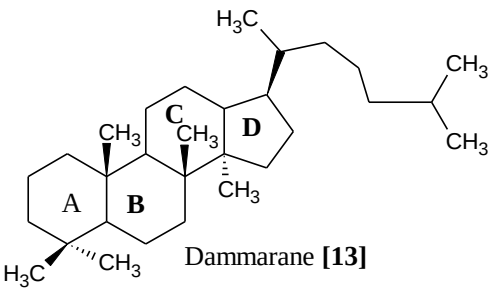

Dammarane **[13]**

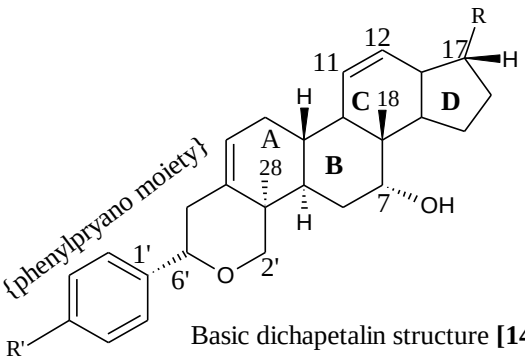

Basic dichapetalin structure **[14]**

A total of thirty-two (32) dichapetalin hybrid triterpenoids have been isolated from eight *Dichapetalum* species namely *D. madagascariense, D. gelonioides, D. mombuttense, D. leucosia, D. zenkeri, D. ruhlandii, D. eickii* and *D. filicaule*. Thirteen of these dichapetalins, A-M were isolated initially from two species namely *D. madagascariense* and *D. gelonioides* whiles the remaining nineteen were recently isolated from *D. gelonioides, D. eickii, D. mombuttense, D. leucosia, D. zenkeri* and *D. filicaule*. The table (Table 2.2) below shows the occurrence of the dichapetalins in the different *Dichapetalum* species investigated.

TABLE 2.2: Occurrence of the dichapetalins in investigated *Dichapetalum* species.

***Dichapetalum* species**[Ref.]	**Dichapetalin type isolated**	**Plant Part**
D. madagascariense[12,13]	A [**22**], B [**27**], C [**15**], D [**16**], E [**17**], F [**18**], G [**19a, b**], H [**19a, b**], M [**31**].	Roots
D. gelonioides[14,18]	A [**22**], I [**23**], J [**24**], K [**25**], L [**26**], [**20**], [**21**], [**29**], [**30**], [**36**], [**37**], [**38**], T [**35**], V [**40**], [**41**], [**42**], [**43**], [**44**] U [**39**]	Stem bark/Leaves
D. ruhlandii[16]	A [**22**].	Roots
D. mombuttense[16]	A [**22**], L [**26**], N [**28**].	Roots
D. leucosia[16]	C [**15**], I [**26**], P [**34**], S [**33**].	Roots
D. zenkeri[16]	A [**22**], B [**27**], L [**26**], O [**45**], P [**34**], Q [**46**], R [**47**].	Roots

D. eickii[16]	A [**22**], M [**31**].	Roots
D. filicaule[17]	A [**22**], X **[32]**.	Roots

Significantly, dichapetalin A **[22]** has been isolated in all the *Dichapetalum* species investigated so far except *D. leucosia*. *D. gelonioides*[13,18] has up to date produced the highest number of dichapetalins (total of 18), most of which are structural analogues of each other followed by *D. madagascariense* from which a total of nine dichapetalins have been isolated.

It is also worth mentioning that majority of the dichapetalins have been isolated from the roots of the plants except for *D. geloniodes*[14,18] where they were isolated from the stem bark and leaves of the plant. It is also reported that the stem bark of *D. madagascariense* indicated the presence of dichapetalin A [**22**] on TLC as part of a complex mixture while chemical investigation of both the root and stem of *D. barteri*[44] did not show the presence of dichapetalins.

The dichapetalins can be distinguished mainly by the nature of the side chain at C-17 which can be grouped into four namely methyl ester, lactone, spiro-ketal, and lactol side chains.

I. Dichapetalins with Methyl ester side chain.

Dichapetalins C [**15**], D [**16**], E [**17**], F [**18**], G [**19a/19b**], H [**19a/19b**], 7-dehydrodichapetalin G [**20**] and 7-dehydrodichapetalin E [**21**] have a methyl ester side chain.

The methyl ester group consists of either;

I. An open chain terminating in a primary alcohol for dichapetalins C [**15**] and F [**18**], or its stearic acid esterified analogue as applies to dichapetalin D [**16**], **or**

II. The primary alcohol cyclizes with the oxo substituent at C-23 to give a 3-methyl furanyl moiety in dichapetalin E [**17**] or a cyclic methyl ketal in the case of dichapetalins G [**19a/19b]** and H [**19a/19b]** which are isomeric ketals with the 11,12-dihydro basic skeleton.

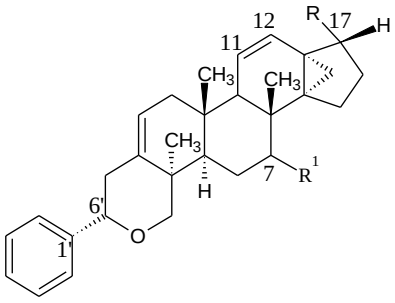

Dichapetalin basic structure [**14**]

R

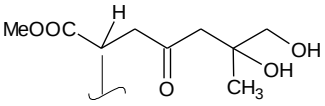

R^1 = OH, Dichapetalin C [**15**]

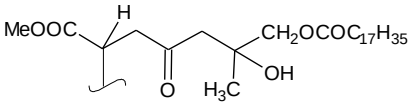

R^1 = OH, Dichapetalin D [**16**]

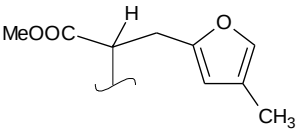

R^1 = OH, Dichapetalin E [**17**]

R^1 = O, 7-dehydro [21]

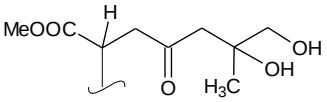

R^1 = OH, Dichapetalin F [**18**]

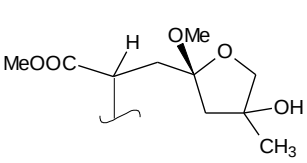

R^1= OH, G or H(11,12-dihydro) [**19a**]

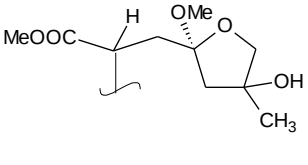

R^1 = OH, G or H(11,12-dihydro) [**19b**]

R^1 = O, 7-dehydro [**20**]

Figure 1: Dichapetalins with methyl ester side chain.

As can be seen from Figure 1 above, the oxidation of the C_7 hydroxyl group in dichapetalins E [**17**] and G [**19b**] results in 7-dehydrodichapetalin E [**21**] and 7-dehydrodichapetalin G [**20**] respectively.

II. Dichapetalins with lactone side chain.

Dichapetalins A [**22**], B [**23**], I [**24**], J [**25**], K [**26**], L [**27**], N [**28**], 21—dehydrodichapetalin Q [**29**] and 2'α-hydroxydichapetalin Q [**30**] possess a lactone side chain. Within the lactone side chain group, dichapetalins A [**22**], B [**23**], I [**24**], J [**25**], K [**26**], L [**27**] 21—dehydrodichapetalin Q [**29**] and 2'α-hydroxydichapetalin Q [**30**] have similar side chain comprising a 5-membered lactone with an allyl alcohol substituent. The differences in their structures are the presence of 11, 12- double bond, a 12-β-OH group, methoxy on the benzene ring of the phenylpyrano moiety and the cyclopropane moiety replaced by a tertiary methyl and a double bond.

Dichapetalins J [**25**] and K [**26**] are methoxylated variants of dichapetalins I [**24**] and A [**22**] respectively which according to Fang[14] *et al* are likely to be extraction artifacts due to the use of methanol as solvent. Dichapetalin B [**27**] is a hydroxylated analogue of dichapetalin A [**22**] at $C_{22.}$

21—dehydrodichapetalin Q [**29**] and 2'α-hydroxydichapetalin Q [**30**] within the 5-membered lactone and allyl alcohol substituent group lack the cyclopropane moiety but instead have a tertiary methyl and double bond. Dichapetalin Q [**46**] and 21-dehydrodichapetalin Q [**29**] are similar but the presence of γ-lactone carbonyl group in the latter and lactol in the former distinguishes them. The presence of a hemiacetal group in 2'α-hydroxy-21-dehydrodichapetalin Q [**30**], which is the first to be reported in the *Dichapetalum* genus with a hydroxyl group at $C_{2'}$, differentiates it from 21-dehydrodichapetalin Q [**29**].

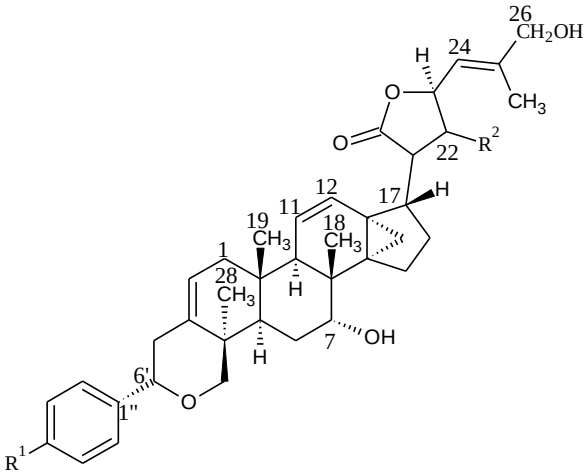

Dichapetalin	R^1	R^2	Other
A [**22**]	H	H	-
B [**23**]	H	OH	-
I [**24**]	H	H	11, 12- dihydro 12-β- OH
J [**25**]	OMe	H	11, 12- dihydro 12-β- OH
K [**26**]	OMe	H	-
L [**27**]	H	H	11, 12- dihydro

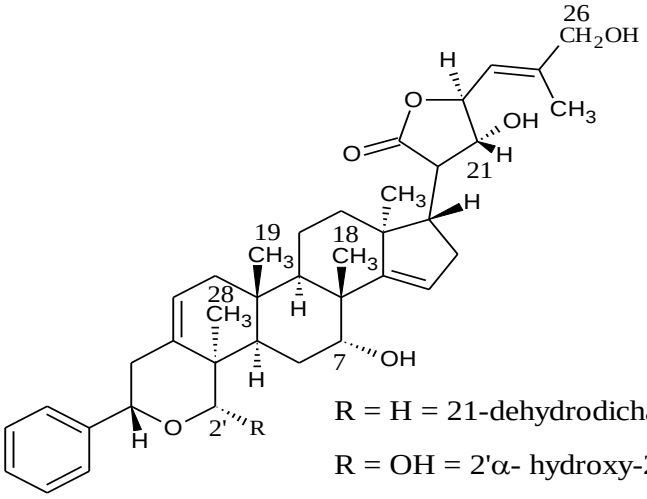

R = H = 21-dehydrodichapetalin Q **[29]**

R = OH = 2'α- hydroxy-21-dehydrodichapetalin Q [**30]**

Figure 2: Dichapetalins with 5-membered lactone and allyl alcohol side chain

Dichapetalin N [**28**] is the last member of the group with lactone side chain. It has a 5-membered lactone and α, β-unsaturated carbonyl on the side chain. It differs from dichapetalin A [**22**] by the presence of CHO group at C_{26} whereas dichapetalin A [**22**] has CH_2OH group at this position.

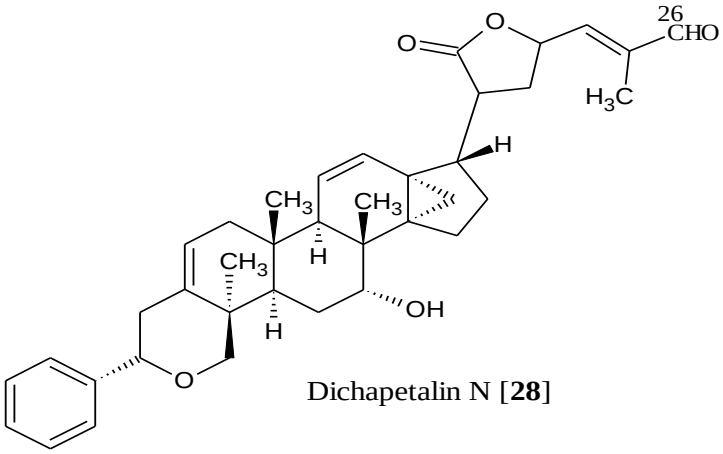

Dichapetalin N [**28**]

III. Dichapetalins with Spiroketal side chain.

Dichapetalins, M [**31**], P [**34**], X [**32**], have structural differences on C_{17} as already mentioned among the dichapetalins. The side chain of dichapetalin X [**32**] has a spiro-ketal ring with a β-hydroxybuturate substituent and a C_{22}-OH group. Both dichapetalins M [**31**] and P [**34**] have the spiro-ketal ring in their side chain but the β-hydroxybuturate is replaced with a methyl ester. The other dichapetalins with the spiro-ketal moiety in their side chain are; dichapetalin S [**33**], dichapetalin T [**35**], dichapetalin U [**39**], dichapetalin V [**40**], 6α-hydroxydichapetalin V [**41**], 22-deoxy-4''-methoxydichapetalin V [**42**], dichapetalin W [**43**] and 4''-demethoxy-7-dichapetalin W [**44**].

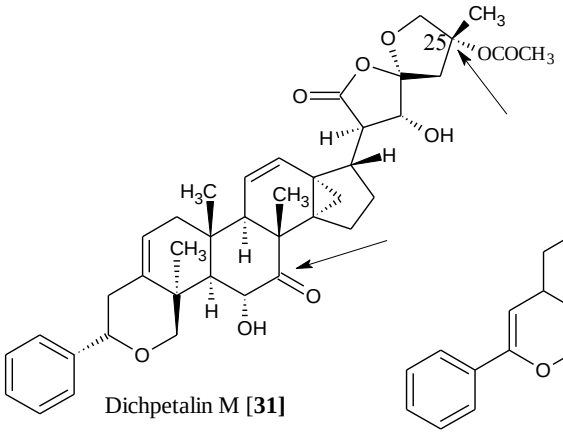

Dichpetalin M [**31**]

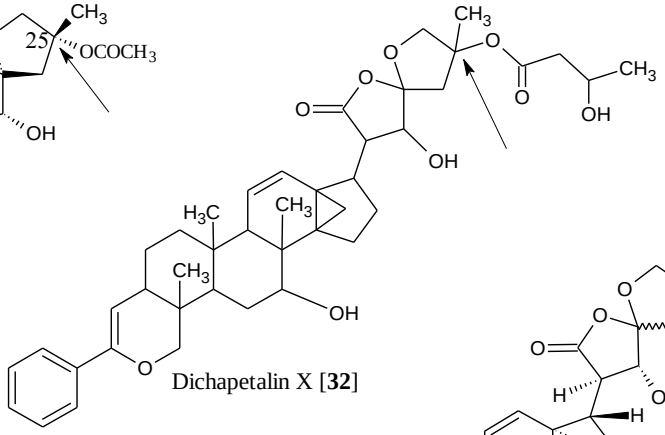

Dichapetalin X [**32**]

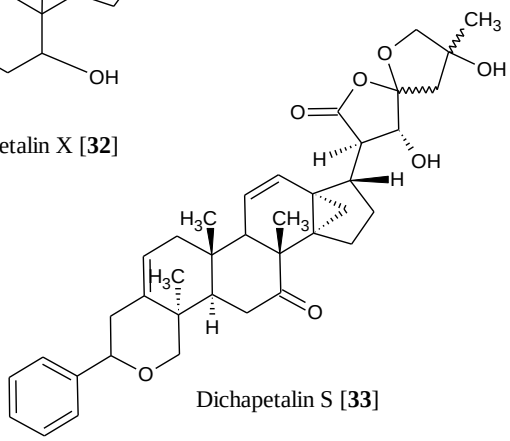

Dichapetalin S [**33**]

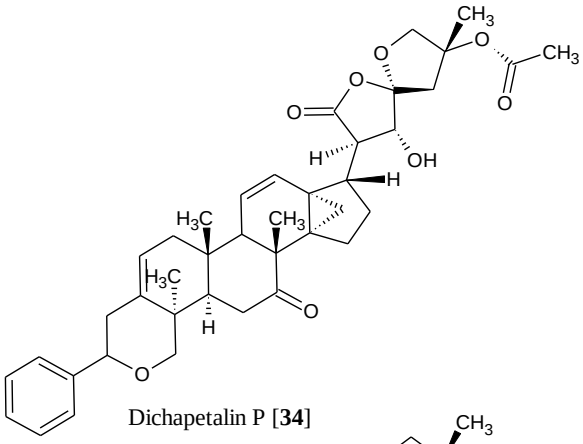

Dichapetalin P [**34**]

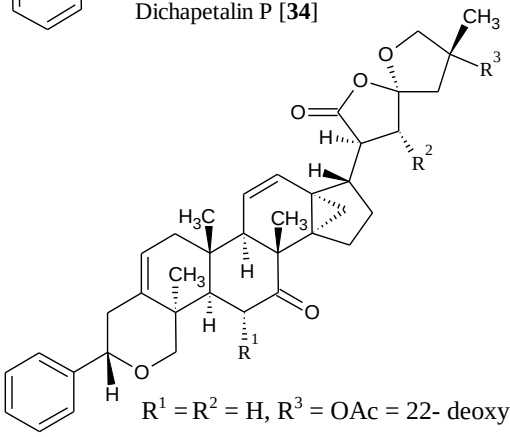

$R^1 = R^2 = H$, $R^3 = OAc$ = 22- deoxydichapetalin P [**36**]

$R^1 = H$, $R^2 = R^3 = OH$ = 25- De-O- acetyldichapetalin P [**37**]

$R^1 = R^2 = R^3 = OH$ = 25- De-O- acetyldichapetalin M [**38**]

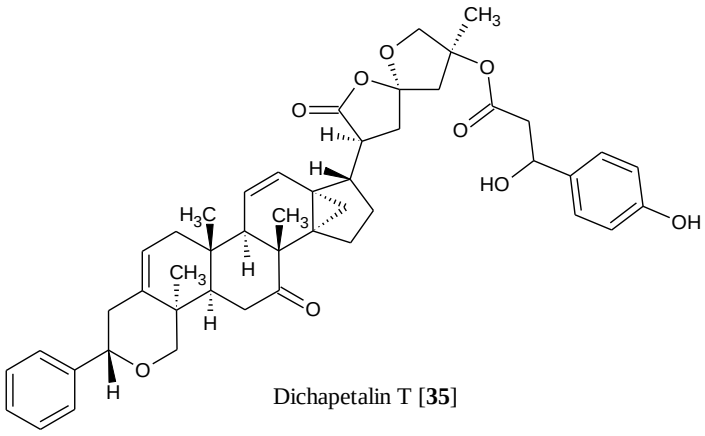

Dichapetalin T [**35**]

Figure 3: Dichapetalins with a spiroketal side chain.

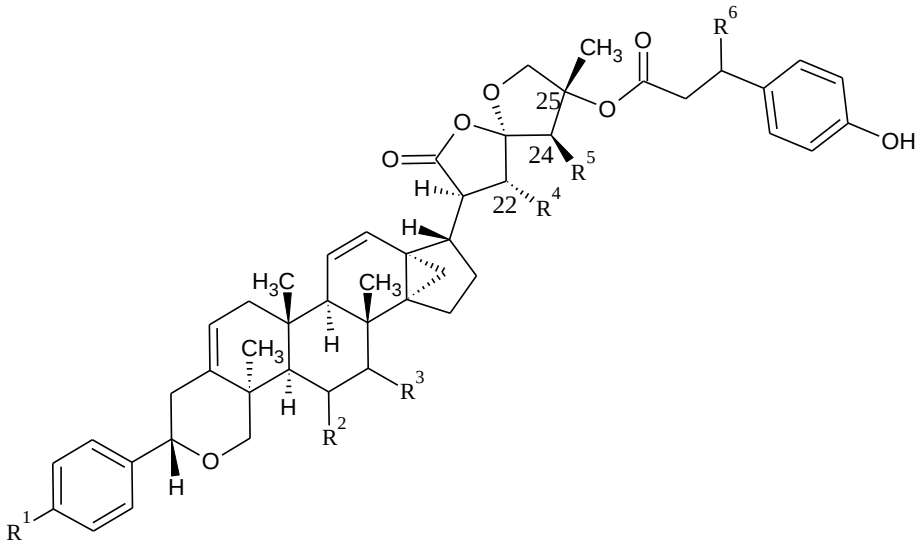

R^1	R^2	R^3	R^4	R^5	R^6	Dichapetalin Type
H	H	O	H	H	OH	Dichapetalin U [**39**]
H	H	O	OH	H	OH	Dichapetalinn V [**40**]
H	OH	O	OH	H	OH	6α–hydroxydichapetalin V [**41**]
OCH_3	H	O	H	H	OH	22- Deoxy-4"- methoxydichapetalin V [**42**]
OCH_3	H	O	H	OH	H	Dichapetalin W [**43**]
H	H	OH	H	OH	H	4"- Demethoxy-7-dihydrodichapetalin W [**44**]

Figure 3: Dichapetalins with spiroketal side chain**.**

Dichapetalins T [**35**] and U [**39**] are stereoisomers with structures similar to 22-deoxydichapetalin P [36] except at C_{25} where the acetoxy group in the latter is replaced by a β-hydroxy (4-hydroxyphenyl)- propanoyloxy group in the former. Dichapetalins T [**35**] and U [**39**] have structural difference only at C_{24} where the C_{24} methylene group in the spiro-ketal system occupies the α-position in the former but is in the β-position in the latter. In dichapetalin V [**40**], the methylene group at C_{22} in dichapetalin U [**39**] is replaced by a hydroxyl group. Dichapetalin V

[**40**] is distinguished from 6α-hydroxydichapetalin V [**41**] by the presence of a hydroxyl group at the $C_{6\alpha}$ position in the latter. Both 22-deoxy-4''-methoxydichapetalin V [**42**] and dichapetalin W [**43**] are methoxylated at $C_{4''}$ but there is hydroxyl group at C_{22} in 22-deoxy-4''-methoxydichapetalin V [**42**] as opposed to the hydroxyl group at C_{24} in dichapetalin W [**43**]. Unlike dichapetalin W [**43**], 4''-demethoxy-7-dichapetalin W [**44**] has no methoxy group and instead of the carbonyl group at C_7 in dichapetalin W, it has a hydroxyl group in this position.

IV. Dichapetalins with Lactol side chain.

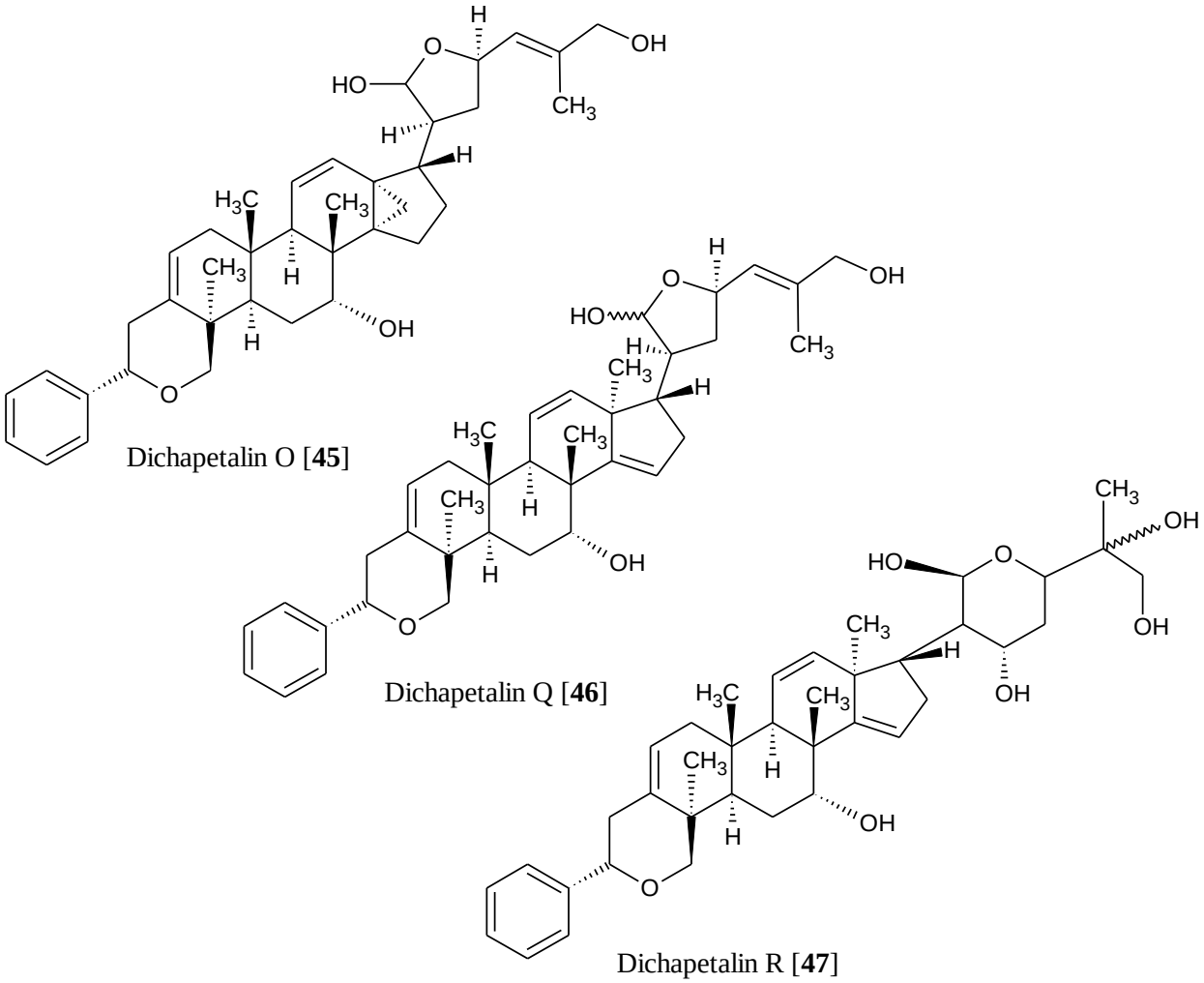

Figure 4: Dichapetalins with lactol side chain.

Dichapetalins O [**45**], Q [**46**] and R [**47**] have lactol in the side chain. Dichapetalins Q [**46**] and R **[47]** are first to be reported to contain a tertiary methyl and double bond instead of the cyclopropane ring of the dammaranes. Dichapetalin O [**45**] and A [**22**] structurally share a common backbone configuration but the presence of a hemiketal in dichapetalin O [**45**] as opposed to the lactone side chain in dichapetalin A [**22**] distinguishes them.

2.3.2 Biological Activities of the Dichapetalins

Biological studies carried out on the dichapetalins including brine shrimp, anthelmintic, antifeedant, nematicidal, antifungal, nitric oxide and anticholinestrase inhibitory activities, anti-HIV and cytotoxicity studies have shown significant activities only with the dichapetalins with lactone or spiroketal side chain. Only dichapetalin C among the dichapetalins with methyl ester side chain has showed significant activity.

In a brine shrimp lethality test, dichapetalin A [**22**] showed significant cytotoxic activity (LC_{50} = 0.31μg/ml) which is seven times higher than podophyllotoxin[45], dichapetalin M [**31**] was found to be very active (LC_{50} = 0.011 μg/ml), twenty-eight times more potent than dichapetalin A [**22**][46].

Dichapetalin A [**22**] has showed significant cytotoxic activities to different cancer cells *in vitro* with varying sensitivities in the respective cancer cell systems. It showed high selectivity against the human colorelectal carcinoma cell line HCT116 with EC_{50} greater than 10.1 μg/ml but broad selectivity against the human colorectal adenocarcinoma cell line Colo-25 with EC_{50} = 7.0 μg/ml. Against the human ovarian adenocarcinoma cell line, dichapetalin A [**22**] exhibited high sensitivity, SW626 (EC_{50} =0.2 μg/ml) and SKOV-3 (EC_{50} = 0.5μg/ml) but broad activity was observed for the human ovarian adenocarcinoma cell line OVcAR-3 (EC_{50} = 5.8 μg/ml). For the human Burkitt's lymphoma leukemia cell line NAMALWA, dichapetalins A [22] was found to be

highly selective (EC_{50} = 0.2 µg/ml) but broad sensitivity towards the human promyelocytic leukemia cell line HL-60 (EC_{50} = 6.4 µg/ml). Towards L1210 murine leukemia cell line, EC_{90} less than 0.0001µg/ml has been reported for dichapetalin A [**22**]. Broad to high selective anti-cancer activities have been exhibited by dichapetalin A [**22**] in the following cell lines: hormone-dependent cancer cell line LNCaP (EC_{50} = 7.0 µg/ml), human prostate cancer cell lines NC1-H460 (EC_{50}= 0.8µg/ml), DU 145 (EC_{50} = 7.6 µg/ml), human lung adenocarcinoma cell lines A549 (EC_{50} = 0.7 µg/ml), HOP-62 (EC_{50} = 0.5 µg/ml), Lu-1 (EC_{50} = 4.1µg/ml)[14,16].

The following cancer cell lines exhibited broad cytotoxic activities towards dichapetalin A [**22**]: the human melanoma WM266-4 (EC_{50} = 9.9µg/ml)[13], human umbilical endothelial cells HUVEC (EC_{50} = 5.5 µg/ml), human neuroblastoma SKNSH (EC_{50} = 6.9 µg/ml), pancreatic adenocarcinoma cell lines BxPC 3 (EC_{50} = 1.8 µg/ml), renal adenocarcinoma TK10 (EC_{50} = 7 µg/ml), human breast adenocarcinoma cell line MCF-7 (EC_{50} = 2.1 µg/ml) and MDAMB-231 (7.6 µg/ml), human colon tumor cell lines Col-2 (EC_{50} = 6.1 µg/ml) and KM- 12 (EC_{50} = 5.1 µg/ml) and human breast ductal carcinoma T47 (EC_{50} = 1.3 µg/ml). However, the human breast cancer cell line was resistant towards dichapetalin A [**22**] recording EC_{50} greater than 20 µg/ml[14,16].

Long *et al*[16] have profiled the cytotoxic activities of dichapetalin A against 16 cancer cell lines as shown in the Table 2.3 below.

TABLE 2.3: Cytotoxicity of dichapetalin A [**22**] against some cancer cell lines[16].

Cell Line	**Tumor Type**	**Dichapetalin A [EC_{50} (µg/mL)]**
HCT-116	Human colorectal carcinoma	0.1
NAMALWA	Human Burkitt's lymphoma	0.2
SKOV-3	Human Ovarian adenocarcinoma	0.5

HOP-62	Human lung cancer	0.5
A549	Human lung adenocarcinoma	0.7
NCI-H460	Human prostate carcinoma	0.8
T47D	Human breast ductal carcinoma	1.3
BxPC3	Human pancreatic adenocarcinoma	1.8
KM-12	Human colon carcinoma	5.1
OVcAR-3	Human ovarian adenocarcinoma	5.8
HL-60	Human acute promyelocytic leukemia	6.4
Colo-205	Human colorectal adenocarcinoma	7.0
TK10	Human renal adenocarcinoma	7.0
MDAMB-231	Human breast adenocarcinoma	7.6
DU145	Human prostate carcinoma	7.6
WM 266-4	Human melanoma	9.9

They found out that the human colorectal carcinoma HCT116 (EC_{50} = 0.1µg/mL) recorded the highest sensitivity towards dichapetalin A [**22**] which was 68-fold greater than the most resistant to dichapetalin A [**22**] (human melona WM266-4 EC_{50} = 9.9µg/mL). They used these cancer cell lines as references to further profile the cytotoxic and anti-proliferative properties of dichapetalins B, C, I, L, M, O, P, Q, R and S. The results are summarized in table 2.4 below.

All the tested dichapetalins indicated varying cytotoxic potencies on the two cancer lines investigated. More interestingly, dichapetalin P [**34**] was found to be four times more potent than dichapetalin A [**22**] on HCT116 cells and 74-fold more active on WM 266-4. Even though both dichapetalins A [**22**] and P [**34**] have lactone in their side chains, dichapetalin P [**34**] has a constrained and hence more stable lactone ring moiety provided by the spiro-ketal. This structural

feature could be responsible for the remarkable activity of dichapetalin P [**34**]. The importance of the constrained lactone ring moiety side chain for activity is further illustrated by the fact that dichapetalin M [**31**], a 6α-hydroxy derivative of dichapetalin P [**34**] recorded the highest cytotoxic activities of EC_{50} = 0.007 and 0.05µg/mL on HCT116 and WM 266-4 cell lines respectively. Possibly the hydroxyl group in dichapetalin M [**31**] is required for activity due to its higher activity compared to that of dichapetalin P [**34**].

Dichapetalin B [**27**], initially isolated by Addae-Mensah and co-workers but never described in terms of biological activity was found nearly as active as dichapetalin P [**34**] on the two cell lines[16]. Dichapetalin N [**28**] was also very potent but dichapetalins O [**45**], Q [**46**] and R [**47**] which lack the lactone side chain showed decreased activity on the cell lines. Dichapetalin S [**33**] was found to be more active than dichapetalins L [**26**], O [**45**], Q [**46**] and R [**47**] on both cell lines probably due to the fact that dichapetalin S [**33**] shares some structural similarities to dichapetalins A [**22**] and P [**34**] which may be vital for activity.

Table 2.4 below shows the chemosensitivities of some dichapetalins on HCT116 and WM 266-4 cancer lines as investigated by Long *et al*[16].

TABLE 2.4: Chemosensitivities of some dichapetalins on HCT116 and WM 266-4 cancer cell lines[16].

Dichapetalin type	**HCT116 [EC_{50} (µg/mL)]**	**WM 266-4 [EC_{50} (µg/mL)]**
A [**22**]	0.1	9.9
B [**27**]	0.05	0.2
C [**15**]	0.3	2.1
I [**23**]	0.2	6.0

L [**26**]	0.4	2.0
M [**31**]	0.007	0.05
N [**28**]	0.05	0.9
O [**45**]	0.5	5.0
P [**34**]	0.04	0.2
Q [**46**]	1.5	15.9
R [**47**]	2.6	19.3
S [**33**]	0.3	0.8

In a separate study by Fang *et al*[14] on the *in vivo* evaluation of dichapetalin A [**22**] (isolated from *D. gelonioides* collected in the Philippines) using the hollow fiber model at 1-6mg/kg doses, no significant growth inhibition was observed. Their observation further confirmed earlier investigations by Addae-Mensah and co-workers in 1996[9] as well as Achenbach *et al* in 1995[10]. Thus though dichapetalin A [**22**] has showed interesting and significant cytotoxic activities *in vitro*, however results from *in vivo* studies are insignificant. In the anti-HIV activity test of dichapetalins A [**22**] and M [**34**] against HIV-1/IIIB in MT-4 cells using the Tetrazolium-base colorimetric assay, dichapetalins A [**22**] and M [**34**] elicited activities at concentrations toxic to the cells and therefore no significant and selective anti-HIV activity was observed[46].

In their recent report, Jing[18] and co-workers tested the cytotoxic activities of dichapetalin U [**39**], V [**40**], W [**43**] and 7-dehydrodichapetalin E [**21**] against five cancer cell lines namely; HL-60 Human promyelocytic leukemia, SMMC-7721 Human hepatocellular cell line, A-549 Human alveolar basal-epithelial cell line, MCF-7 Human breast adenocarcinoma cell line and SW480 Human colon adenocarcinoma cell line. Dichapetalin V [**40**] recorded significant and broad cytotoxicity against all the tested cancer cell lines particularly for A-549 and MCF-7 (IC_{50} = 3 and

3.5 μM respectively). Their experiment proved dichapetalin V [**40**] to be a better cytotoxic agent than cisplatin (IC_{50} = 8.3 and 16.1μM for A-549 and MCF-7 respectively) against A-549 and MCF-7 cell lines. In the same experiment, dichapetalin U [**39**] showed selective activity towards A-549 (IC_{50} = 26.8 μM) and MCF-7 (IC_{50} = 8.2 μM) but dichapetalin W [**43**] did not show any activity against all the tested cancer lines. Moderate activities were observed for 7-dehydrodichapetalin E [**21**] but were broader compared to the recorded activities of dichapetalin U [**39**] against all the tested cell lines.

Jing[18] *et al* evaluated the feeding deterrent activities and nematicidal effects of the dichapetalins isolated from *D. gelonioides*. Dichapetalin A [**22**], 7-dehydrodichapetalin G [**20**] and 21-dehydrodichapetalin Q [**29**] exhibited antifeedant activities with EC_{50} = 3.1, 3.1 and 3.4μg/cm^2 respectively against beet armyworm (*Spoderata exugua*). The observed activities were found to be comparable to that of commercial neem oil (1% azadirachtin) which gave EC_{50} = 2.7 μg/cm^2 in the same experiment. The hydroxyl group at C_7 (in dichapetalin A [**22]** and 21-dehydrodichapetalin Q [**29**]) and the tetrahydrofuran side chain of 7-dehydrodichapetalin G [**20**] are implicated in the increased anti-feedant activity since dichapetalins with *p*-methoxylated C-6' phenyl ring in the same experiment recorded lower anti-feedant activities. In the nematicidal studies, all the compounds tested exhibited general nematicidal effects but were far less toxic to the nematodes compared with avermectin. Only 25-de-*O*-acetyldichapetalin P [**36**] and 4"-demethoxy-7-dihydrodichapetalin W [**44**] showed significant nematicidal activities causing 46.3 (± 3.6%) and 61.8 (± 5.1%) mortality respectively at 100μg/ml over 72hr period.

Jing[18] and co-workers evaluated the antifungal activities of dichapetalin A [**22**], 22-deoxydichapetalin P [**36**] and dichapetalin U [**39**] isolated from *D. gelonioides* against four pathogenic fungi namely; *Colletotetrichum gloeosporioides, C. musae, Fusarium oxysporum* f. sp.

niveum and Rhizoctonia solani. Dichapetalin U [**39**] significantly inhibited the growth of all four fungal strains with the diameter of inhibition zone ranging from 12.4(±1.1) – 13.8(±1.0) mm. The antifungal activities observed for dichapetalin U [**39**] were comparable to that of nystatin against all the fungal strains. Dichapetalin A [**22**] and 22-deoxydichapetalin P [**36**] showed activities less potent than dichapetalin U [**39**] even though against *C. musae*, 22-deoxydichapetalin P [**36**] showed higher antifungal activity than dichapetalin A [**22**] and U [**39**].

Dichapetalin A [**22**] proved to be a potent inhibitor of microphage nitric oxide (NO) production with IC_{50} = 0.02μM compared to MG132 Proteasome inhibitor (IC_{50} = 0.1μM). However, compared to the proteasome inhibitor, dichapetalin A [22] is a weak acetylcholinestrase (AChE) inhibitor as dichapetalin A [**22**] measured AChE inhibition of 28.6 ±0.7 % while proteasome inhibitor recorded AChE inhibition of 59.9 ± 2.2 % in the same experiment[20].

In a separate study, dichapetalins A [**22**] and X [**35**] isolated from the roots of *D. filicaule* gave IC_{50} values of 162.4 and 523.2 μg/ml respectively in an anthelmintic activity test against clinical isolates of hookworm eggs[17].

2.4 Dichapetalins from Other Sources and their Biological Activities

Tuchinda[15] *et al* in their search for anti-cancer agents from plants isolated five new phenylpyranotriterpenoids; Acutissimatriterpenes A **[49]** -D [**52**], and E [**48**] from the ethyl acetate extract of the aerial parts of *Phyllanthus acutissima*. Their work represents the first report of the isolation of dichapetalin-type triterpenoids with a spiro-ketal side chain from the genus *Phyllanthus*.

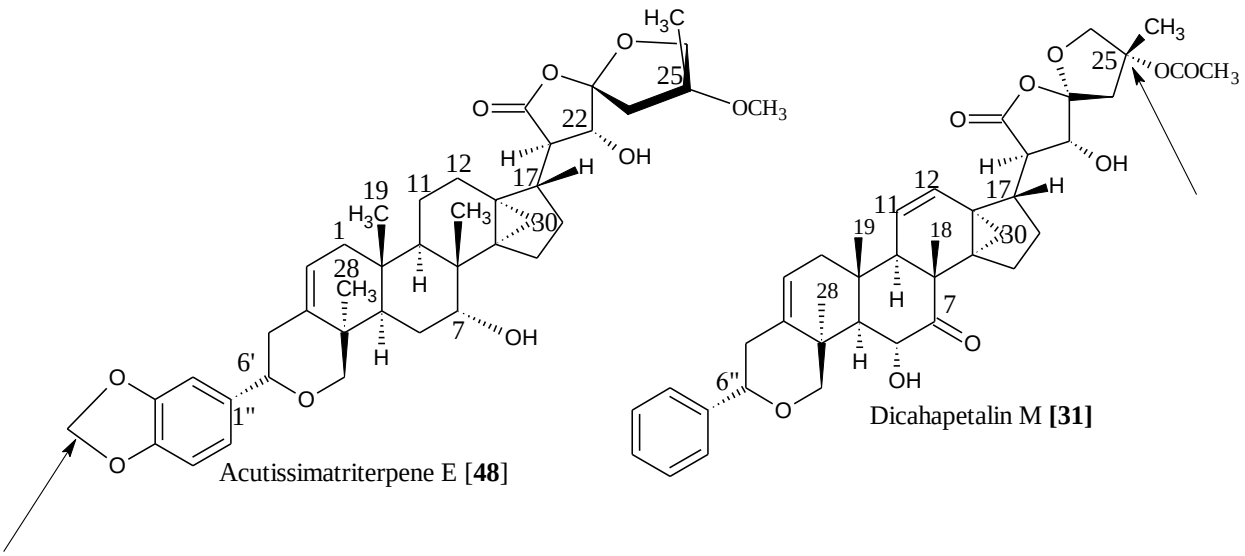

Figure 5: Structural difference between the dichapetalins and acutissimatriterpenes.

The C_{-17} side chain and the presence or otherwise of a methylenedioxy unit in the phenylpyrano moiety distinguishes the acutissimatriterpenes from the dichapetalins as shown in Figure 5 above.

As can be seen from the structures [**48**]-[**52**], acutissimatriterpenes A [**49**] and C [**51**] are methylenedioxy analogues of acutissimatriterpenes B [**50**] and D [**52**] respectively. Acutissimatriterpenes A [**49**] and B [**50**] are isometric ketals of acutissimatriterpenes C [**51**] and D [**52**] considering the side chain groups. Though acutissimatriterpenes A [**49**], B [**50**], and E [**48**] have similar tetrahydrofuran configuration, the only difference is the presence of hydroxylated alkane in E [**35**] at C_{22}. Again the spiroketal side chains of dichapetalin M [**31**] and acutissimatriterpenes A [**49**], B [**50**], and E [**48**] are similar except at the C-25 where the acetoxy group in dichapetalin M is replaced by a methoxy group in A [**49**], B [**50**] and E [**48**].

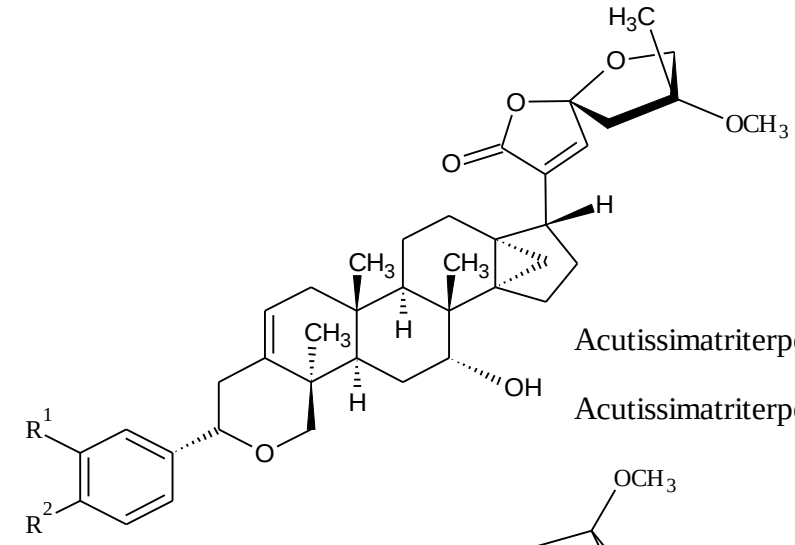

Acutissimatriterpene A: $R^1 = R^2 = O\text{-}CH_2\text{-}O$ [**49**]

Acutissimatriterpene B: $R^1 = R^2 = H$ [**50**]

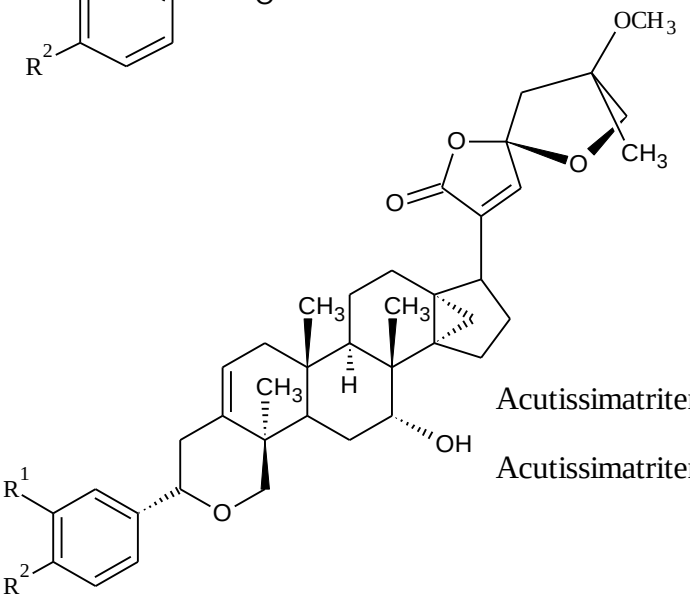

Acutissimatriterpene C: $R^1 = R^2 = O\text{-}CH_2\text{-}O$ [**51**]

Acutissimatriterpene D: $R^1 = R^2 = H$ [**52**]

Figure 6: Dichapetalin-type triterpenoids isolated from *Phyllanthus acutissima.*

The isolated acutissimatriterpenes were tested against a panel of six cancer cell lines namely; P-388 murine lymphocyte leukemia, KB human nasopharyngeal carcinoma, Col-2 human colon cancer, MCF-7 human breast cancer, Lu-1 human lung cancer and ASK rat glioma. The results according to Tuchinda *et al* indicated that acutissimatriterpene A [**49**] and acutissimatriterpene B **[50**] were active against murine lymphocyte leukemia giving EC_{50} = 0.4 and 0.5µg/ml respectively whereas acutissimatriterpene E [**48**] showed significant activities against murine lymphocyte

leukemia (EC_{50} = 0.005µg/ml), human breast cancer (EC_{50} = 1.1µg/ml) and human lung cancer (EC_{50} = 3.1µg/ml). While the remaining cell lines did not show any significant activity, acutissimatriterpenes C [**51**] and D [**52**] showed insignificant activities (EC_{50} > 5µg/ml) against all the cancer lines tested.

Results also from anti-HIV-1 activities employing cell-based cytotoxic and syncytium assays using MC99 virus and 1A2 cell line system showed various levels of activities for acutissimatriterpenes A-E (Selectivity index = >1.5- >8.1). For this particular study, it can be hypothetically stated that the presence of C_{22}- OH and a non-substituted phenyl ring are crucial for activity.

In an HIV-1 RT assay, acutissimatriterpenes A [**49**] and B [**50]** were moderately sensitive (> 50 to 70% inhibition at 200µg/ml) followed by acutissimatriterpenes D [**52**] and C [**51**] at 37% and 11% inhibition respectively, whiles acutissimatriterpene E [**48**] was the least active (-0.5% inhibition). Again the presence of an unsaturated C_{20}-C_{22} and a non-substituted phenyl group may be important for the observed activities. These results as observed by Tuchinda and co-workers presents the only significant activities of the dichapetalins in anti-HIV studies.

2.5 Other Compounds Isolated From Previously Investigated *Dichapetalum* Species

The stem bark of *D. gelonioides*[14,18] afforded apart from dichapetalins A, I, J and K, two nordaboranditerpenoids; *ent*-16-nor-3-oxodolabra-1,4(18)-diene-2-ol-15-oic acid [**53**] and *ent*-16-nor-5α,13α(methyl)-2-oxodolabra-3-en-3-ol-15-oic acid [**54**], zeylanol [**55**], 28-hydroxyzeylanol [**56**] and betulinic acid [**57**].

Chemical investigation of the roots and stem of *D. barteri*[44] even though did not show the presence of any dichapetalin, a new triterpene belonging to the friedo-oleanane family named 2-hydroxy-3-oxo-D:A-friedooleanan-29-oic-acid **[58**] was isolated in addition to betulinic acid [**57**], betulonic

acid [**59**], friedelan-3-one [**60**], friedelan-3β-ol [**61**], canophyllal [**62**], canophyllol [**63**] and 7 homologous long chain esters of E-ferulic acids.

The petroleum ether and acetone-chloroform extracts of the roots of *D. filicaule*[17] also afforded friedelan-3-one [**60**] and friedelan-3β-ol [**61**], in addition to glycerol monostearate [**64**], pomolic acid **[65**] and a mixture of stigmasterol [**66**] and β-sitosterol [**67**] from the acetone-chloroform extract only. This presented the first report for the isolation of pomolic acid from the Dichapetalaceae[17].

Long[16] *et al* isolated the abietic acid derivative pyracrenic acid [**68**] from the roots of *D. mombuttense*. The roots and stem back of *D.madagascariense* afforded friedelan-3-one [**60**] and friedelan-3β-ol [**61**] in addition to a mixture of stigmasterol [**66**] and β-sitosterol [**67**], zeylanol [**55**], sucrose [**69]**, stearic acid [**70**] and potassium salts.

In addition to fluoroacetate, phytosterols, tannins, organic acids, resins, two amino acids (namely N-methyl serine [**71**], N-methyl alanine [**72**]), and methyl pentoside trigonelline [**73**] have been isolated from *D. cymosum*[47].

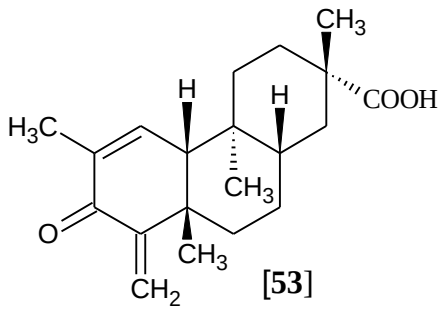

[**53**]

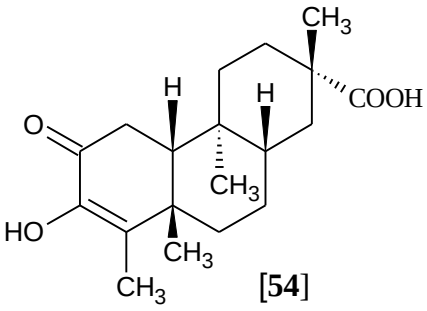

[**54**]

Figure 7: Other compounds isolated from some *Dichapetalum* species.

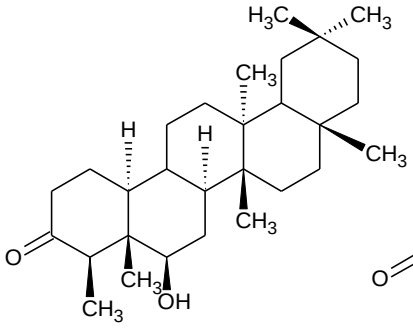

Zeylanol [**55**]

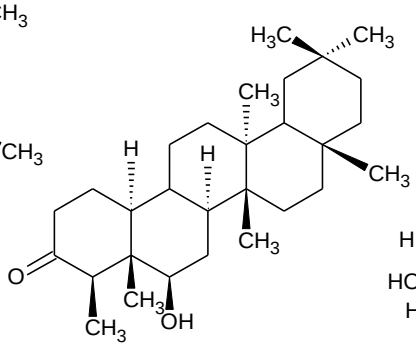

28-hydroxyzeylanol [**56**]

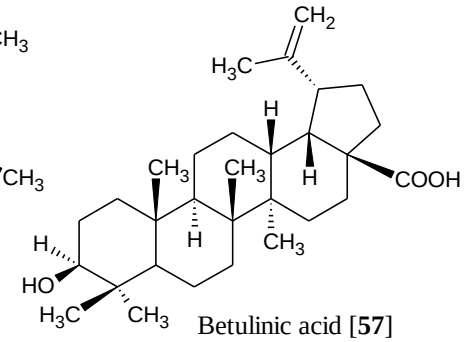

Betulinic acid [**57**]

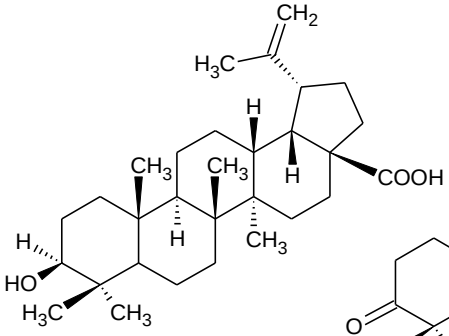

[**58**]

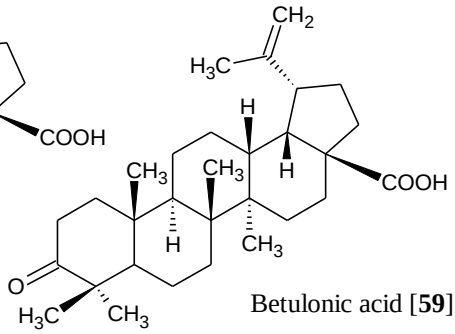

Betulonic acid [**59**]

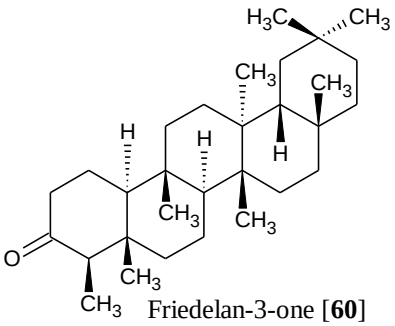

Friedelan-3-one [**60**]

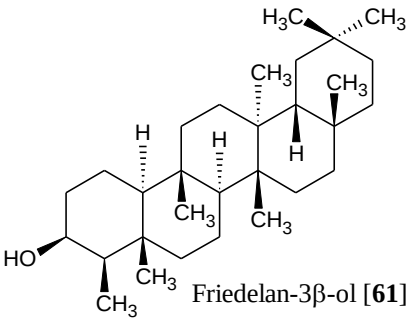

Friedelan-3β-ol [**61**]

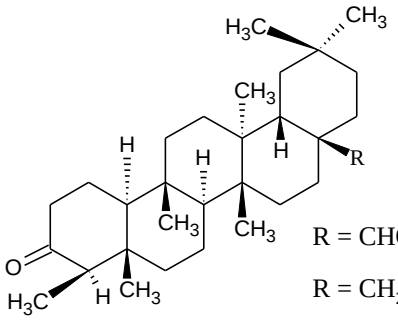

R = CHO = Canophyllal [**62**]

R = CH_2OH = Canophyllol [**63**]

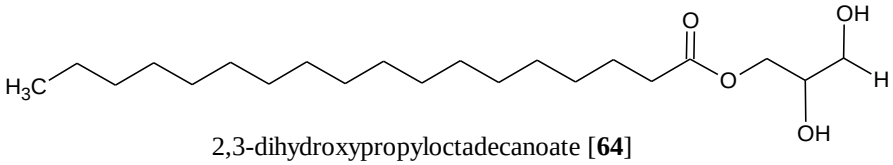

2,3-dihydroxypropyloctadecanoate [**64**]

Figure 7 continued.

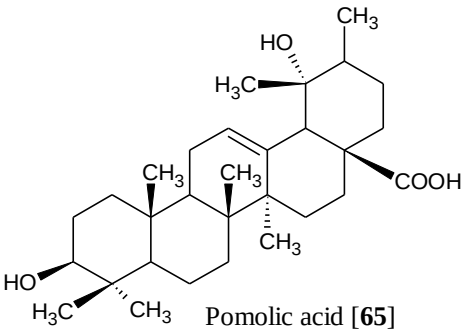

Pomolic acid [**65**]

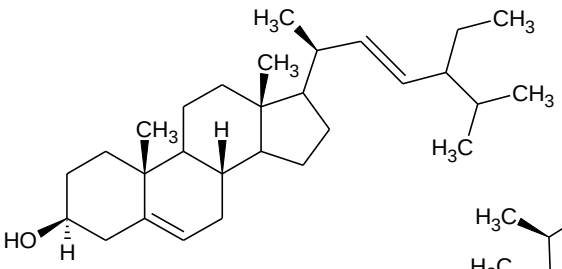

Stigmasterol **[66]**

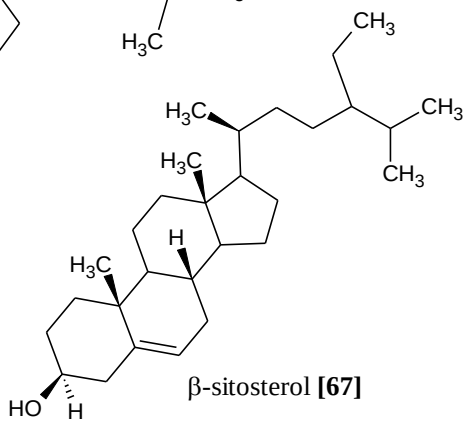

β-sitosterol **[67]**

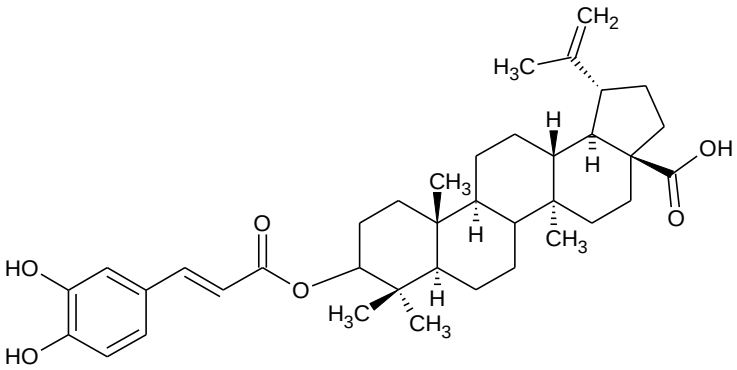

Pyracrenic acid [**68]**

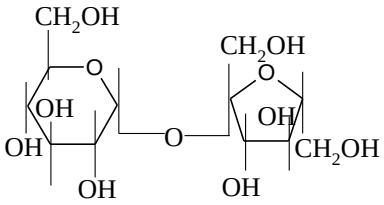

Sucrose [**69**]

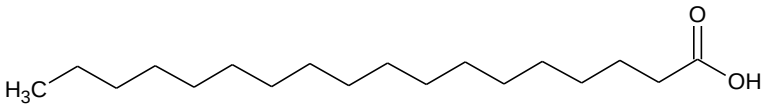

Stearic acid [**70**]

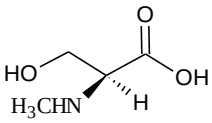

N-methylserine [**71**]

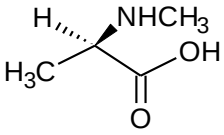

N-methylalanine [**72**]

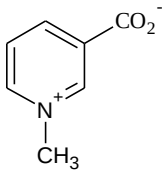

Trigonelline [**73**]

Figure 7 continued.

2.6 Schistosomiasis: A Major Neglected Parasitic Disease in Ghana.

Infectious diseases are one of the leading causes of morbidity and mortality in the developing worlds. Majority of these diseases are caused by parasites that belong to the diseases of poverty or neglected tropical diseases. Among these parasites include the causative agents of trypanosomiasis, leishmaniasis, schistosomiasis, lymphatic filariasis and onchocerciasis[24]. Schistosomiasis is endemic to most tropical and sub-tropical regions of the globe as well as part of Asia and South America and according to the World Health Organization (WHO) report, it is the second most prevalent tropical disease after malaria[20]. More than 200 million people are infected with the disease world-wide, with higher prevalence occurring among children[22]. In the year 2000, a survey of the disease specific-mortality indicated that 70 million out of a total of 682 million people had experienced haematuria and 32 million, dysuria associated with schistosomiasis infection[48]. According to the report, 18 million out of those infected suffered bladder cancer and 10 million, hydronephrosis[22]. In Sub-Saharan Africa, it is estimated that 280,000 deaths are reported yearly due to schistosomiasis infection[22]. The disease therefore constitutes an important health problem in Africa[22]. In Ghana, the disease is wide-spread in all the regions and the prevalence of schistosomiasis infection is estimated between 54.8-60%, indicating that it is still a problem in some parts of the country[23].

Schistosomiasis is caused by blood-dwelling fluke worms of the genus *Schistosoma*, with *S. mansoni* (in Africa, Middle East, South America and the Caribbean), *S. haematobium* (in Africa and Middle East), and *S. japonicum* (in China, Indonesia, Philippines) as the main disease causing species[19]. The adult worms colonize the veins of either the portal vein system (in the case of *S. mansoni* and *S. japonicum*) or the urinary bladder plexus (*S. haematobium*) and can live for several years. Egg production is both responsible for both transmission of the parasite and aetiology of the

disease. Schistosomal species are distinguished by differences in their morphology; both in parasite stage and their eggs, and by the intermediate snail host that supports the transmission of parasites[19] (Figure 8).

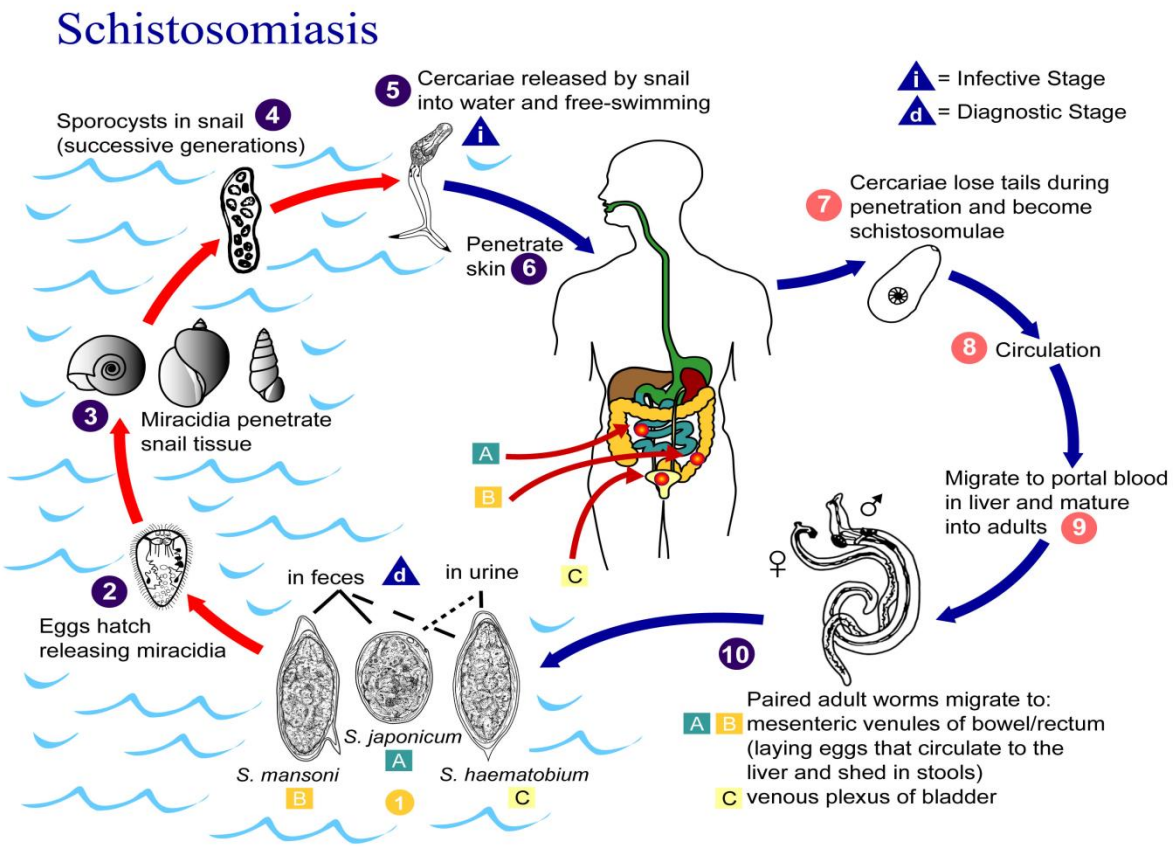

Figure 8: Life Cycle of *Schistosoma* species[19]

The infection of *Schistosoma* species occurs when the larvae of the parasites are liberated by the infected intermediate snail host, which once in contact with the definite human host, penetrates the skin. In the human host, the schistosomulae migrate to the liver via the bloodstream where they mature into adult male and female forms. After mating, the worms migrate to either the mesenteric intestinal veins or the venous plexus of the urinary system. The female worms then release the

eggs which are able to pass the epithial of blood vessels and reach the intestinal lumen, the bladder or urethra lumen in order to be expelled by stools or urine[19].

2.6.1 Control of Schistosomiasis

Even though there is no consensus about the best strategy to control the disease, prevention and control strategies are based on improving the sanitation conditions and treating patients as well as controlling the intermediate vectors[49]. A combination of the approaches above is being considered for interrupting the life cycle of *Schistosoma sp*[50,51]. Current strategies have focused on the periodic treatment of people living at risk areas with anti-schistosomal drugs in order to reduce morbidity and transmission[52].

2.6.2 Drugs for Treating Schistosomiasis

Chemotherapy is the global strategy adopted in the fight against *Schistosoma* spp. infection. Current treatment of *Schistosoma* species infection relies on metrifonate [**74**], oxamniquine [**75**] and praziquantel [**76**][53].

Metrifonate [**74**] or O,O- dimethyl-2,2,2-trichloro-1-hydroxyethylphosphonate was derived from an organophosphorus insecticide. It is recommended by WHO for treating *S. haematobium* infection since it has selective activity against the urogenital disease[54]. Metrifonate [**74**] acts as a reversible inhibitor of acetylcholinestrase, this inhibitory activity at low concentration causes a selective paralysis of the parasite's muscles making it prone to being carried out by the bloodstream to either the liver (for *S. mansoni*) or to the lungs (for *S. haematobium*). At higher concentrations, metrifonate [**74**] is toxic to humans, and at lower concentration *S. mansoni* unlike *S. haematobium* is able to go back to the mesenteric veins in the intestines to re-establish the infection[53].

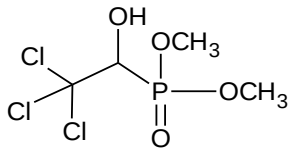

Metrifonate [**74**]

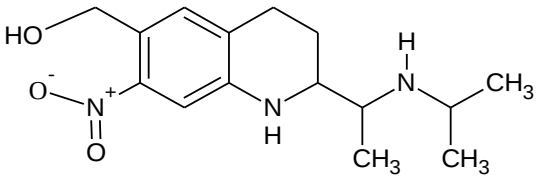

Oxamniquine [**75**]

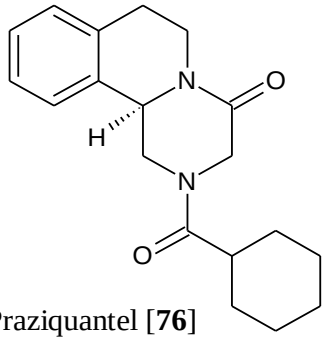

Praziquantel [**76**]

Figure 9: Anti-Schistosomiasis drugs.

Oxamniquine **[75]** or 1,2,3,4- tetrahydro-2-[isopropylamino]methyl(-)-7-nitro-6-nitro-quinoline methanol is reported to be a substrate of sulfotransferase that produces an ester which is able to react with nucleic acids and thereby interferes with replication and transcription processes in the *Schistosoma* spp.[54]. It causes an increased motility and tegument damage and it is more active against *S. mansoni* and hence recommended for treating *S. mansoni* infection. Due to its restricted use to *S. mansoni* and the high cost of production coupled to the emergence of resistant strains, oxamniquine **[75]** is not used in control campaigns even though it has less cytotoxic effects in humans compared to metrifonate **[74]**[54].

Praziquantel **[76]** or 2-(cyclohexanecarbonyl)-3, 6, 7, 11btetrahydro-1H-pyrazino[2,1-a]isoquinil-4-one is the drug of choice for treating the three human pathogenic species of schistosoma-*S. mansoni*, *S. japonicum* and *S. haematobium*. It is a safe and low cost drug and has been used for over 2 decades for control strategies and patients treatment in countries like China, Brazil, Cambodia, Egypt, Morocco and Saudi Arabia[55]. The drug is suggested to induce membrane alterations, producing a Ca^{2+} entry in the muscle cells and paralysis in the contracted state[56]. The paralyzed parasites are then carried by the bloodstream. Due to its large scale usage for control programs over a long period, the resistance of *S. mansoni* to praziquantel has been reported in

Egypt[23], and also diminished efficacy as well as resistance of the other strains of schistosoma has been reported in the field and in the laboratory[58,59,60].

The classical strategy of alternating treatments to avoid the development of resistance is very crucial. Since vaccines, safe and affordable drugs are lacking to treat schistosomiasis especially in the tropics and sub-tropics, there has been a growing interest in the scientific community to search for extracts and new compounds from plant origin with anti-schistosomal properties[61,62].

2.6.3 Natural Products as Potential Source for the Control of Schistosomiasis.

Nature has always served as a unique source of structures of high phytochemical diversity, many of them showing interesting biological and medicinal purposes. It is estimated that over 70% of the African population still rely on traditional herbs for curative purpose. Plants have been used extensively in the treatment of various diseases including schistosomiasis especially in Africa and Asia[61]. The variety of the application of these herbal extracts indicates their ethno-pharmacological potential as sources of active compounds.

Ndamba[61] *et al* have documented a list of 47 plants from different plant families used in the treatment of urinary schistosomiasis. The extract of one of them, *Pterocarpus angolensis* (Leguminosae) was prepared as described by traditional healers in Zimbabwe. After treating some previously exposed mice with the extract from the stem bark of *angolensis,* the results were found to be similar to the efficacy of praziquantel[62]. Other researchers have also confirmed the anthelmintic potencies against schistosomula of *S. mansoni* of the extracts from the root and stem bark of *Abrus precatorius* (Fabaceae) and *Elephantorrhiza goetzei* (Mimosaceae)[62]. More recently, studies are focusing on the isolation, identification and validation of the active phytochemicals within the plant extracts.

The most interesting antischistosomal compounds so far are derivatives of artemisinin; artemether **[82**] and artesunate **[81**]. Artemether has been found to be active against immature schistosomes and it has been suggested that artemether be used together with praziquantel for schistosomiasis treatment[63]. Table 2.5 below presents a brief review of natural products from plant and plant-derived sources with schistosomal properties.

Table 2.5: Potential anti-schistosomal drugs from plants (and natural product-derived) sources.

Compound/Source	**Relevant Data**
Curcumin **[77]** *Curcuma longa*[64]	Effective *in vitro* against *S. mansoni* adult worms; 100% mortality in both male and female worms at 50µg/ml, loss of motor activity, reduction in oviposition and separation of male and female worms.
2-hydroxychrysophanol **[78]** and Kwanzoquinone E **[79]** *Hemerocallis fulva*[65]	Effective *in vitro* against *S. mansoni* adult worms at 50 and 25µg/ml respectively. 35% and 80% mortality in male and female worms recorded for the former and latter respectively.
Quercetin-3-O-β-D-rhamnoside **[80]** *Schefflera vivosa*[66]	Effective *in vitro* against *S. mansoni* worms at 100µg/ml, 25% mortality recorded in male and female worms, reduction in motor activity observed.
Artesunate **[81]** and artemether **[82]** *Artemisia annua*[63]	Effective against immature schistosome in experimentally infested mice-150-300mg/kg; 67-77% mortality in male and female. Reduction in the oviposition and motor activity, disruption in tegument.
Vernodalin **[83]** *Vernonia amygdalina*[67]	Effective *in vivo* against *S. mansoni* in mice, inhibition of the oviposition and reduction in motor activity
Epiisopiloturin [**84**] *Pilocarpus mycrophyllus*[68]	Effective *in vitro* against *S. mansoni* worms, 100% mortality observed at 300µg/ml in male and female worms, causes tegument disruption in the worms.

Phytol **[85]** (Synthetic)[69]	Effective *in vitro* against *S. mansoni* worms; reduction in egg-laying observed at 25µg/ml.
Piplartine **[86]** *Piper tuberculatum*[70]	Effective *in vitro* against *S. mansoni* worms; 100% mortality in male and female worms at 15.8µM, and 100% mortality in schistosomula.
E/Z-Nerolidol **[87]** (Synthetic)[71]	Effective *in vitro* against *S. mansoni* worms; 100% mortality in male and female adult worms at 31.2 and 62.5µM, reduction in motor activity.
Favaspidic acid [**88**] and Desaspidin [**89**] *Dryopteris spp.*[72]	Effective *in vitro* against *S. mansoni* worms; 100% mortality in male and female worms observed at 50 and 25µMrespectively. Reduction in motor activity and tegument disruption.
Allicin **[90]** *Alium sativum*[73]	Effective against *S. mansoni* male worms *in vitro*; disruption of tegument observed at 10-20µg/ml.

As indicated in Table 2.5, several *in vitro* studies have been conducted in search for new drugs or possible leads for the control of schistosomiasis. The extensive phytochemical investigations reveal the presence of potential anti-schistosomals from different plant classes with different functionalities like alkaloids, terpenes, amides and lactones among others.

Even though little *in vivo* studies have been conducted compared to *in vitro* studies, the results from the *in vitro* studies are worth considering and should inspire the pathway to conducting *in vivo* studies to validate their antischistosomal properties. Also the search of new possible drugs must be intensified and optimized from other plant families like the Dichapetalaceae.

Many phytochemicals from the *Dichapetalum* species investigated have revealed interesting pharmacological activities like anticancer, anthelmintic and antifeedant among others. Most of these compounds are terpenoids in nature and compared to the structures shown below, they may provide potential anti-parasitic agents or leads for the treatment of *Schistosoma* infections. The *Dichapetalum* species abound in the tropics and most of them have not been investigated.

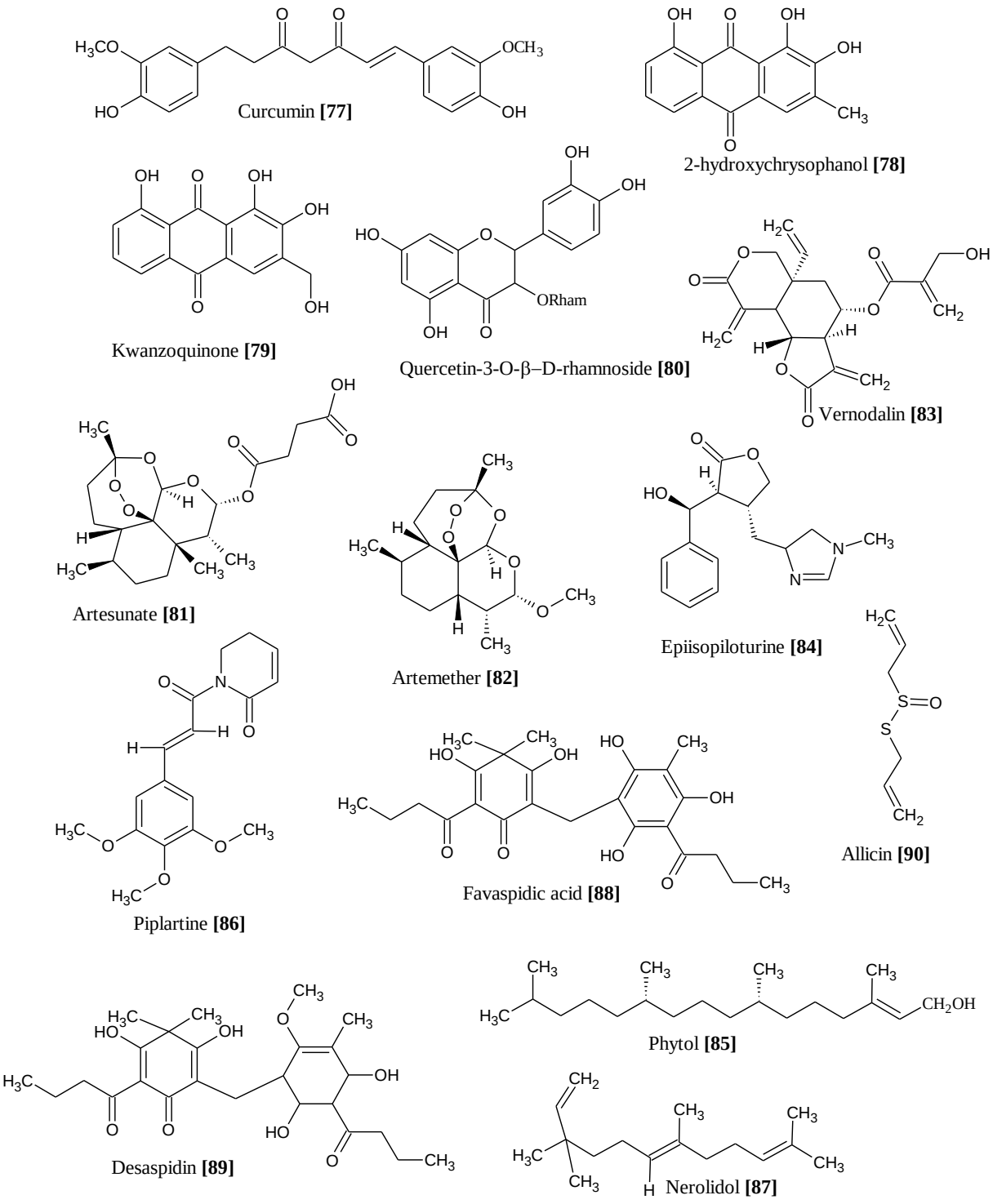

Figure 10: Potential anti-schistosomal drugs.

CHAPTER THREE

THE PRESENT INVESTIGATION

3.1 Summary

The stem of *D. crassifolium*, collected from Kuntanase in the Ashanti Region of Ghana was chopped into small pieces and pulverized after air drying for one month. The pulverized plant material (5.0kg) was successively extracted with three different solvents: petroleum ether (PE), ethyl acetate (EA) and methanol (MeOH) using Soxhlet extraction. The process yielded 34g of PE, 55g of EA and 25g of MeOH crude extracts.

Isolation and purification of the isolates from all extracts were achieved by column chromatography, thin layer chromatography (TLC) and recrystallization to yield 14 solids. Three (3) of these solids came from the PE extract, eleven (11) from the EA extract but none from the MeOH extract.

The solids isolated from the PE extract were identified as friedelan-3-one, friedelan-3β-ol and a mixture of friedelan-3-one and friedelan-3β-ol by comparative TLC, co-melting point and by comparing their IR data with authentic samples and available literature data. These solids were also isolated both as pure compounds and as a mixture from the ethyl acetate extract.

In addition to friedelan-3-one, friedelan-3β-ol and a mixture of the two, seven (7) other solids were isolated from the ethyl acetate extract. One of them (DCS-E4), was identified as the very common mixture of stigmasterol and β-sitosterol by co-TLC, co-melting point and IR data with reference samples and literature information. The solid DCS-E6 was identified as pomolic acid and another solid (DCS-E7) was identified as the previously isolated and identified

phenylpyranotriterpenoid compound, dichapetalin M, also by co-TLC and melting point with authentic samples in addition to ^{1}H and ^{13}C NMR data. DCS-EM was obtained as a mixture of dichapetalin M and two other unknown solids based on TLC. Also, DCS-E8 was identified as maslinic acid after comparing its ^{1}H and ^{13}C NMR data with reference data. The identities of DCS-E5, DCS-E9 and DCS-E11 are unknown due to impurity and paucity of material.

Investigation of the methanol extracts did not yield any solid.

3.2 INVESTIGATION OF EXTRACTS FROM THE STEM OF *D. CRASSIFOLIUM*

3.2.1 Phytochemical Screening of the PE, EA and MeOH Crude Extracts

Phytochemical screening tests were carried out on the petroleum ether, ethyl-acetate and methanol crude extracts to determine the class of compounds present in them. The results of the phytochemical screening tests are summarized in Table 3.1 below.

TABLE 3.1: Phytochemical Screening Test Results on the Crude Extracts of *D. crassifolium.*

Class of compounds	PE extract	EA extract	MeOH extract
Alkaloids	-	-	-
Anthraquinones and anthracene	-	-	-
Flavonoids and leucoanthocyanins	-	-	-
Cardiac glycosides	-	-	+
Saponins	-	-	-
Tannins	-	+	+
Terpenoids	+	+	+

Legend: **(+)** = present and **(-)** = absent

The results of the phytochemical screening test indicated that the chemical constituents of the stem of *D. crassifolium* are steroids in nature.

3.2.2 Investigation of the Petroleum Ether (PE) Extract

The dried pulverized stem of the plant material (5.0kg) was defatted via Soxhlet extraction with petroleum ether (40-60^{o}C) for 24 hours continuously. Concentration of the extract gave a total of 34.0g of a dark-greenish syrup-like crude matter coded as DCS-P. Phytochemical screening on DCS-P indicated the presence of terpenoids only. DCS-P was kept in the refrigerator until further investigation. Scheme 3 below summarizes how the phytochemicals present in the extract were isolated.

Scheme 3: Investigation of PE Extract.

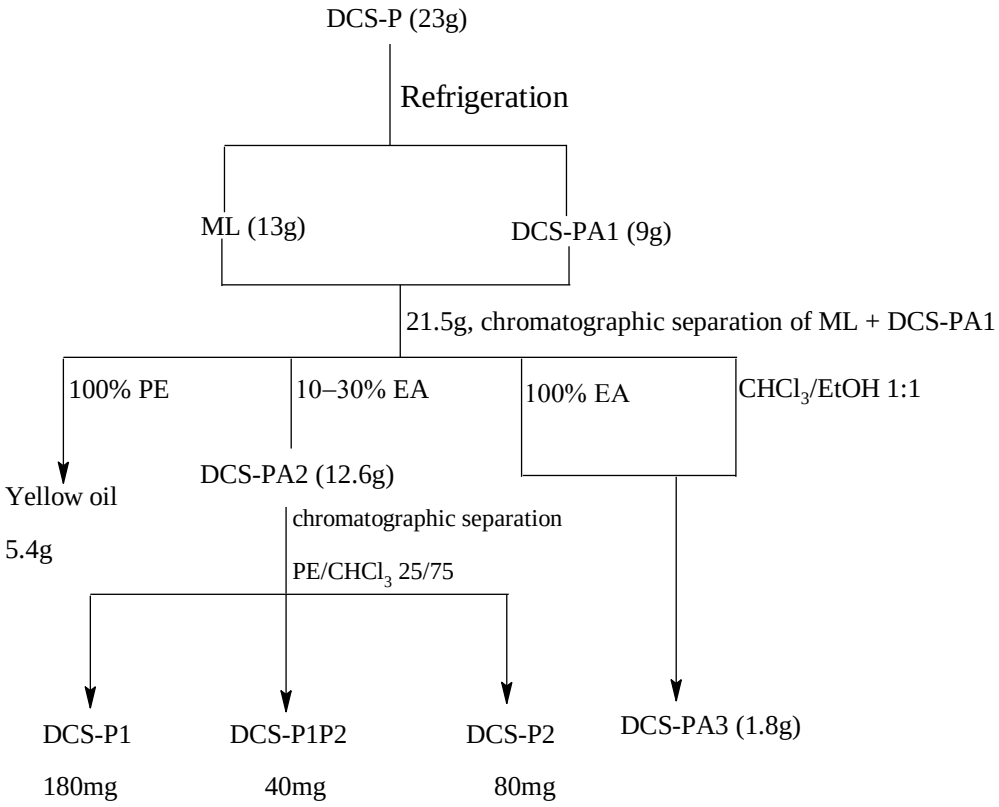

Upon refrigeration, DCS-P was observed to have precipitate and supernatant portions. The supernatant (mother-liquor, ML) was filtered off and TLC in petroleum ether/ ethyl acetate (28:1), was run on both the solid portion DCS-PA1 and the mother liquor, ML. After staining with anisaldehyde spray reagent, the two portions revealed comparable spots (over 14) and hence were put together (21.5g), dissolved in chloroform and mixed with silica gel (6g) and air dried. This was later put on a glass column pre-loaded with silica gel (230g). The column was first eluted with 100% petroleum ether, then with petroleum ether and ethyl acetate mixtures until 100% ethyl acetate. The column was finally washed with chloroform/ethanol 1:1mixture.

Fractions F021-F073, eluted with 10-30% of ethyl acetate in petroleum ether were combined based on their similar TLC profiles. This was coded DCS-PA2, which gave 4 spots on TLC (Petroleum ether/ethyl acetate: 14:0.5). The sub-fraction DCS-PA2 (12.6g), was again put on a smaller glass column pre-loaded with silica gel (80g) and eluted with petroleum ether/chloroform: 25/75 mixture. The column fractions yielded the solids DCS-P1 (120mg, 1 spot), DCS-P2 (70mg, 1 spot) and a mixture of these two solids coded DCS-P1P2 (20mg, 2spots) after recrystallization from ethanol. The 100% ethyl acetate fraction and the fraction obtained after washing the column (chloroform/ absolute ethanol 1:1) were also found to be the same on TLC and hence were combined (coded DCS-PA3) and safely kept in the refrigerator for future investigation.

3.2.2.1 Isolation and identification of friedelan-3-one, DCS-P1

DCS-P1 was obtained as white needle-like crystals after recrystallization from ethanol with melting point of 249-251^{o}C. On TLC, DCS-P1 was observed as a single yellow spot with anisaldehyde spray reagent after heating. The yellow color lasted for a short time. The following R_{fs} were recorded in the following solvent systems: 100% $CHCl_3$, R_f = 0.94; petroleum ether/EtOH

(15:1), R_f = 0.79; petroleum ether/acetone (12:0.5), R_f = 0.82; petroleum ether/ ethyl acetate (14:0.5), R_f = 0.87 but the color faded quickly upon exposure to air. The spot also stained with iodine to give a dark grayish coloration which lasted temporarily. Comparative TLC and mixed melting point with a reference sample identified DCS-P1 as friedelan-3-one. The reference sample had a melting point of 250-252ºC and showed the same R_f as DCS-P1 run in the solvent systems above. The IR data of the two compounds were comparable especially in the fingerprint region.

The IR data of DCS-P1 and friedelan-3-one are presented in Table 3.2 below.

TABLE 3.2: IR frequencies of DCS-P1 compared to that of friedelan-3-one.

Frequency (cm^{-1}) of DCS-P1	Peak Intensity	Frequency (cm^{-1}) of friedelan-3-one[17]	Peak Intensity	Interpretation
3003.19, 2926.86 2869.70	Strong	3003, 2971, 2926, 2869	Strong	C-H stretch; alkanes
1715.54	Strong	1715	Strong	C=O stretch; ketones
1462.80, 1389.39	Strong	1463, 1389	Strong	$C(CH_3)_2$ bending vibration; alkanes

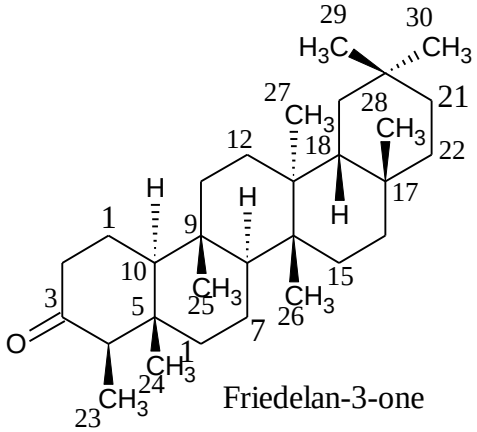

Friedelan-3-one

Friedelan-3-one, also called friedooleanan-3-one, DA-friedooleanan-3-one, friedelin, friedeline or 3-friedelanone has the IUPAC name (4R, 4aS, 6aS, 6aS, 6bR, 8aR, 12aR, 14aS, 14bs) – 4, 4a, 6a, 6b,8a, 11,11, 14a- octamethyl -2, 4, 5, 6, 6a, 7, 8, 9, 10, 12, 12a, 13, 14, 14b-tetradecahydro-1H-picen-3-one with a molecular weight of 426.73g/mol[12].

In the family Dichapetalaceae, friedelan-3-one has been isolated from *D. barteri*, *D. madagascariense*, *D. gelonioides* and *D. filicaule*. However, it has also been isolated from other different plant families among which are; *Maytenus ilicifolia* (Celastraceae)[74], *Ageratum conyzoides* (Asteraceae)[75], the stem bark of *Hymenocardia acida* (Hymenocardiaceae)[76], *Calophyllum cordata-oblongum* (Calophyllaceae)[77], root bark of *Tripterygium hypoglaucum* (Celastraceae)[78] and from the plant *Virola Calophylla* (Myristicaceae)[79].

Contrary to previous thought that terpenoids are biologically inactive, there is continuing evidence to confirm that terpenoids have broad spectrum of pharmacological activities coupled with low toxicity profile[80]. Apart from their use in most Asian countries for their anti-inflammatory, analgesic, antipyretic, hepatoprotective, cardiotonic, sedative and tonic effects[80,81], several other activities including antioxidant, antimicrobial, antiviral, antiangiogenic, antiallergic, antipruritic, spasmolytic and cytotoxicity have been reported[82, 83, 84].

The anti-ulcerogenic activity of friedelan-3-one has been suggested by Queiroga[74] *et al* after isolating it from *Maytenus ilicifolia*. Duraipandiyan[85] and co-workers have suggested the potential antifungal effect of friedelan-3-one. Duraipandiyan as well as Kumari[86] *et al* have investigated the anti-inflammatory activity of friedelan-3-one. Kumari and co-workers isolated friedelan-3-one in addition to surionol, daucosterol, ursolic acid, cycloeucaneol, nimbiol, sugiol and 3β-hydroxyglutin-5-ene from *Cammiphora berryi* and investigated their anti-inflammatory activity

via an *in vitro* soybean lipoxygenase (SBL) assay. Among all the isolates, friedelan-3-one showed the highest significant activity with IC_{50} = 35.8µM. Erasmienne[87] and co-workers also have confirmed the antiplasmodial activity of friedelan-3-one isolated from *Endodesmia calophylloides*.

3.2.2.2 Isolation and identification of friedelan-3β-ol, DCS-P2

DCS-P2 was obtained as a glassy-white, rod-like crystalline solid. It was soluble in chloroform and stained with iodine vapor to give a dark-brown coloration only upon longer exposure. The melting point was determined to be 272-274^{o}C. It stained purple with anisaldehyde spray reagent on TLC upon heating. The purple color lasted for a longer time. The following R_f values were measured after running TLC on this solid in the following solvent systems: 100% $CHCl_3$, R_f = 0.81; petroleum ether/EtOH (15:1), R_f = 0.46; petroleum ether/ acetone (12:0.5), R_f = 0.5, petroleum ether/ ethyl acetate (14:0.5), R_f = 0.61. After running comparative TLC and melting point on DCS-P2 and a reference sample, DCS-P2 was identified as friedelan-3β-ol based on its comparable R_f and melting point with the reference sample. The reference material had a melting point of 271-273^{o}C. The IR data obtained for DCS-P2 was comparable to that of the reference sample.

TABLE 3.3: Comparison of IR data of DCS-P2 with that of friedelan-3β-ol

IR frequency (cm^{-1}) of DCS-P2	Intensity of Peak	IR Frequency (cm^{-1}) of Friedelan-3β-ol[17]	Intensity of Peak	Interpretation
3476.97	Strong	3479	Strong	O-H stretch; alcohol
2932.17, 2870.58	Strong	2911, 2869	Strong	C-H stretch; alkanes
1447.72, 1384.96	Strong	1451, 1385	Strong	$C(CH_3)_2$ bend; alkanes

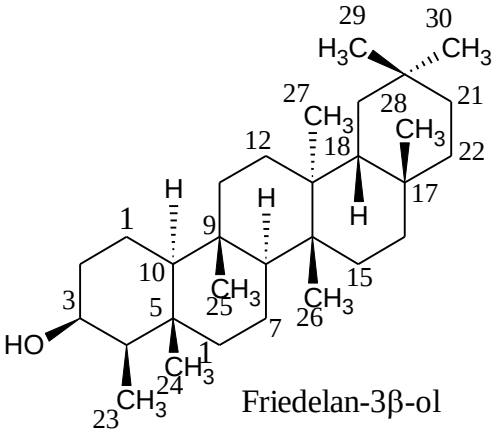

Friedelan-3β-ol

Friedelan-3β-ol, is synonymous with epi-Friedelinol, epifriedelanol, friedelinol and 3β-friedelinol has the IUPAC name (3S, 4R, 4aS, 6aS, 6bR, 8aR, 14aS)- 4, 14a, 6a, 6b, 8a, 11, 11, 14a-octamethyl- 1, 2, 3, 4, 5, 6, 6a, 7, 8, 9, 10,12, 12a 13, 14, 14b-hexadecahydropicen-3-ol. It has a molecular weight of 428.73g/mol[12].

From the plant family Dichapetalaceae, friedelan-3β-ol, like friedelan-3-one, has also been isolated from *D. barteri*, *D. madagascariense*, *D. gelonioides* and *D. filicaule*. In literature, friedelan-3β-ol has been isolated from other different plant families like *Meytenus ilicifolia* (celastraceae)[74], *Drynarai quercifolia* (Polypodiaceae)[87], *Ulmus pumila* L. (Ulmaceae)[88], *Ipomoea cairica* (Convolvulaceae)[89] and *Myricaria paniculata* (Myrtaceae)[90].

Apart from anti-ulcerogenic activity as suggested by Queiroga[74] and co-workers for friedelan-3β-ol, Yang[91] *et al* have suggested its possible use in controlling aging related diseases.

3.2.2.3 Isolation of a mixture of friedelan-3-one and friedelan-3β-ol, DCS-P1P2

The solid DCS-P1P2 was obtained as white needle-like crystals after recrystallization from ethanol. The melting point was determined to be 236-246^{o}C. It showed 2 spots on TLC and stained yellow and purple with anisaldehyde spray reagent with the following R_{fs} when run in the

following solvent systems: 100% $CHCl_3$, R_f = 0.94, 0.81; petroleum ether/ EtOH (15:1), R_f = 0.79, 0.46; petroleum ether/acetone (12:0.5), R_f = 0.87, 0.51; petroleum ether/ ethyl acetate (14:0.5), R_f = 0.87, 0.61. DCS-P1P2 was identified as a mixture of fridelan-3-one (DCS-P1) and friedelan-3β-ol (DCS-P2) after running comparative TLC with DCS-P1, DCS-P2 and as authentic sample in the above solvent systems. Its lower melting point probably suggests the higher amount of friedelan-3-one than friedelan-3β-ol in the mixture as indicated by the sizes of the spots on TLC. The IR data for this mixture revealed prominent peaks at 3477, 1178 cm^{-1} for an OH stretch, a strong and sharp signal at 1710cm^{-1} for a carbonyl stretch and also the presence of a gem dimethyl group at 1449 and 1383 cm^{-1}.

3.3 Investigation of the Ethyl Acetate (EA) Extract

The defatted plant material was air dried and successively extracted with 10L of ethyl acetate for 24 hours. A total of 65g of crude extract was obtained after extracting 5.0kg of the plant material. The crude extract was dark-greenish in appearance and TLC in petroleum ether/ethyl acetate 10:3 indicated over 14 spots. This extract was coded DCS-EA and Scheme 4 below summarizes how work was carried out on the extract to obtain the isolates.

DCS-EA was fractionated with wide increase in polarity into 13 fractions, DCS-EA1 - DCS-EA13. The similarity of some of the fractions on TLC resulted in the combination of DCS-EA1 and DCS-EA2 into DCS-EAA1, DCS-EA3 and DCS-EA4 into DCS-EAA2; DCS-EA5, DCS-EA6 and DCS-EA7 into DCS-EAA3; DCS-EA8, DCS-EA9 and DCS-EA10 into DCS-EAA4; DCS-EA11 and DCS-EA12 into DCS-EAA5 and finally elution with absolute ethanol gave fraction DCS-EAA6, giving a total of six fractions in all.

The separate sub-fractions, DCS-EAA1 to DCS-EAA5 were each purified further by column chromatography.

Scheme 4. Summary of Work Carried out on Ethyl Acetate extract**.**

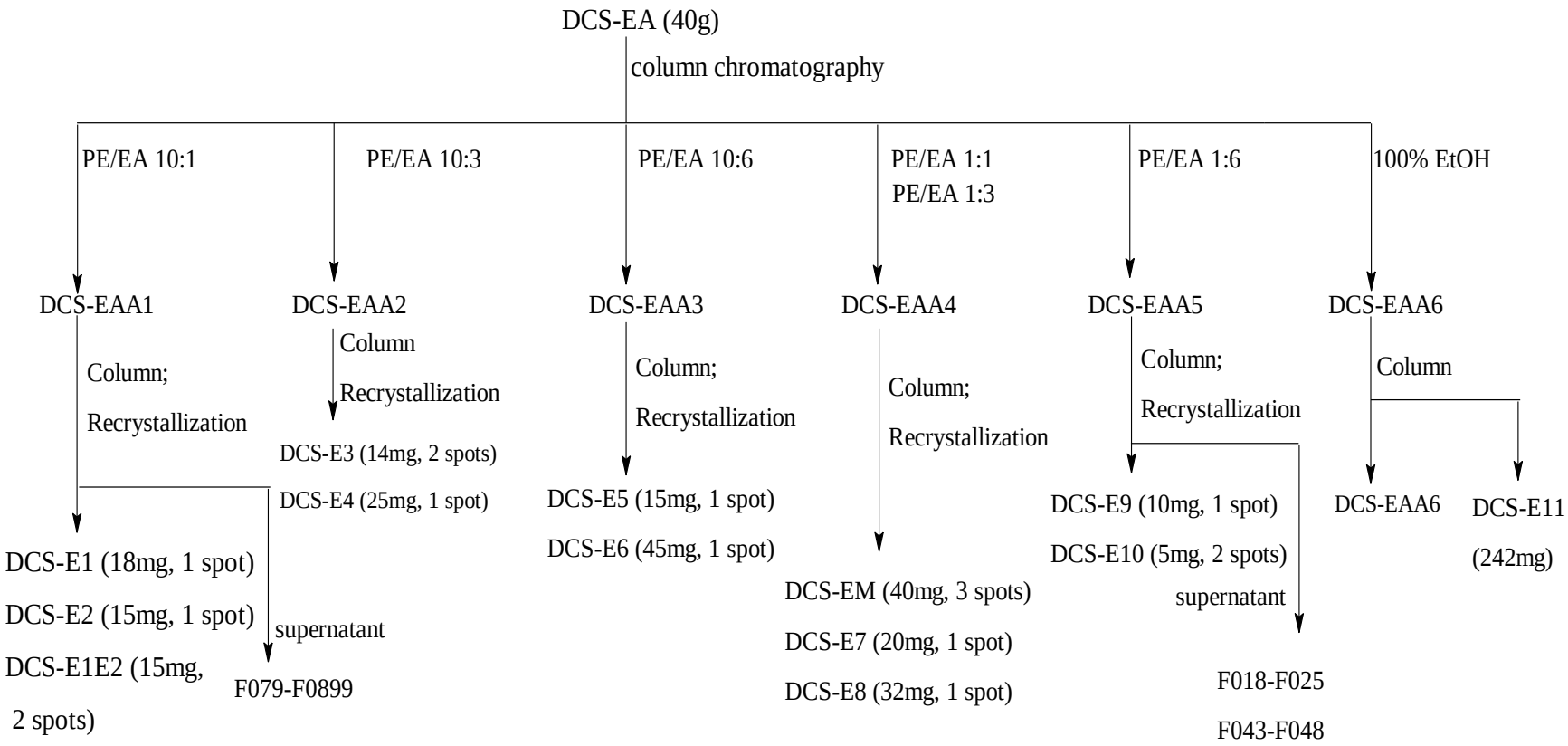

3.3.1 Purification and identification of friedelan-3-one, DCS-E1

DCS-E1 was obtained as white needle-like crystals after recrystallization from ethanol. It was the first solid to precipitate from the sub-fraction DCS-EAA1 during the chromatographic separation. The melting point was determined to be 248-250^{o}C and found to be soluble in chloroform. It appeared as a yellow spot (which faded quickly) on TLC after staining with anisaldehyde spray reagent in the following mobile phase compositions: 100% chloroform, R_f = 0.92; petroleum ether/ acetone (12:0.5), R_f = 0.80; petroleum ether/ethanol (15:1), R_f = 0.77; petroleum ether/ethyl acetate (14:0.5), R_f = 0.85. Based on the comparable R_f values, melting points and IR data of DCS-E1, DCS-P1 and with an authentic sample, DCS-E1 was identified as friedelan-3-one. The reference material had a melting point of 250-252^{o}C. The IR data recorded significant peaks at 3003.19, 2926.86, 2869.70, 1715.54, 1462.80 and 1389.39 cm^{-1}.

3.2.3.2 Purification and identification of friedelan-3β-ol, DCS-E2

The next solid from sub-fraction DCS-EAA1 during the chromatographic separation was DCS-E2, obtained as a glassy, white rod-like crystals with a melting point of 272-274^{o}C. DCS-E1 gave a purple spot on TLC run in the following solvent systems when sprayed with anisaldehyde reagent: 100% chloroform, R_f = 0.79; petroleum ether/ethanol (15:1), R_f = 0.42; petroleum ether/acetone (12:0.5), R_f = 0.48; petroleum ether/ethyl acetate (14:0.5), R_f = 0.59. DCS-E2 does not fluoresce under UV light; it however stained with iodine over long exposure. Based on the comparable R_{fs}, melting points and IR data of DCS-E2, DCS-P2 and an authentic sample, DCS-E2 was identified as friedelan-3β-ol**.** The reference material had a melting point of 271-273^{o}C. The IR data recorded significant peaks at 3476.97, 2932.17, 2870.58, 1447.72 and 1384.96 cm^{-1}.

3.3.3 Purification and identification of mixture of friedelan-3-one and friedelan-β-ol, DCS-E1E2 and DCS-E3

The solids DCS-E1E2 and DCS-E3 were similar in all respect to the already isolated solid DCS-P1P2. They were obtained as white crystals after recrystallization from ethanol and gave two spots; yellow and purple with comparable R_f values as DCS-P1P2. The IR data recorded for both were similar in addition to their comparable melting points. DCS-E1E2 and DCS-E3 were therefore identified as a mixture of fridelan-3-one and friedelan-3β-ol.

3.3.4 Purification and identification of a mixture of β-sitosterol and stigmasterol, DCS-E4

The next solid isolated from sub-fraction DCS-EAA2 was DCS-E4, obtained as white crystalline solid after recrystallization from petroleum ether/acetone mixtures and the melting point was determined to be 138-140^{o}C. DCS-E4 gave a single orange spot with anisaldehyde spray reagent on TLC run in the following mobile phase compositions: 100% chloroform, R_f = 0.50; petroleum ether/ethanol (15:1), R_f = 0.20; petroleum ether/ ethyl acetate (10:4), R_f = 0.82; petroleum ether/ acetone (12:0.5), R_f = 0.21. The melting point recorded for the reference sample was 139-141^{o}C. Based on comparable R_f values, melting point and IR data of DCS-E4 with a reference material, DCS-E4 was identified as a mixture of β-sitosterol [**39**] and stigmasterol [**40**]. The IR data of the reference sample and that of DCS-E4 is presented in Table 3.4 below.

TABLE 3.4: Infrared values of DCS-E4 compared to that of β-sitosterol/stigmasterol mixture

IR (*KBr*) ν_{max} cm^{-1} DCS-E4	Peak Intensity	IR (*KBr*) ν_{max} cm^{-1} Ref.[12,14]	Peak intensity	Interpretation
3434.43	Strong, broad	3434	Strong, broad	O-H stretch, alcohol
2936.20, 2882.60	Strong, sharp	2933, 2886	Strong, sharp	C-H stretch, alkane

1639.76	Weak	1641.11	Weak	C=C stretch, alkene
1463.99,1382.79, 1062.30	Medium	1464.23,1382.03, 1061	Medium	C-H bending vibration, alkane

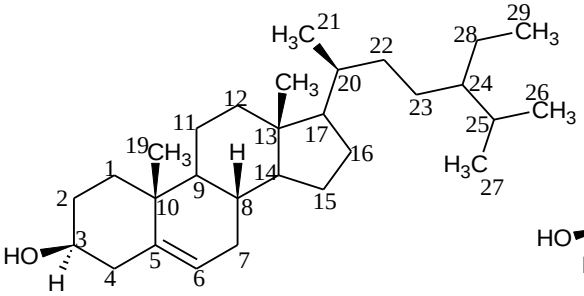

β-Sitosterol [39]

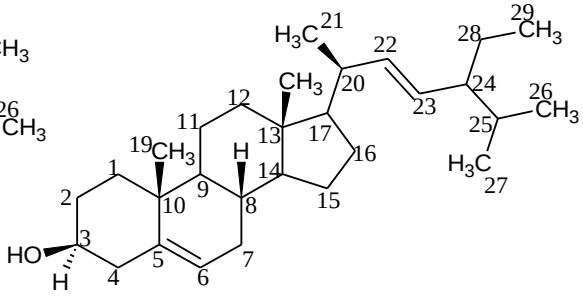

Stigmasterol [40]

The two compounds, β-sitosterol [**39**] and stigmasterol [**40**] structurally differ only at $C_{22} - C_{23}$ due to unsaturation in the latter and as a result are often isolated together as a mixture. Also due to the electronic effects of the C=C carbons in stigmasterol [**40**], the chemical shifts of the protons and carbons in the environment of the unsaturation would be slightly higher (deshielded) than in β-sitosterol [**39**].

Steroids, being terpenoids are metabolites of isopentyl pyrophosphate oligomers and represent the largest group of phytochemicals. There are over 20,000 terpenoids in nature which occur in different plants including sea-weeds as well as wax-like coatings of various fruits and medicinal herbs like apples, cranberries, figs, olives, mistletoe and lavender among others[92,93].

Terpenoids are biosynthesized in plants by the cyclization of squalene, which is then converted to squalene 2, 3-oxide from which the precursor of phytosterols, cycloartenol [**39a**] is derived[94]. Cycloartenol [**39a**], a polycyclic sterol unique to plants, is alkylated at C_{-24} to produce a triene [**39c**] through a series of steps (Scheme 5), C_{-14} sterol reductase and a Δ^8- Δ^7 isomerase act on the

triene to form 24-methylenelophenol, a branch point in the pathway. Parallel pathways lead to the membrane sterols sitosterol from which stigmasterol is derived[95].

Bulk sterols are integral parts of the membrane lipid bilayer, where, in conjunction with phospholipids, they regulate membrane permeability and fluidity. Sitosterol is believed to regulate membrane fluidity and permeability in plants membranes by restricting the mobility of fatty acyl chains in a similar manner to cholesterol in mammalian cells. It may be involved in how plants membranes adapt to changes in temperature[95].

Scheme 5: Biosynthetic Pathways of sterols required for Normal Plant Development.

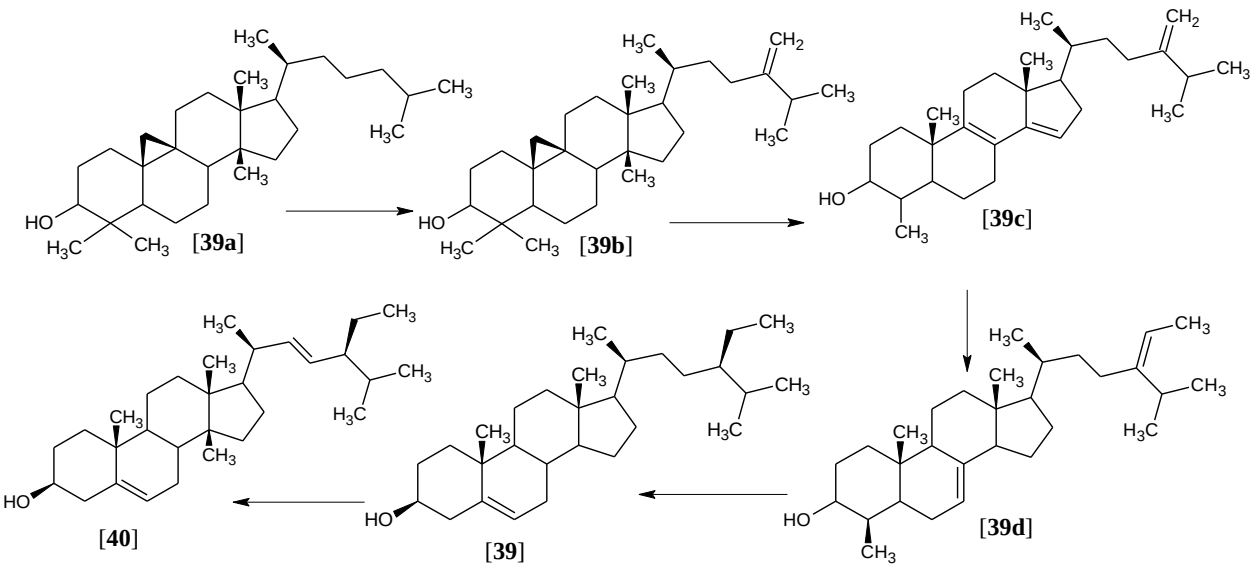

β-sitosterol, isolated from *Cissus quadrangularis*, according to Garinma[96] *et al* has demonstrated anti-inflammatory and anti-hemorrhoidal activities. Chandler[97] and co-workers have also confirmed the anti-hypercholesterolemic activity of β-sitosterol and stigmasterol. Stigmasterol has been reported to regulate the activity of the Na^+/K^+- ATPase in plants, similar to that of cholesterol in animal cells and again more specifically for cell differenciation and proliferation[95].

3.3.5 Purification of DCS-E5 and DCS-E6 (DCS-E6 identified as pomolic acid)

DCS-E5 and DCS-E6 were the only solids isolated from sub-fraction DCS-EAA3. They were isolated as powdery white solids after recrystallization from a mixture of diethyl ether and chloroform (10/3) and the melting points were determined to be 264-266^{o}C and 268-270^{o}C respectively. DCS-E5 and DCS-E6 gave a purple spot with vanillin spray reagent on TLC run in petroleum ether/chloroform/acetone (7:3:5), R_f = 0.52. DCS-E5/DCS-E6 also gave a single violet spot with anisaldehyde spray reagent on TLC run in the following mobile phase compositions: 100% chloroform, R_f = 0.24; petroleum ether/acetone (10:3), R_f = 0.41; petroleum ether/diethyl ether (3:7), R_f = 0.58; petroleum ether/ethyl acetate (10:6), R_f = 0.87. The IR data recorded for both solids is presented in Table 3.5 below. Comparison of the ^{1}H and ^{13}C NMR data of DCS-E6 with those of a reference sample confirmed DCS-E6 as pomolic acid [**65**]. No other spectroscopic data was obtained for DCS-E5 due to paucity of material.

Table 3.5: IR data for DCS-E5 and pomolic acid, DCS-E6

IR (*KBr*) ν_{max} cm^{-1} DCS-E5	Peak intensity	IR (*KBr*) ν_{max} cm^{-1} DCS-E6	Peak intensity	Interpretation
3436.94	Strong	3446.79	Strong	O-H stretch
2927.99	Strong	2928.60	Strong	C-H stretch, alkane
1691.94 1633.22	Strong Weak	1690.31	Strong	C=O stretching vibration of carboxylic acid.
1461.71, 1385.91	Medium	1461.59, 1385.57	Medium	C-H bending vibration, alkanes
1237.70,1157.91, 1029.73	Weak	1236.91,1157.03, 1029.73	Weak	C-H bending vibrations

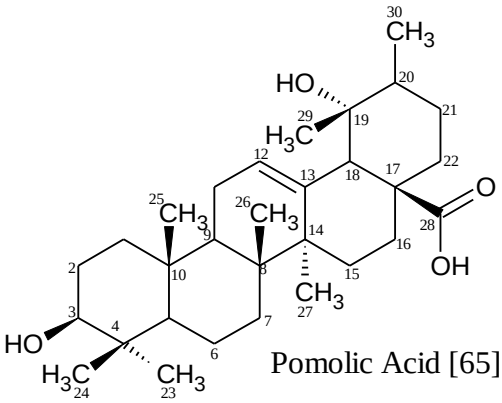

Pomolic Acid [65]

The ^{13}C-NMR data recorded for DCS-E6 revealed the presence of 30 carbons, with chemical shifts ranging from 15.1-180.6 ppm. The carbon signal at δ_C 180.6 was assigned to the carboxyl functional group at C-28 and this is further confirmed by the presence of broad, intense O-H stretching absorption in the recorded IR spectrum for DCS-E6. The downfield signals at δ_C 78.9 and 73.0 were assigned to C-3 and C-19 respectively. Even though these are sp^3 carbons, the observed downfield shifts is as a result of their attachment to electronegative hydroxyl groups. The sp^2-alkene type carbons, C-12 and C-13 were assigned chemical shifts of δ_C 129.1 and 138.0 respectively. Apart from C- 13 and C-19, the quaternary carbons were assigned chemical shifts of δ_C 41.1 (C-4), 38.6 (C-8), 37.5 (C-10), 47.1 (C-14) and 47.5 (C-17). Five of the tertiary methyl carbons were assigned the following chemical shifts; δ_C 23.6 (C-23), 16.5 (C-24), 15.4 (C-25), 16.0 (C-26) and 25.4 (C-27). The signals at δ_C 25.9 and 15.1 were assigned to C-29 and C-30 respectively. The ^{13}C NMR assignment is summarized in Table 3.6 below.

After assigning all the ^{1}H and ^{13}C-NMR signals of DCS-E6 and comparing with a reference data, DCS-E6 was clearly identified as the ursane-type triterpene acid, pomolic acid [**65**].

Table 3.6: Comparison of ^{13}C Chemical Shifts of DCS-E6 (Pomolic acid) with reference data.

^{13}C No.	DCS-E6 (δ_C in $CD_3OD/CDCl_3$)	Reference data of Pomolic acid (δ_C in $CD_3OD/CDCl_3$)[17]
1	39.8	39.6
2	29.6	29.4
3	78.9	78.6
4	41.1	41.0
5	55.1	55.0
6	18.4	18.4
7	32.7	32.6
8	38.6	38.4
9	48.6	48.7
10	37.5	37.3
11	24.4	24.0
12	129.1	128.7
13	138.0	137.9
14	47.1	46.9
15	28.0	28.0
16	26.9	26.5
17	47.5	47.3
18	53.1	53.0
19	73.0	72.8
20	36.9	36.7
21	27.2	27.7
22	38.4	38.3
23	23.6	23.4
24	16.5	16.5
25	15.4	15.4
26	16.0	16.0
27	25.4	25.2
28	180.6	180.6
29	25.9	25.8
30	15.1	15.1

The ^1H NMR (Figures 11a-c) recorded for DCS-E6 revealed several signals ranging from δ_H 1.2 - 2.2 for overlapping sp^3-hybridized methylene and methine protons of pomolic acid. The signal at δ_H 5.35 (1H, t, J = 6Hz) was assigned to H-12 and the signal at δ_H 3.40 (1H, m) was assigned to H-3. For the methyl protons, H-29 was assigned δ_H 1.26 (3H, d, J = 7.2Hz), H-30 was assigned δ_H

0.95 (3H, d, J = 12Hz) and H-26 was assigned δ_H 0.78 (3H, d J = 10.8Hz). These appeared as multiplets due to long range proton-proton coupling. The other methyl protons appeared as singlets and resonated at the following frequencies; δ_H 1.21 (H-24), 0.99 (H-25) and 0.92 (H-23). The prominent signal at δ_H 7.30 is due to residual $CDCl_3$ in the solvent used in obtaining the spectrum.

The chemical shift value of δ_H 2.49 (2H, ddd, J_1 = 8.8, J_2 = 9.6, J_3 = 6.6Hz) was assigned to H-2, the downfield shift suggesting neighboring electronegative groups. The observed multiplicity at δ_H 2.49 could be explained by the fact that there was an initial coupling to the methylene protons at H-1 into a triplet and each signal of the triplet was further split into a doublet by the methine proton at H-3. The signal at δ_H 2.63 (1H, s) was assigned to H-18 and not H-9 primarily due to the electronegative neighboring environment (OH and COOH) of H-18 compared to H-9.

The signal at δ_H 2.18 (1H, d, J = 7.8) was assigned to H-9. The signal at δ_H 3.21 (2H, dd, J_1 = 15, J_2 = 7.8) was assigned to H-11, the signal at δ_H 1.98(2H, d, J = 5Hz) was assigned to H-16 while the signal at δ_H 1.96 (2H, d, J = 4.6Hz) was assigned to H-22.

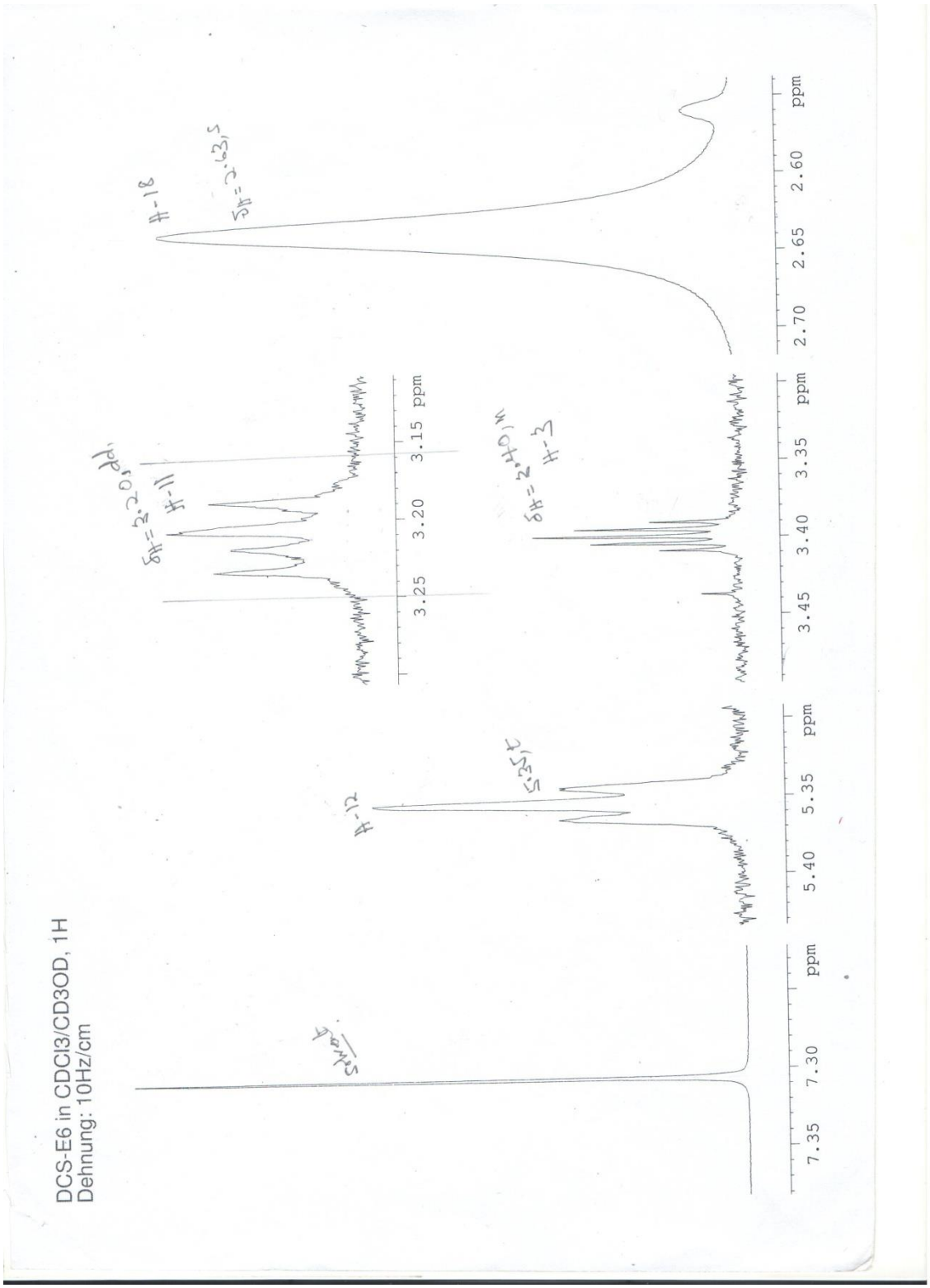

Figure 11a : Expanded [1]H NMR of DCS-E6.

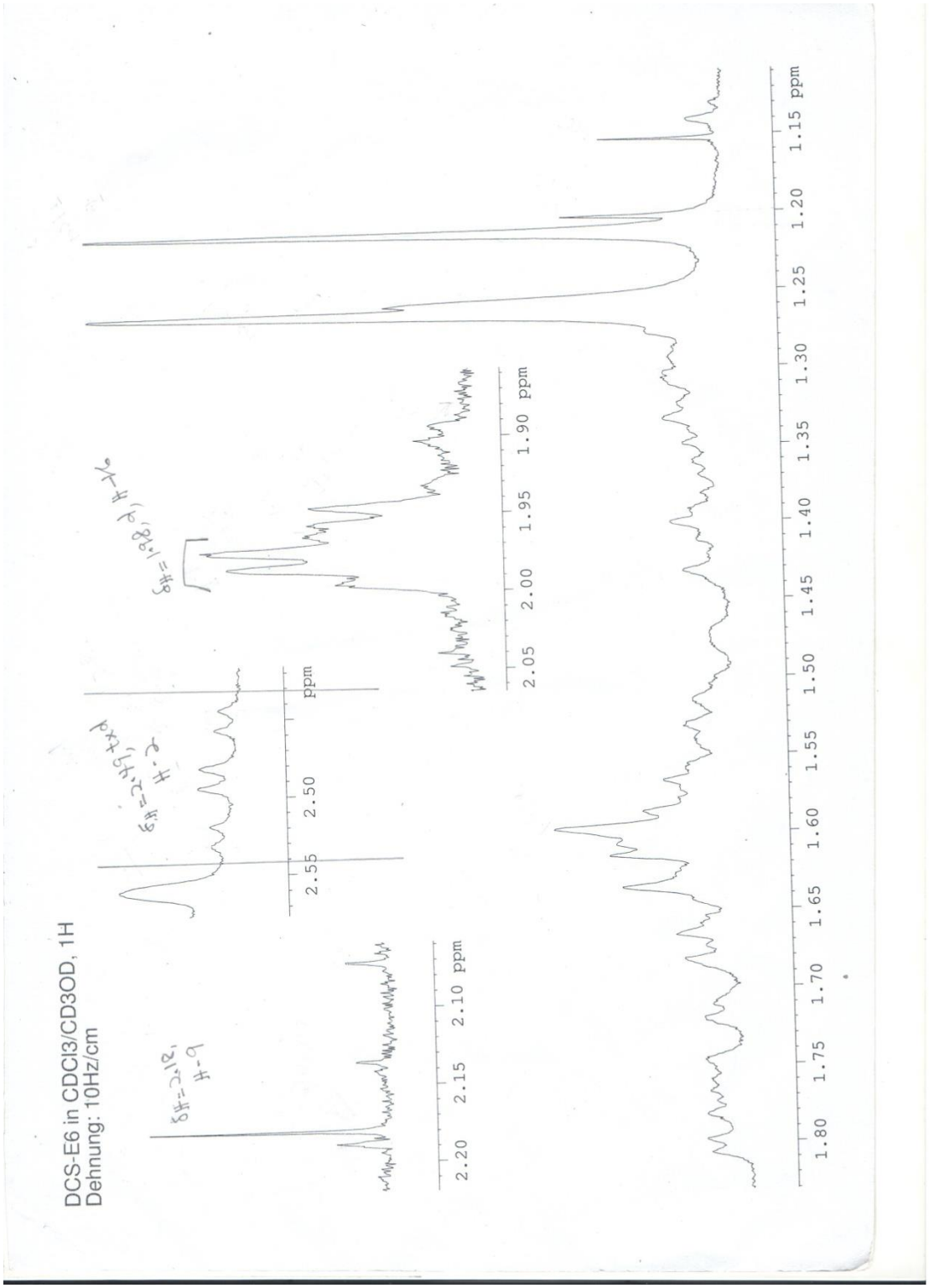

Figure 11b: Expanded ^{1}H NMR of DCS-E6.

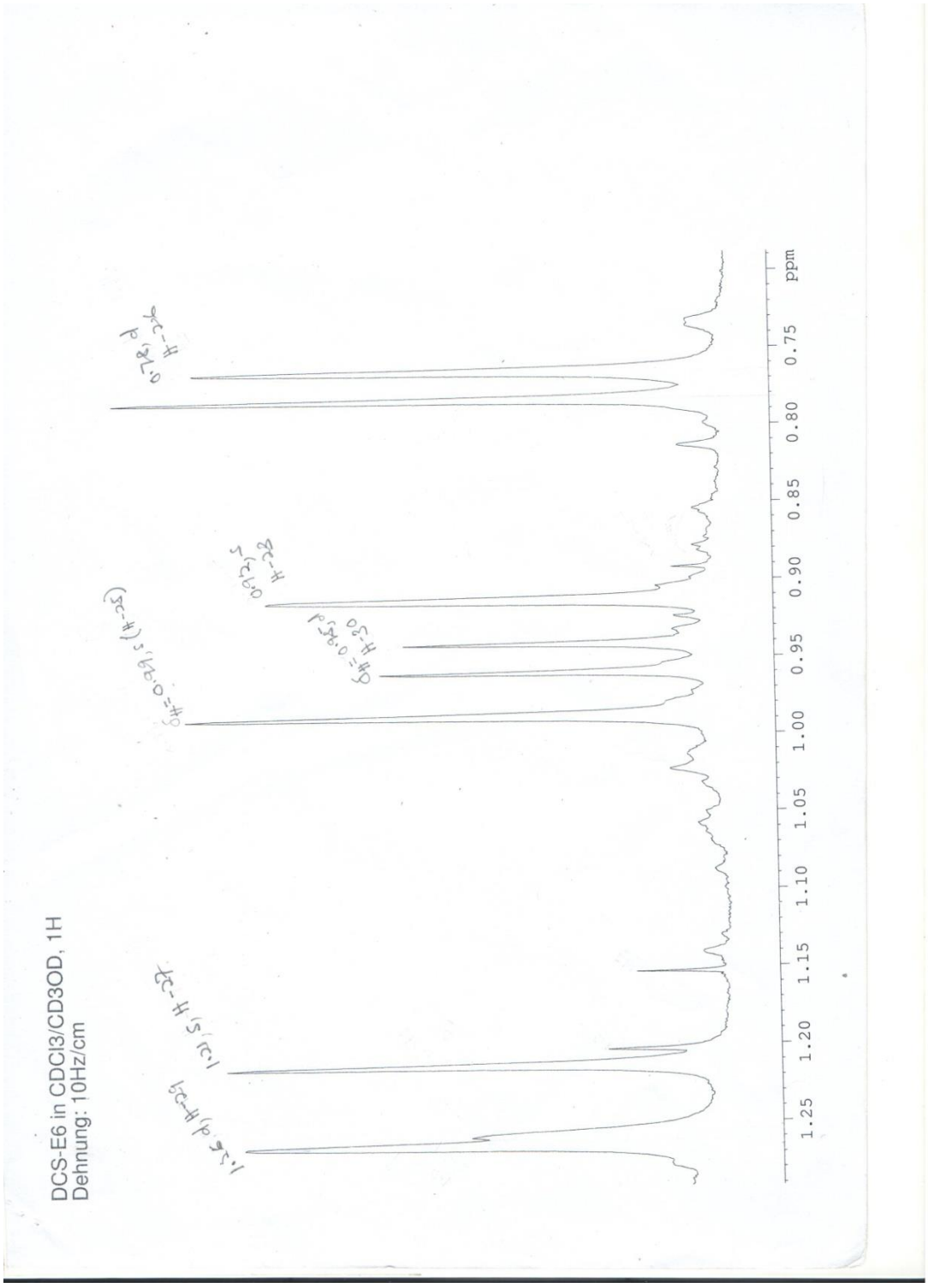

Figure 11c: Expanded ^{1}H NMR of DCS-E6.

Literature is replete with several biological activity studies on pomolic acid (PA). For instance, PA isolated from the methanolic extract of *Planchonella duclitan* (Blanco) by Tzoug-Huei[98] *et al* demonstrated cytotoxicity towards human colorectal carcinoma cell line HT29 and human breast carcinoma cell line MCF-7. They recorded IC_{50} (µM) values of 24.1 ± 4.2 and 32.4 ± 3.8 for PA towards HT29 and MCF-7 respectively, after treating the cells with different concentration of the test compounds over 72hr period. Also, Wu X-D[99] *et al* have reported the moderate cytotoxic activity of PA towards HL 60, SMMC-7721, A-549, MCF-7 and SW480 cell lines using the MTT method. PA has also shown apoptotic and anti-proliferative properties against leukemia cell line HL-60, human gastric adenocarcinoma MK-1, human uterine carcinoma HeLa and murine melanoma B16F10 cells[100,101].

Kuang[102] and co-workers have investigated the *in vitro* α-glucosidase inhibitory effect of PA among other triterpenoids isolated from the roots of *Sanguisorba tenuifolia* var. Alba. From their results PA demonstrated moderate α-glucosidase inhibitory effect with IC_{50} (mM ± SEM, mM) value of 1.84 ± 0.12. They therefore concluded that these '*triterpenoids of the EtOAc-soluble fraction may be the potential anti-hypoglycemic agents in the plant as they have been shown to induce an anti-diabetic effect'*.

Among nine triterpene acids isolated from the ethanol extract of the leaves of *Perilla frutescens*, Banno[103] *et al* investigated the anti-inflammatory effect of PA (in addition to anti-tumor promoting effects). After evaluating the anti-inflammatory effect of PA with respect to 12-*O*-tetradecanoylphorbol-13-acetate (TPA)-induced inflammation (1µg/ear) in mice, they observed an inhibition of inflammation value of ID_{50} = 0.12mg/ear. Also Estrada[104] and co-workers have investigated the hypotensive and anti-platelets properties of pomolic acid on rats.

To my best of knowledge, this is the second time pomolic acid is being reported to have been isolated from the Dichapetalaceae even though the compound has been isolated from different plants families over the past years.

3.3.6 Purification and identification of dichapetalin M, DCS-E7

The solid DCS-E7 was isolated as a white amorphous solid from sub-fraction DCS-EAA4. The melting point recorded for DCS-E7 is 282-284^{o}C after recrystallization from a mixture of diethyl ether/chloroform (10/3). DCS-E7 stained violet on TLC when sprayed with either anisaldehyde or vanillin spray reagent in the following mobile phase compositions: petroleum ether/ethyl acetate (1:1), R_f = 0.74; petroleum ether/acetone/chloroform (7:5:5), R_f = 0.76; diethyl ether/acetone (7:3), R_f = 0.78; petroleum ether/acetone (10:8), R_f = 0.82. Comparable R_f values were obtained for DCS-E7 and a reference sample, dichapetalin M[12] in the above solvent systems. The melting point of the reference sample was 280-282^{o}C, comparable to that of DCS-E7. The IR data for both compounds (shown in Table 3.7) were also comparable especially in the fingerprint region except for the presence of a broad peak at 1618.38cm^{-1} of small intensity in the IR spectrum obtained for DCS-E7. The identity of DCS-E7 was further supported by comparing the ^{1}H and ^{13}C-NMR data with that of the reference sample.

TABLE 3.7: Infrared data of DCS-E7 compared to that of a reference, dichapetalin M.

IR (*KBr*) ν_{max} cm^{-1} DCS-E7	Peak intensity	IR (*KBr*) ν_{max} cm^{-1} Dichapetalin M[12]	Peak intensity	Interpretation
2976.95, 2943.43, 2882.64	Strong	2919, 2853	Strong	C-H stretching vibration of alkanes
1770.96, 1750.12, 1699.79	Strong	1772, 1751, 1701	Strong	C=O stretch of lactone, ester and α-hydroxy ketone
1368	Strong	1367	Strong	C-H bend for alkanes

1246	Strong	1244	Strong	O-H bending vibration of alcohol
1098.27, 1039.35	Strong	1096.4, 1039.4	Strong	C-O-C bending vibration of ether
694.96	Variable	691.1	Variable	$-C_6H_5$ bending vibration

The ^{13}C-NMR (and ^{1}H NMR, Table 3.8) spectrum for dichapetalin M showed a total of 38 signals from δ_C 14.4 to 213.7. The α-hydroxy ketone at C-7 (with a corresponding IR band at 1699.79cm^{-1}) resonated at a frequency of 213.7 and the signal at δ_C 174 was assigned to the carbonyl carbon, C-21, of the lactone ring. The following signals were recorded for the carbons of the benzene ring; δ_C 142.5 (C-1''), 128.4 (2''/6''), 125.8 (3''/5'') and 127.4 (4''). The alkenic carbons were assigned the following signals; 116.3 (C-2), 141.3 (C-3), 120.1 (C-11) and 131.6 (C-12).

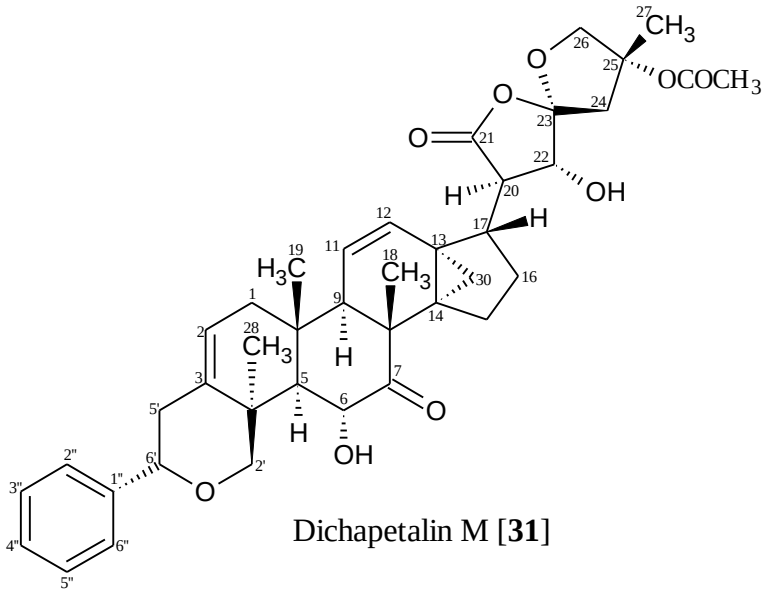

Dichapetalin M [**31**]

Seven sp^3-hybridized carbons occurred downfield due to the deshielding effect of the oxygen atom attached to them. They are; δ_C 111.3 (C-23), 85.5 (C-25), 81.3 (C-6'), 78.5 (C-26), 72.1 (C-22) and 71.3 (C-6/2'). The spirocyclic ring carbon, C-23, has two deshielding oxygen atoms attached

to it and the downfield chemical shift observed for C-25 is as a result of the electronegative acetoxy group attached to it. The downfield chemical shift observed for C-6' is due to the attached benzene ring and the oxygen atom.

The remaining twenty signals between δ_C 14.4-59.1 are for methyl, methylene and methane carbons. The following chemical shifts were assigned to the methyl carbons; δ_C 17.1 (C-18), 18 .2 (C-19), 22.0 (C-27), 26.7 (C-28) and 21.8 ($AcCH_3$). All the remaining signals agreed well with literature data and the recorded melting point of 282-284^{o}C for DCS-E7 further supports its identity as dichapetalin M.

Table 3.8: Comparison of ^{1}H and ^{13}C NMR data of DCS-E7 (dichapetalin M) with literature data

^{13}C No.	**DCS-E7 ($CDCl_3$)** δ_C/ppm	δ_H/ ppm	**Dichapetalin M ($CDCl_3$)[12,13]** δ_C/ ppm	δ_H/ ppm
1	40.1	2.2[a], 1.65[a], d, 3.1Hz	40.0	2.19[a], 1.64[a]
2	116.6	5.39, d, *J*= 4.8Hz	116.6	5.38, d, *J* = 7.0Hz
3	141.3	-	141.3	-
4	39.9	-	39.9	-
5	59.1	1.65[a]	59.1	1.64[a]
6	71.3	4.60, dd, J_1= 10.4Hz, J_2= 3.6Hz, 3.81(OH, d, *J* = 4.2Hz)	71.3	4.59,dd, J_1= 13.0Hz, J_2=4.5Hz, 3.79 (OH, d, *J*= 4.5)
7	213.7	-	213.7	-
8	47.1	-	47.0	-
9	52.1	-	52.1	1.97[a]
10	36.9	-	36.9	-
11	120.1	5.41	120.1	5.41, dd, J_1= 10, J_2= 2.5Hz
12	131.6	6.33, dd, J_1= 8.3Hz, J_2= 4.3Hz	131.6	6.33, dd, J_1= 10, J_2= 3Hz
13	31.6	-	31.6	-
14	36.5	-	36.5	-
15	26.7	1.99[a], 2.2[a]	26.7	1.99[a], 2.19[a]
16	23.6	1.78, m	23.7	1.32, 1.76, m
17	40.5	2.55, m	40.5	2.55, m
18	17.1	1.23, s	17.1	1.21, s
19	18.2	1.35, s	18.2	1.34, s
20	47.3	2.96, dd, J_1= 8.3Hz, J_2= 4.1Hz	47.3	2.96, dd, J_1= 10, J_2= 5.5Hz
21	174.0	-	174.0	-
22	72.1	4.18, d, 8.3Hz, 2.46 (OH, d, 8.3Hz)	72.1	4.18, dd, J_1= 10Hz, J_2 = 10Hz, 2.45 (OH, d, *J* = 10.0Hz)

23	111.3	-	111.3	-
24	45.7	2.86, 2.52, d, *J*= 16.7Hz	45.7	2.86, 2.50, d, *J* = 15.0Hz
25	85.1	-	85.1	-
26	78.5	4.32, d, *J*= 8.3Hz, 3.98, d, *J*=8.3Hz	78.5	4.33, d, *J* = 10Hz, 4.09, d, *J* = 10Hz
27	22.0	1.70, s	22.0	1.70, s
28	26.7	1.54, s	26.6	1.53, s
30	14.4	1.28, d, *J* = 8.3Hz, 1.02, d, *J*=8.3Hz	14.4	1.28, d, *J* =6.0Hz, 1.02,d, *J*=6.0Hz
2'	71.3	4.32, 3.92, d, 8.3Hz	71.3	4.32, 3.92, d, *J* = 10.0Hz
5'	40.1	2.70, t, *J*= 11.4Hz, 2.25,dd, J_1 = 11.4Hz, J_2 = 2.1Hz	40.1	2.69,t_{br}, *J* = 13.5Hz, 2.25,dd, J_1= 13.5, J_2 = 2.5Hz
6'	81.3	4.36[a]	81.3	4.34, dd, J_1 = 11.5, J_2 = 2.5Hz
1"	142.5	-	142.5	-
2''/6''	128.4	7.41, d, *J*=3.6Hz	128.4	7.40, d, *J* = 7.5Hz
3''/5''	125.8	7.35, t, *J*= 3.6Hz	125.8	7.35, t, *J* = 7.5Hz
4''	127.4	7.28, t, *J*= 3.6Hz	127.5	7.28, t, *J* = 7.5Hz
AcCO	170.4	-	170.4	-
$AcCH_3$	21.8	2.06,s	21.8	2.08, s

[a] Overlapping signals

Dichapetalin M was first isolated in 2008 from the roots of *D. Madagascariense*[13] and roots of *D. eickii*[16] in 2013. In a brine shrimp bioassay its measured cytotoxicity of LC_{50} = 0.011µg/ml was approximately 200-fold more potent than podophyllotoxin[45]. Long[16] *et al* have revealed dichapetalin M as the most potent cytotoxic member of the dichapetalins, recording cytotoxic activities of EC_{50} = 0.007µg/ml on HCT116 and EC_{50} = 0.05µg/ml on WM 266-4 cell lines respectively.

3.3.7 Purification and identification of Maslinic Acid, DCS-E8

The solid DCS-E8, white and powdery in appearance with a melting point of 256-258°C was isolated from sub-fraction DCS-EAA4 and was recrystallized from a mixture of chloroform/acetone (2:5). DCS-E8 stained purple with anisaldehyde spray reagent on TLC run in the following solvent systems: petroleum ether/ethyl acetate (1:1), R_f = 0.43; petroleum ether/acetone/chloroform (7:3:3), R_f = 0.54; diethyl ether/acetone (7:3), R_f = 0.78; petroleum

ether/acetone (10:8), R_f = 0.78. The IR data recorded for DCS-E8 showed peaks at 3443.97 cm^{-1} (O-H stretching vibrations), 2941.14 cm^{-1} (C-H stretching vibration), 1692.67 cm^{-1}(C=O stretching vibration, 1461.82 and 1385.04 cm^{-1} (C-H asymmetric bending vibration), 1270.26 cm^{-1} (C-O-H bending vibration) and 1051.37cm^{-1} (C-O stretching vibration) .

The ^{13}C NMR spectrum obtained for DCS-E8 (Table 3.9) confirmed the presence of 30 carbons consisting of three sp^2 hybridized-carbons (two of the alkene type and one C=O) and two sp^3-hybridized carbons attached to hydroxyl groups. The other twenty-five carbons are six sp^3-hybridized quaternary, seven methyl, nine methylene and three methine carbon signals.

The signal at δ_C 180.8 was assigned to the carboxyl group at C-28 (Maslinic acid [**91**]) which is further supported by the strong C=O stretching vibration band (1692.67 cm^{-1}) recorded in the IR spectrum of DCS-E8 for carboxylic acid. The signals at δ_C 122.2 and 144.1 were assigned to C-12 and C-13 respectively as these downfield shifts are expected for sp^2-hybridized carbons of the alkene type, while the values at δ_C 68.8 and 83.7 were assigned to C-2 and C-3 respectively. Even though C-2 and C-3 are sp^3-hybridized, the observed downfield shift is due to their attachment to the electronegative hydroxyl groups.

The following chemical shifts were assigned to the methyl carbons; δ_C 28.7 (C-23), 16.6 (C-24), 16.8 (C-25), 17.0 (C-26), (C-27), 32.7 (C-29) and 23.6 (C-30). The signal at δ_C 46.5 was assigned to C-17 (downfield due to the electronegative COOH group) and the signal at δ_C 49.0 was assigned to C-9, which is downfield compared to the signal at δ_C 41.3 (C-18) supposedly due to the electronegative hydroxyl groups on the ring adjacent to C-9.

From the ^1H NMR spectrum recorded for DCS-E8 (in CDOD/$CDCl_3$), the signal at δ_H 5.26 (1H) was assigned to H-12 on the sp^2-hybridized carbon, C-12. The signal at δ_H 2.83(1H, dd, J_1 = 6Hz,

J_2 = 13Hz) was assigned to H-18, the signal at δ_H 3.66 (1H, td) was assigned to H-2. The observed multiplicity is due to first coupling of the signal to the methylene protons at H-1, then each signal of the resulting triplet split further into a doublet by the methine proton at H-3. The downfield chemical shift of 3.66 (for a proton bonded to sp^3-hybridized carbon) indicates the presence of electronegative bonded groups. The signal at δ_H 3.45 was assigned to H-3.

The signal at δ_H 1.95 (2H, ddd, J_1 = 11.6Hz, J_2 = 9.6Hz, J_3 = 9.6 Hz) was assigned to H-16 and the signal at δ_H 1.90 (1H, dd, J_1 = 4.2, J_2 = 7.8) was assigned to H-9 while the signal at δ_H 1.61 (2H, dd, J_1= 11.3, J_2 = 11.3 Hz) was assigned to H-11.

Finally the following chemical shifts were assigned to the methyl protons; δ_H 1.14 (3H, s, H- 27), 1.02 (3H, s, H-23), 0.98 (3H, s, H-25), 0.93 (3H, s, H-30), 0.90 (3H, s, H-29), 0.81 (3H, s, H-26) and 0.78 (3H, s, H-24).

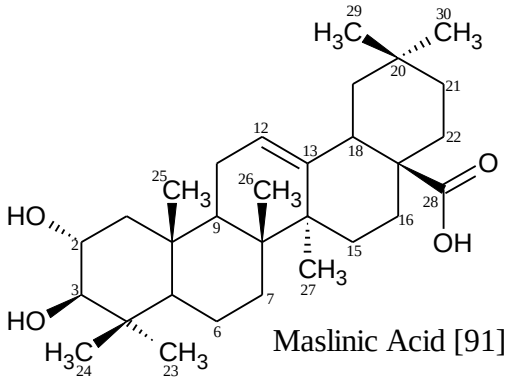

Maslinic Acid [91]

The figure (Figure 12) below presents part of the expanded ^{1}H NMR spectrum recorded for DCS-E8.

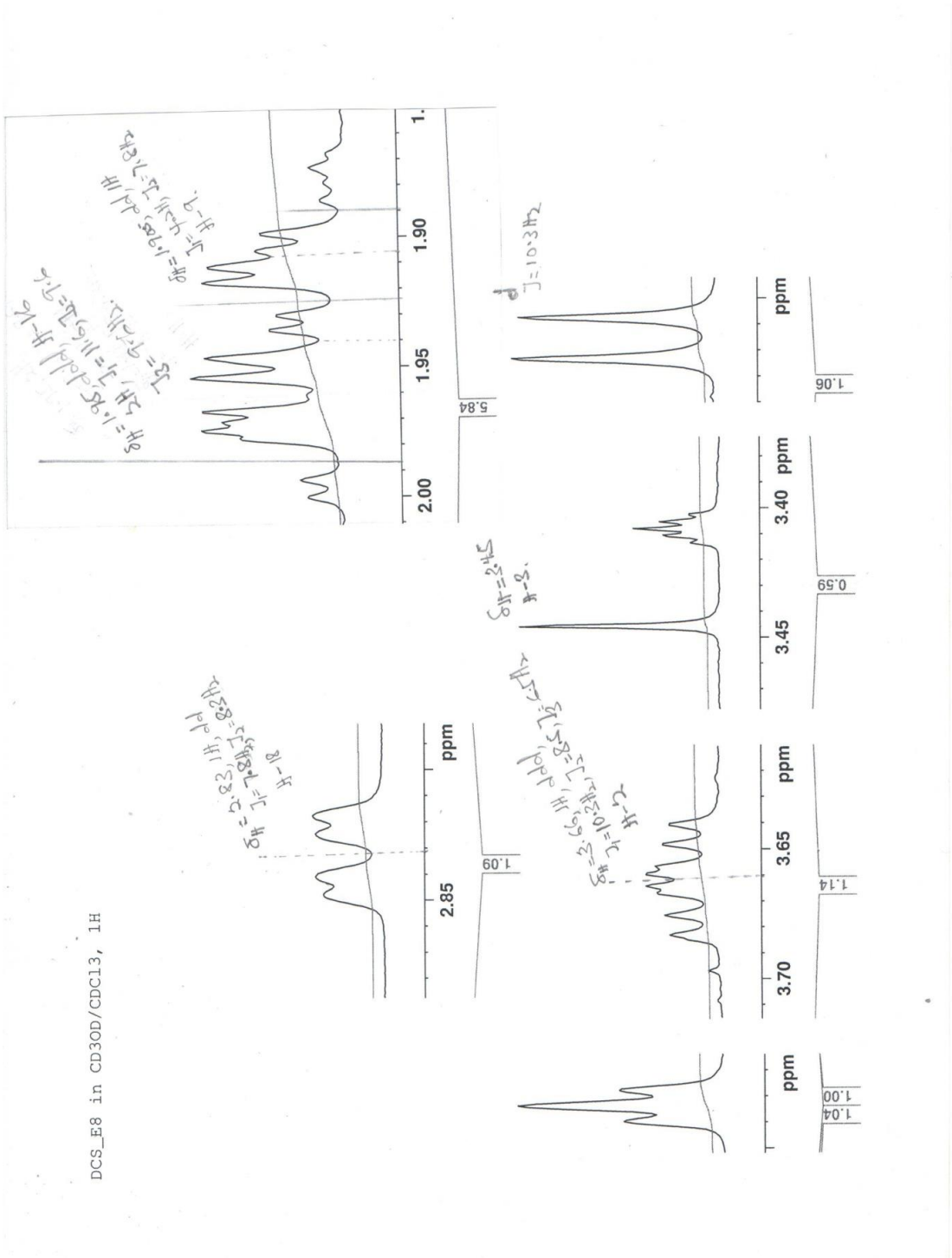

Figure 12: Expanded ^{1}H NMR of DCS-E8

Table 3.9: ^{1}H and ^{13}C Chemical Shifts of DCS-E8 (Maslinic acid) and reference data.

^{13}C No.	DCS-E8 (in $CD_3OD/CDCl_3$)		Literature data of Maslinic Acid (in CD_3OD)[105]	
	δ_C/ppm	δ_H/ppm	δ_C/ppm	δ_H/ppm
1	47.7		48.2	-
2	68.8	3.66 (1H, ddd, J_1= 10.3, J_2= 8.5, J_3= 6.5 Hz)	69.5	3.62 (1H, ddd, J_1 = 11.3, J_2 = 9.6, J_3 = 4.5)
3	83.7	3.45(1H, d, 10.3Hz)	84.4	2.91(1H, d, J = 9.6)
4	39.3	-	40.5	-
5	55.4	-	56.7	-
6	18.5	--	19.6	-
7	32.7	-	33.9	-
8	39.4	-	40.6	-
9	49.0	1.90 (1H, dd, J_1=4.2, J_2= 7.8Hz)	49.3	1.70 (1H, dd, J_1= 14.0, J_2 = 14.0Hz)
10	38.3	-	39.3	-
11	23.6	1.61 (2H, dd, J_1 = 11.3, J_2= 11.3Hz)	24.7	-
12	122.2	5.26	123.5	5.26 (1H, dd, J_1 = 3.5, J_2 = 3.5)
13	144.1	-	145.4	-
14	42.0	-	42.8	-
15	27.8	-	28.8	-
16	23.1	1.95(2H, ddd, J_1=11.6, J_2=9.6,J_3= 9.6 Hz	24.0	2.02 (2H, ddd, J_1 = 13.3, J_2 = 13.3, J_3 = 3.9)
17	46.5	-	47.7	-
18	41.3	2.83 (1H, dd, J_1= 7.8, J_2=8.3	42.8	2.86 (1H, dd, J_1 = 14.1, J_2 = 3.9)
19	46.3	-	47.3	-
20	30.8	-	31.7	-
21	34.0	-	35.0	-
22	33.2	-	33.9	-
23	28.7	1.02 (3H, s)	29.3	1.02 (3H, s)
24	16.6	0.78 (3H, s)	17.1	0.81 (3H, s)
25	16.8	0.98 (0.98)	17.5	1.01 (3H, s)
26	17.0	0.81 (3H, s)	17.8	0.82 (3H, s)
27	26.0	-	26.4	-
28	180.8	-	181.9	-
29	32.7	0.90 (3H, s)	33.6	0.91 (3H, s)
30	23.6	0.93 (3H, s)	24.1	0.95 (3H, s)

Maslinic acid (also called crategolic acid) or (2α, 3β)-2, 3-dihydroxyolean-12-en-28-oic acid is widely distributed in natural plant sources. A number of researchers have assessed the biological activities of maslinic acid using different experimental modules and these have proved that maslinic acid exerts anti-tumor, anti-diabetic, anti-oxidant, cardioprotective, anti-HIV, neuroprotective, anti-parasitic and growth-stimulating effects[106].

Rufino-Palomares[107] and co-workers have investigated the mechanism of maslinic acid with respect to its inhibitory effects on the growth of HT29 colon-cancer cells. Their result indicated that '*treatment with maslinic acid resulted in a significant inhibition of cell proliferation in a dose-dependent manner and causes apoptotic death in colon-cancer cells.* They found out *that maslinic acid inhibits considerably the expression of Bcl-2 whilst increasing that of Bax; it also stimulates the release of mitochondrial cytochrome-c and activates caspase-9 and caspase-3'.* According to them, '*all these results points clearly to the activation of the mitochondrial apoptotic pathway in response to the treatment of HT29 colon-cancer cells with maslinic acid'*.

Lozano-Mena[106] *et al* have recently comprehensively reviewed several researches relating to the biological importance of maslinic acid and '*their results provide evidence of the potential of maslinic acid as a nutraceutical, not only for health promotion, but also as a therapeutic adjuvant in the treatment of several disorders'.*

Even though maslinic acid has been isolated from several other plants families, this current investigation reports for the first time, the isolation of this pentacyclic triterpene from the family of Dichapetalaceae.

Even though the solid DCS-EM was isolated from this sub-fraction (DCS-EAA4), it was not pure and several TLCs run alongside the solids DCS-E6, DCS-E7 and DCS-E8 in the different solvent

systems indicated that DCS-EM is a mixture of pomolic acid, dichapetalins M and maslinic acid. The melting point was determined to be 253-265^{o}C. No attempt was made to purify it after a few trials proved futile.

3.3.8 Purification and isolation of DCS-E9, DCS-E10 and DCS-E11

Sub-fraction DCS-EAA5 was partitioned into four fractions; F018-F025, F028-F033, F036-F041 and F043-F048. The solid DCS-E9 was obtained from fraction F028-F033 after washing with diethyl ether. The solid was filtered off, dried and melting point measured to be 116-119^{o}C. DCS-E9 stained pink with anisaldehyde on TLC run in petroleum ether/ethyl acetate (1:1), R_f = 0.16; petroleum ether/acetone/chloroform (7:5:5), R_f = 0.17; petroleum ether/acetone (10:8), R_f = 0.32; petroleum ether/ethanol (10:2), R_f = 0.45. The IR data obtained for DCS-E9 showed significant peaks at 3433.97cm^{-1} (strong, broad) for O-H stretching vibration of alcohol , 2918.33, 2849.26cm^{-1} (strong, sharp) for C-H stretching vibration of alkanes , 1622.62cm^{-1} (strong) for C=O stretching vibration of ester and 1467.12 and 1384.51 cm^{-1}(CH_2, CH_3 bending vibration of alkanes) and 1121.71cm^{-1} for CO-O bending vibrations. Initial ^{13}C-NMR obtained for DCS-E9 predicted it to be a fatty acid, but due to the impure nature and paucity of the material, no further data was obtained to fully identify DCS-E9.

The solid DCS-E10 (5mg, 4 spots) was obtained from the fraction F036-F041 via triturating with ethyl acetate. The solid stained with iodine but not with anisaldehyde spray reagent and it was whitish and powdery in appearance. The melting point was determined to be 124-137^{o}C. No other data was obtained for this solid due to its impure nature and paucity of material.

After eluting DCS-EAA6 with 50% ethanol solution, the resulting fractions were colloidal in nature making separation of solute impossible. Upon the addition of small amount of 0.1M HCl,

the solute coagulated. The solute was filtered, dried to afford DCS-E11; brown in appearance and soluble only in chloroform/ethanol mixtures with a melting point of 175-178^{o}C. On TLC in solvent systems with polarities close to 100% ethanol, it appeared as a streak and stained yellow to brown with anisaldehyde spray reagent. The IR data recorded revealed strong and broad peaks at 3390.53cm^{-1} for O-H stretch, 2920.13, 2850.01cm^{-1} for C-H stretch, 1653.30cm^{-1} for C=O stretch, and peak at 1515.18cm^{-1} for C=C aromatic. No further data was obtained on DCS-E11 due to its impure nature.

3.4 *In Vitro* Screening of the crude extracts, Friedelan-3-one, a mixture of β-Sitosterol and Stigmasterol, and dichapetalin M For Anti-Schistosomal Activity.

Schistosomiasis is a neglected tropical parasitic disease caused by trematode parasites of the genus *Schistosoma* and affects several millions of people worldwide. Due to its widespread usage over the past four decades, there has been reported incidence of resistance of field and laboratory strains of *Schistosoma* against praziquantel, the only drug of choice for schistosomiasis treatment. Hence, the search for new and safe anti-schistosomal agents has intensified more recently. In the light of recent investigations suggesting that the dichapetalins have broad spectrum of biological activities[18] coupled with the urgent need of potential anti-schistosomal agents, the crude extracts (petroleum ether, ethyl acetate and methanol extracts) as well as three isolates; friedelan-3-one, mixture of β-sitosterol and stigmasterol, and dichapetalin M from the stem of *D. crassifolium* were screened for their anti-schistosomal activities.

The six samples with unknown anti-schistosomal activities were tested against field isolates of human *Schistosoma eggs* to ascertain their ovicidal properties. Thus, the *in vitro* anti-schistosomal activities of the test samples were carried out using the ovicidal method (Egg Hatch Assay, EHA)

with praziquantel as the standard drug. Field isolates of human *Schistosoma* eggs were obtained after extracting them from urine samples collected from 120 participants at Tomefa, a rural community in the Ga West District around the Weija dam in the Greater-Accra Region of Ghana. Over 80% of the participants were school children aged between 8 and 14years. The modified Kotze[108] *et al* technique was employed to identify, purify and extract the eggs from 4L of urine sample at the Noguchi Memorial Institute of Medical Research.

The *in vitro* anti-schistosomal activity test was conducted in 96 well-plates. EHAs were set up by plating the purified egg suspension (50µl containing approximately 25 eggs) in a 96-well plate. Stock solutions were prepared (2mg/ml for each isolate and 5mg/ml for each crude extract) in DMSO for each test sample and by serial dilution (dilution factor = 0.5), different concentrations were prepared to the 7th well for each test sample. To each well already containing the egg solution, 50µl of test sample solution was added. The tests were conducted in duplicates. Water and praziquantel (2mg/ml stock solution) were used as negative and positive controls respectively. The plates were incubated at room temperature for 24 hrs after which eggs and unhatched eggs were counted using inverted light microscope and the percent egg hatch 100µl of formalin was added to each well to stop the hatching process. The number of hatched (larvae) inhibition calculated from the relation:

$$\%\ \text{egg hatch inhibition (\%EHI)} = \frac{\#\ \text{unhatched}}{\#\ \text{unhatched} + \#\ \text{larvae}} \times 100$$

The %EHI was plotted against log of concentration. Extrapolation of the 50% EHI on the curve gave the half maximal inhibitory concentration (IC_{50}) of the test samples. The tables below (Table 3.10 A and B) present the %EHI of the test samples at the different concentrations.

Table 3.10A: %EHI recorded for the duplicate test at different concentrations of extracts, pure compounds and standard, praziquantel.

% EHI						
Extracts						
Concentration µg/ml	Petroleum Ether		Ethyl Acetate		Methanol	
5000	83.3	87.5	92.8	100	100	100
2500	87.5	75	100	100	100	100
1250	66.7	83.3	78.6	87.5	66.7	66.7
625	66.7	75	83.3	66.7	53.8	47.6
312.5	23.0	25.0	33.3	54.5	14.3	33.3
156.25	40.0	36.4	44.4	50.0	16.7	0
78.125	14.3	14.3	50.0	41.7	16.7	25

Pure Compounds

Concentration µg/ml	Friedelan-3-one		Stigmasterol/Sitosterol		Dichapetalin M	
2000	100	100	75	100	66.7	66.7
1000	80	80	72.7	72.7	75	66.7
500	66.7	50	83.3	66.7	50	50
250	50	66.7	66.7	75	54.5	47.6
125	16.7	0	44.0	0	38.5	0
62.5	0	25	25	25	14.3	0
31.25	0	14.3	0	11.1	0	16.7

Praziquantel

Concentration µg/ml		
2000	100	100
1000	100	100
500	100	100
250	100	83.3
125	83.3	83.3
62.25	90	77.8
31.125	76.9	75.0

Table 3.10B: *In vitro* average % EHI values at different concentrations of extracts, pure compounds and praziquantel. Data are mean ± SEM.

Mean % EHI			
Extracts			
Concentration µg/ml	Petroleum Ether	Ethyl Acetate	Methanol
5000	85.4 ± 2.1	96.4 ± 5.4	100 ± 0.0
2500	81.3 ± 6.3	100 ± 0.0	100 ± 0.0
1250	75.0 ± 5.8	83.1 ± 4.5	66.7 ±0.0
625	70.6 ± 3.9	75.0 ± 8.3	50.7 ± 2.9
312.5	24.0 ± 1.0	43.9 ± 10.6	23.8 ± 9.5
156.25	38.2 ± 1.7	47.2 ± 2.8	8.4 ± 4.0
78.125	14.3 ± 0.0	45.9 ± 6.2	20.9 ± 3.7

Pure Compounds			
Concentration µg/ml	Friedelan-3-one	Stigmasterol/Sitosterol	Dichapetalin M
2000	100 ± 0.0	87.5 ± 12.5	66.7 ± 0.0
1000	80.0 ± 0.0	72.7 ± 0.0	70.9 ± 4.2
500	58.4 ± 8.4	75.0 ± 8.3	50.0 ± 0.0
250	58.4 ± 8.4	70.9 ± 4.2	51.1 ± 3.4
125	8.4 ± 4.2	22.2 ± 11.1	19.3 ± 9.7
62.5	12.5 ± 6.3	25.0 ± 0.0	7.2 ± 3.6
31.25	7.20 ± 3.6	5.6 ± 2.8	8.4 ± 4.2

Praziquantel	
Concentration µg/ml	
2000	
1000	100 ± 0.0
500	100 ± 0.0
250	91.7 ± 8.4
125.25	83.3 ± 0.0
62.5	83.9 ± 6.1
31.25	76.0 ± 1.0

Generally, the %EHI increased steadily with increasing concentration of test sample, thus the %EHI was concentration-dependent. At a concentration of 1250 µg/ml, all the crude extracts exhibited %EHI > 50% with the ethyl acetate extract showing the highest %EHI of 83.3. The observed %EHI for the ethyl acetate and methanol extract were the same (100%) at a concentration of 2500µg/ml. The ethyl acetate extract demonstrated higher inhibition activity between the concentrations of 78.125-312.5µg/ml compared to the methanol extract. The petroleum ether extract showed %EHI of 85.4 at a concentration of 5000µg/ml and after two serial dilutions to a concentration of 1250µg/ml, it recorded %EHI of 75.0, higher than that of the methanol extract at the same concentration.

Among the isolates, friedelan-3-one showed %EHI of 100% at a concentration of 2000µg/ml, comparable to that of the standard, praziquantel, at the same concentration. At this same concentration (2000µg/ml), the %EHI recorded for β-sitosterol/stigmasterol was 87.5, whiles dichapetalin M exhibited %EHI of 66.7. All the isolates showed %EHI > 70% at a concentration of 1000µg/ml. The observed %EHI for friedelan-3-one at 1000 µg/ml was 80%, then after dilution to 500 µg/ml, the %EHI was 58%. Praziquantel exhibited the same %EHI of 100% at concentrations of 1000 and 500 µg/ml. At a concentration of 250µg/ml, the %EHI of β-sitosterol/stigmasterol was 70.9 whiles that of friedelan-3-one was 58.4, that of dichapetalin M was 51.1 and that observed for praziquantel was 91.7.

Furthermore, between concentrations of 125-62.5µg/ml, the β-sitosterol/stigmasterol mixture was more potent than friedelan-3-one and dichapetalin M. The standard, praziquantel, was still significantly active at lower concentrations compared to the isolates and crude extracts.

The calculated IC_{50} values for the test samples are presented in Table 3.10C below.

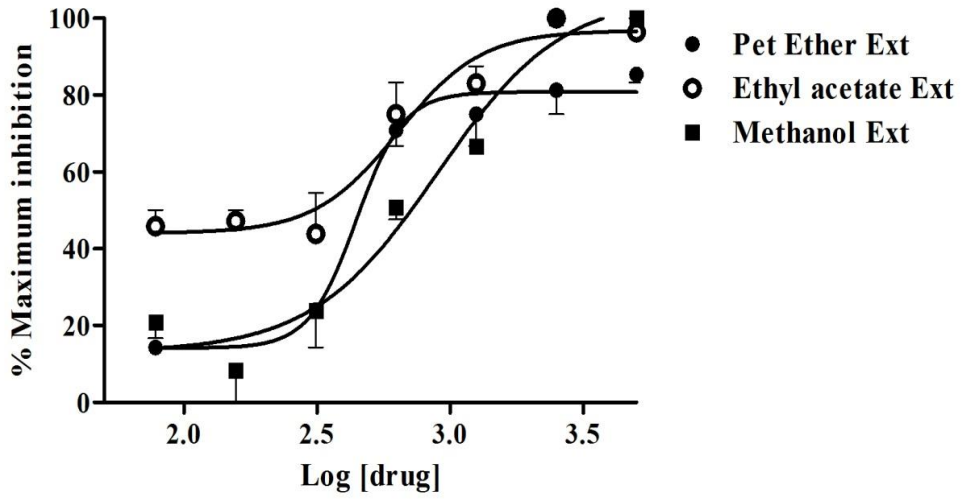

Figure 13: Concentration-dependent effect of Petroleum ether, Ethyl acetate and Methanol extracts of the stem of *D.crassifolium* on the egg hatching of *Schistosoma* species (*S. mansoni and S. haematobium*) Each point is mean ± S.E.M (n=2).

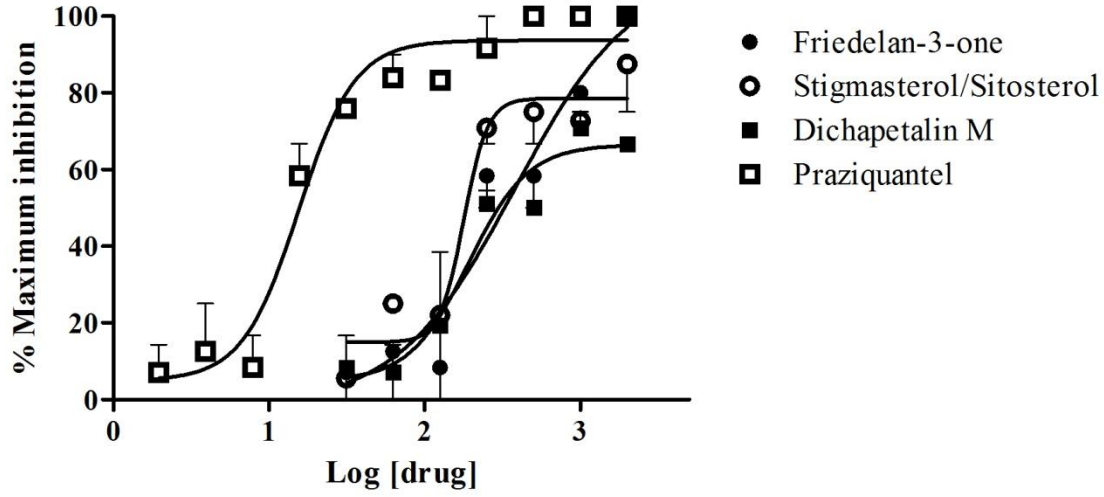

Figure 14: Concentration-dependent effect of isolates; friedelan-3-one, stigmasterol/sitosterol and dichapetalin M from the stem of *D.crassifolium* and standard, praziquantel, on the egg hatching of *S. mansoni and S. haematobium* species. Each point is mean ± S.E.M (n=2).

Table 3.1C: *In vitro* half maximal inhibitory concentration (IC_{50}) of the test samples

Test Sample	**IC_{50} (µg/ml) ± S.E.M**
Crude Extracts	
1. Petroleum Ether	443.70 ± 0.04
2. Ethyl Acetate	638.00 ± 0.08
3. Methanol	893.70 ± 0.08
Isolates	
4. Friedelan-3-one	378.10 ± 0.23
5. β-sitosterol/stigmasterol	177.90 ± 0.10
6. Dichapetalin M	191.00 ± 0.12
Standard	
7. Praziquantel	15.47 ± 0.06

Analysis from the GraphPad Prism graphs above (Figures 13 - 14) of the half maximal inhibitory concentration IC_{50} of the isolates gave the most effective inhibitory agent to be the mixture of β-sitosterol/stigmasterol, with an IC_{50} value of 177.9 ± 0.10 µg/ml followed by dichapetalin M with an IC_{50} value of 191 ± 0.12 µg/ml. Friedelan-3-one recorded an IC_{50} = 378.1 ± 0.23 µg/ml. The calculated IC_{50} for the standard praziquantel was 15.47 ± 0.06 µg/ml. Hence, the results show that praziquantel still remains a potent anti-schistosomal agent.

The crude extracts; petroleum ether, ethyl acetate and methanol showed IC_{50} values of 443.7 ± 0.04, 638.0 ± 0.08 and 893.7 ± 0.08 µg/ml respectively. Thus, the petroleum ether crude extract exhibited the most effective *in vitro* ovicidal activity in the study among the crude extracts.

Even though the ethyl acetate extract produced the compounds that exhibited high EHI activity - β-sitosterol/stigmasterol and dichapetalin M, it was not as active as the petroleum ether extract,

which yielded only the less active friedelins. Possibly, the presence of polar constituents such as tannins in the ethyl acetate fraction as indicated in the phytochemical screening did not enhance its ovicidal activity. Also there may be poor synergistic effect among the constituents of the ethyl acetate extract, including the mixture of β-sitosterol and stigmasterol, and dichapetalin M. The methanol extract which contains mainly tannins showed the poorest activity suggesting that tannins may not influence the observed egg hatching activity.

Previous investigations have confirmed the anti-schistosomal potencies of other terpenoids like phytol, where a reduction in egg-laying was observed at 25 µg/ml in *S. mansoni* worms[69], also nerolidol[71], where 100% mortality was observed in male and female adult worms at concentrations of 31.2 and 62.5µM respectively, and the effect of (+)-limonene epoxide on *S. mansoni* adult worms at a concentration of 25 µg/ml was similar to that of praziquantel, with reduction and mortality of all worms after 120hrs[109].

3.5 CONCLUSION

In the present study, the stem of *D. crassifolium* was investigated. The petroleum ether extract yielded friedelan-3-one, friedelan-3β-ol and a mixture of friedelan-3-one and friedelan-3β-ol. The ethyl acetate extract yielded pomolic acid, dichapetalin M and maslinic acid as well as the friedelins and a mixture of β-sitosterol and stigmasterol. No solid was isolated from the methanol extract. These compounds were identified and characterized using comparative thin-layer chromatography, comparative melting point, mixed melting point, IR, ^{1}H and ^{13}C NMR spectroscopy.

The crude extracts as well as some of the purified isolates were screened for their potential *Schistosoma* species (*S. mansoni* and *S. haematobium*) egg hatch inhibition activities. The

petroleum ether, ethyl acetate and methanol crude extracts gave IC_{50} values of 443.7 ± 0.04, 638.0 ± 0.08 and 893.7 ± 0.08 µg/ml respectively. Also among the tested isolates, friedelan-3-one, β-sitosterol/stigmasterol and dichapetalin M gave IC_{50} values of 378.1 ± 0.23, 177.9 ± 0.12 and 191.0 ± 0.12 µg/ml respectively. Hence among the crude extracts, the petroleum ether extract exhibited the most active egg hatch inhibition activity and also for the tested isolates, the mixture of β-sitosterol and stigmasterol was most active.

The observed egg hatch inhibition activity of the mixture of β-sitosterol/stigmasterol and dichapetalin M were about 11 and 12 fold respectively less active compared to that of the standard, praziquantel (IC_{50} = 15.47 ± 0.06 µg/ml), used in the study.

This study constitutes the first report of the chemical and biological investigation of the stem of *Dichapetalum crassifolium*. Maslinic acid is also reported for the first time from the *Dichapetalaceae*.

3.6 RECOMMENDATIONS

Further spectroscopy is recommended to elucidate the structures of the unknown solids; DCS-E5 and DCS-E9. The use of modern chromatographic methods must be employed such as reversed-phase and HPLC instead of the conventional normal phase liquid chromatography to isolate more of the compounds present in the plant in future investigations. This is very important since as evidenced from the TLC analysis the isolated compounds are not the only compounds present in the plant.

A comprehensive bioassay-guided isolation procedure should be adopted in order to extend the phytochemical and antimicrobial investigations and to ascertain the active phytochemicals present. Also, synergic effects among the crude extracts and isolated compounds should be investigated

and in future investigations, *in vivo* studies should be included to confirm the *in vitro* anti-schistosomal results.

CHAPTER FOUR

EXPERIMENTAL

4.1 Collection and Preparation of Plant Material

The plant material was collected from Kuntanase, a town located in the Ashanti Region of Ghana and identified as of *D. crassifolium* at the National Herbarium, Department of Botany (Specimen code: DCR001), University of Ghana. The stem was chopped into smaller pieces and air/shade dried for four weeks after which the dried material was milled.

4.2 General Experimental Procedure

Soxhlet extraction was used as the extraction method of the pulverized stem of the plant. The organic solvents used were petroleum ether (40-60^{o}C), ethyl acetate and methanol. Extraction was done for 24 hours continues for each solvent. The extracts, after each extraction cycle, were concentrated and dried under reduced pressure on Buchi Rotary Vacuum Evaporator and the recovered solvent used for the next extraction.

The main purification procedure used for the isolation of the phytochemicals of each extract was solid-liquid column chromatography using silica gel 60 (Fluka; particle size 0.063-0.2mm) as the stationary phase material. Employing gradient elution technique, chromatographing was started off with petroleum ether (40-60^{o}C) and the polarity of the mobile phase increased steadily until that mobile phase system which elutes the most polar constituents in the extract. Thin layer chromatography (TLC) using aluminium foil slides pre-coated with silica gel (0.2mm thick, Kiesegel 60 F_{254} Merck type) was employed to monitor the progress of the column

chromatographic separation and also to determine the purity of eluates. Where necessary, recrystallization with appropriate solvents was used for further purification of isolates.

Visualization of spots on TLC plates was by Ultraviolet (UV) light, iodine vapor, vanillin and anisaldehyde spray reagent. Melting points of pure isolates were determined with Stuart Scientific Melting Point Apparatus. Isolated known compounds were characterized by their appearance and retardation factor (R_f) on comparative TLC in different solvent systems with very different polarities and co-melting points. ^{1}H and ^{13}C Nuclear Magnetic resonance (NMR) data were obtained on 500MHz NMR spectrometer at the University of Erlangen, Germany. IR data was obtained on FT IR spectrometer at the Food and Drugs Authority, Ghana and visualization of spots under UV lamp was done using UVGL-58 Handheld UV lamp (254-365nm).

4.3 Chemicals and Reagents

Wagner's reagent

2.0g of potassium iodide and 1.27g of iodine were together dissolved in a little distilled water in a volumetric flask and the solution made up to 100cm^3 with distilled water. The presence of alkaloids is indicated by the formation of large brown amorphous and flocculent precipitate after treating the hydrochloric acid solutions of the extracts with a few drops of reagent.

Meyer's reagent

1.36g of mercuric iodide is dissolved in distilled 60cm^3 water and the resulting solution added to the one obtained by dissolving 5g of potassium iodide in 10cm^3 distilled water and the resulting solution made up to 100cm^3 with distilled water. The formation of a pale yellow precipitate when a few drops of the reagent are added to the test solution is indicative of the presence of alkaloids.

Dragendorff's reagent

8g of hydrated bismuth nitrate is dissolved in 20cm^3 concentrated nitric acid and the resulting solution is slowly added to a solution of 27.2g of potassium iodide in 50cm^3 of distilled water with stirring. Crystalline potassium nitrate which precipitates is filtered off and the filtrate made to 100cm^3 with distilled water before being used as a reagent for testing for alkaloids in the test. The solution of the extract is made distinctly acidic with sulphuric acid and completely freed of any ethanol in which the alkaloid precipitates are soluble. Two or three drops of the reagent are used since some of the alkaloid precipitates are soluble in excess reagent. Formation of brown precipitate is indication of the presence of alkaloids.

Anisaldehyde spray reagent

1cm^3 of concentrated sulphuric acid is added to 50cm^3 of glacial acetic acid. To the mixture is added 0.5cm^3 anisaldehyde. The reagent is always prepared fresh and used as spray. The sprayed TLC plates are heated to 110^{o}C for 10 minutes before visualization in visible light. Most organic compounds will stain as blue, violet, green, pink, yellow, red, cream and grey on a light pink background.

Liebermann-Buchard reagent

5cm^3 of redistilled acetic anhydride is cautiously mixed while cooling with 5cm^3 of concentrated sulphuric acid. The resulting mixture is again slowly added, also while cooling on ice to 50cm^3 of absolute ethanol. As a positive indication for the presence of terpenoids in an extract, this reagent when sprayed onto a TLC plate will produce pink to red spots after development followed by heating in an oven at a temperature of 110^{o}C for 15 minutes and then examination under UV lamp.

Iron (III) chloride solution

100cm^3 of iron (III) chloride solution is prepared by mixing 10g of iron (III) chloride and 90cm^3 of distilled water. Two to three drops of the solution are added to 3cm^3 of a test solution. The presence of catechol-type tannins is indicated by the formation of a greenish-blue coloration.

4.4 Solvent Extraction of the Plant Material

4.4.1 Extraction with Petroleum Ether (40-60ºC)

The pulverized stem of the plant (5.0kg), was extracted via Soxhlet extraction in batches. For each batch, 0.5g of plant material was extracted continuously for 24 hours using 3L of petroleum ether. After 2 successive extractions, the extract was filtered and the solvent was evaporated off on vacuum rotary evaporator to obtain the crude extract. A total of 34.0g of a dark-greenish syrup-like crude matter was obtained.

The crude extract on TLC (Petroleum Ether/Ethyl acetate 10/1) indicated over 10 spots, some staining yellow, orange, pink, purple, blue and violet when sprayed with anisaldehyde reagent. Two spots were UV active, appearing as blue and bright green, these spots did not stain either with anisaldehyde or iodine. The anisaldehyde stain was used extensively throughout the petroleum ether crude extract investigation.

4.4.2 Extraction with Ethyl acetate

After the petroleum ether extraction, the defatted plant material was air dried and the extraction repeated as described for the petroleum ether but this time ethyl acetate was the solvent used. The total weight of crude extract obtained after the Soxhlet extraction of 5.0kg of the plant material was 65.0g. TLC on the crude extract (Petroleum ether/ ethyl acetate 10/3) gave more than 10 spots,

some staining yellow, pink, purple, blue and violet with anisaldehyde stain. Most of the spots observed for the petroleum extract were also observed for the ethyl acetate extract.

4.4.3 Methanol Extraction

After the ethyl acetate extraction, the plant material was air dried and the extraction continued using methanol. A total of 2.5kg of plant material was extracted to give 23g of dark-reddish solid, very soluble in chloroform-ethanol mixture. TLC on the crude extract (Petroleum ether/ethyl acetate 10/6) gave several spots, some staining yellow, pink, purple and blue with anisaldehyde stain. Similar spots were also observed as ion the case of the ethyl acetate extract.

4.5 Phytochemical Screening Test Procedure

The petroleum ether extract, ethyl acetate extract and methanol extract were screened separately for alkaloids, anthraquinones and anthracene derivatives, flavonoids and leuco-anthocyanins, cardiac glycosides, terpenoids, tannins, and saponins as follows:

Test for alkaloids

About 0.1g of each of the crude extracts in separate test tubes was added to $5cm^3$ of 2M HCl solution. This was stirred, warmed and filtered. The filtrate from each extract was then divided into three test tubes. To one portion of each test solution was added Dragendorff's reagent; to another portion, Meyer's reagent and to the remaining portion, Wagner's reagent. The absence of a yellowish or reddish brown precipitate in the test tubes indicated the absence of alkaloids.

Test for flavonoids and leucoanthocyanins.

About 0.1g solid of each of the crude dried extract was added to $15cm^3$ of 80% ethanol. The resulting solution was filtered and the filtrate divided into two separate test tubes. To one portion

was added magnesium turnings followed by 0.5cm^3 concentrated hydrochloric acid and observed color changes within 10 minutes. 5cm^3 of concentrated hydrochloric acid was added to the other portion and warmed for 5 minutes. The presence of light pink color in both extracts indicated the presence of flavonoids.

Test for tannins

About 0.5g of each extract was dissolved in 10cm^3 of aqueous methanol and the solution divided into two portions. To one portion, was added freshly prepared iron (III) chloride solution and to the other portion nothing was added to serve as blank. The formation of a dark greenish-blue coloration on addition of iron (III) chloride indicates the presence of tannins.

Test for saponins

The presence of saponins in the extracts was indicated by the fact that there was foaming when some amounts of the extracts were each shaken with water.

The foaming disappeared after the test tube had been set aside for about an hour.

Salkowski's test for cardiac glycosides

About 0.5g of each extract was dissolved in 2cm^3 of chloroform in a test tube. Concentrated sulphuric acid was carefully added down the side of the test tube to form a lower layer. Formation of a reddish brown color at interface indicates the presence of the glycone portion of cardiac glycosides.

Test for anthraquinones and anthracene

About 0.5g of each extract was dissolved in 30cm^3 of distilled water and filtered. The filtrate was shaken up with 10cm^3 benzene in a separating funnel and allowed to stand. The benzene layer was transferred into a test tube and shaken with 5cm^3 of 2M ammonia solution. The absence of red color in the ammonia layer was indicative of the absence anthraquinones in the extract.

4.6 Investigation of the Extracts

4.6.1 Petroleum ether (40-60^{o}C) Extract

A total of 34g of crude extract was obtained after the Soxhlet extraction and concentration on the vacuum rotary evaporator. This was coded DCS-P and kept in the refrigerator. After few days, DCS-P was observed to have solid precipitate and liquid supernatant portions. The supernatant (mother-liquor, ML) was filtered off and TLC in Petroleum ether/ ethyl acetate, 14:0.5 was run on both the solid portion DCS-PA1 and the mother liquor, ML. After staining with anisaldehyde, the two portions revealed comparable spots and hence were put together (20g), dissolved in chloroform and mixed with silica gel (6g) and air dried. This was later put on a glass column pre-loaded with silica gel (230g). The column was first eluted with petroleum ether 100%, then with petroleum ether and ethyl acetate mixtures until 100% ethyl acetate. The column was finally washed with chloroform/ethanol 1:1mixture. The eluates were collected in test tubes, 10 ml each. TLC was run on the eluates to monitor the progress of the chromatographing and to combine comparable eluates.

At 10% of ethyl acetate in petroleum ether, the fractions F021-F073 were combined based on their similar TLC profiles. This was coded DCS-PA2, which gave 4 spots on TLC (Petroleum ether/ethyl acetate: 14/0.5). The sub-fraction DCS-PA2 (5.6g), was again put on a smaller glass

column pre-loaded with silica gel (80g) and eluted with petroleum ether/chloroform: 25/75 mixture. The eluates were collected in smaller test tubes in volumes of 5ml. The column fractions yielded the solids DCS-P1 (60mg, 1 spot), DCS-P2 (40mg, 1 spot) and a mixture of these two solids coded DCS-P1P2 (20mg, 2spots) after recrystallization from ethanol . The 100% ethyl acetate fraction and the fraction obtained after washing the column (chloroform/ absolute ethanol 1:1) were also found to be the same and hence were combined (coded DCS-PA3) and safely kept in the refrigerator. All other isolates were oily in nature.

4.6.2 Ethyl Acetate (EA) extract

The ethyl acetate extract (40g) was loaded onto a chromatographic glass column pre-loaded with silica gel (470g) and eluted quickly with wide increase in polarity, starting from petroleum ether/ethyl acetate mixtures of 10:1, 10:3, 10:6, 1:1, 1:3, followed by 100% ethyl acetate and finally with absolute ethanol.

In all 13 fractions were obtained initially, DCS-EA1 - DCS-EA13, but the similarity of some of the fractions on TLC resulted in the combination of DCS-EA1 and DCS-EA2 into DCS-EAA1, DCS-EA3 and DCS-EA4 into DCS-EAA2; DCS-EA5, DCS-EA6 and DCS-EA7 into DCS-EAA3; DCS-EA8, DCS-EA9 and DCS-EA10 into DCS-EAA4; DCS-EA11 and DCS-EA12 into DCS-EAA5, thus six fractions in all.

The fraction DCS-EAA1 (4.8g) was loaded onto a column pre-loaded with silica gel (75g) and eluted with petroleum ether/chloroform 25/75 throughout. The column fractions yielded the solids DCS-E1 (18mg, 1 spot), DCS-E2 (15mg, 1 spot) and a mixture DCS-E1E2 (15mg, 2 spots) after recrystallization from absolute ethanol. The solids DCS-E1and DCS-E2 spotted yellow and purple respectively with anisaldehyde stain on TLC run in petroleum ether/ethyl acetate (14:0.5). The

solid DCS-E1E2 spotted yellow and purple in the same solvent system on TLC with the same R_f values as the solids DCS-E1 and DCS-E2. The last fraction from the column, F071-F089, was safely kept in the refrigerator for future investigation.

The fraction DCS-EAA2 (3.6g) was loaded on a glass column pre-packed with silica gel (75g) and eluted with petroleum ether/ ethyl acetate (10:1). The eluates were collected in volumes of 5ml and combined based on the TLC profiles. The column fractions (F010-F015) yielded the solid DCS-E3 (14mg, 2 spots) which indicated similar TLC profiles as DCS-P1P2 and DCS-E1E2 after running them in different solvent systems. The column fractions (F018-F024) yielded the solid DCS-E4 (25mg, 1 spot), this solid indicated a spot which stained purple with anisaldehyde spray on TLC in the solvent system; petroleum ether/ethyl acetate (10:4).

The fraction DCS-EAA3 (4.2g) was loaded on a glass column pre-packed with silica gel (75g) and slowly eluted with petroleum ether/ethyl acetate 10:2 then finally with 30% ethyl acetate in petroleum ether. The column fraction yielded the solid DCS-E5 (45mg, 1 spot) which stained blue with anisaldehyde spray on TLC run in petroleum ether/ethyl acetate (10:6).

The fraction DCS-EAA4 (7.4g) was loaded on a glass column pre-packed with silica gel (120g) and slowly eluted starting with petroleum ether/ethyl acetate 10:3 and finally with 40% ethyl acetate in petroleum ether. The solid DCS-E6 (55mg, 3 spots) precipitated from fractions F025-F040, were filtered and recrystallized from a mixture of diethyl ether/chloroform (10:3).

From fractions F054-F071, the solid DCS-E7 (25mg, 1 spot) precipitated and was recrystallized from a mixture of chloroform/diethyl ether (2:5). DCS-E7 stained violet with anisaldehyde spray on TLC run in petroleum ether/ ethyl acetate (10:6). The fractions F075-F091 after concentrating on the vacuum rotary evaporator and recrystallization from 2/5 mixture of chloroform/diethyl ether

afforded the solid DCS-E8 (32mg, 1 spot). DCS-E8 stained purple with anisaldehyde spray on TLC run in petroleum ether/ethyl acetate (10:6). The last fraction, F093-F114 was combined with sub-fraction DCS-EAA5.

DCS-EAA5 (3.8g) was loaded on a glass column pre-packed with silica gel (80g) and eluted slowly with chloroform/ absolute ethanol 95/5 throughout. Based on TLC, four fractions; F018-F025, F028-F033, F036-F041 and F043-F048 were obtained. The solid DCS-E9 (10mg, 1 spot) was obtained from fraction F028-F033 after washing with diethyl ether three times. The solid was filtered off and dried. DCS-E9 stained pink with anisaldehyde on TLC run in petroleum ether/ethyl acetate (1:1) and petroleum ether/acetone/chloroform (7/5/5). When sprayed with anisaldehyde, a grey spot was visualized but was observed as pink when heated. No solid precipitated from fraction F043-F048, there appeared to be solid in fraction F018-F025 but all effort to get the solid even in the smallest amount proved futile. TLCs were run on this fraction in different solvent systems to establish the veracity of the presence of a solid in this fraction. The solid DCS-E10 (5mg, 2 spots) was obtained from the fraction F036-F041via triturating with ethyl acetate since it was very soluble in acetone. The solid stained with iodine but not anisaldehyde and it was dirty white and powdery in appearance.

After eluting DCS-EAA6 with 50% ethanol solution, the resulting fractions were colloidal in nature making separation of solute impossible. Upon the addition of small amount of 0.1M HCl, the solute coagulated. The solute was filtered, dried to afford DCS-E11; brown in appearance and soluble only in chloroform/ethanol mixtures. On TLC, it appeared as a streak and stained yellow to brown with anisaldehyde spray reagent.

4.7 *In vitro* screening of crude extracts and some isolates for anti-schistosomal activity

4.7.1 Schistosome Egg recovery and Concentration from infested urine samples by the modified Kotze *et al*[108] Method.

Materials and Reagents

1. Urine
2. 50ml Falcon tubes
3. 50ml of 0.9% Saline
4. 40ml of 0.015% Brij-35
5. 2 × 250ml beakers
6. 180, 150 and 80µm sieves (Nonaka Rikaki Co. Ltd, Japan)
7. Centrifuge
8. Aspirator

Field isolates of human *Schistosoma* eggs were obtained after extracting them from urine samples collected from 120 participants at Tomefa, a rural community in the Ga West District around the Weija dam in the Greater-Accra Region of Ghana. Ethical clearance for the anti-schistosomal test was obtained at the Noguchi Memorial Institute of Medical Research (Appendix III, pg. 128). Over 80% of the participants were school children aged between 8 and 14years. Urine samples that were positive for schistosome eggs were pooled into 50ml falcon tubes and centrifuged at 500g for 5 minutes. The supernatant was discarded and the deposits suspended in 50ml of 0.9% saline and centrifugation repeated. The sediment was suspended in 40 ml of 0.015% Brij-35 and shaken vigorously. It was centrifuged again at 500g for 5 minutes. The supernatant was discarded and the sediment re-suspended in saline into a 200ml beaker. More saline was added to the 150ml mark.

The suspension was filtered through a stack of three sieves: 180 µm, 150 µm and 80 µm, respectively (Nonaka Rikaki Co. Ltd, Japan). The stack of sieves was thoroughly flushed with a jet of saline to wash the eggs. To prevent air lock, the 150 µm and 80 µm sieves were occasionally separated. At the end of washing, the 80 µm was removed and inclined at approximately 45^{o} to the horizontal and a jet of saline applied to it to wash off the eggs into a beaker. The suspension was centrifuged at 200g for 10 minutes and left for 30 minutes after which the supernatant was aspirated down to 5ml and egg count was estimated in 20µl of solution.

4.7.2 *In vitro* screening of test compounds against schistosome eggs using the 96-well plate-Egg Hatch Assay.

From the 5ml concentrated schistosome egg suspension, three 30µml the suspension was pipetted unto a slide and observed under light microscope. The number of eggs per 30µml was noted and hence the average number of eggs per 30µml determined. From this result the approximate number of eggs in the 5ml concentrated egg solution was calculated.

The test compounds; DCS-P1, DCS-E4, and DCS- E7 (2mg for each) and then 5mg each for the crude extracts (petroleum ether, ethyl acetate and methanol) were dissolved in 1ml of 5% DMSO to give 2mg/ml (for each test isolate) and 5mg/ml (for each crude extract) stock solutions. 100µl of the stock solution of each test compound was pipetted in duplicate into the first wells. By using serial dilution, 50µl dilute solutions of the test compounds were prepared in decreasing order of concentration to the seventh well. Then 50µl of egg solution was added to each well and the presence of eggs ascertained under the inverted microscope. Water and praziquantel (2mg/ml stock solution) were used as negative and positive controls respectively.

Egg Hatch Assays was incubated for 24 hours at ambient temperature and the process of egg hatch was stopped by the addition of 100ml of formalin to each well. The number (#) of hatched eggs and unhatched eggs (larvae) was counted using inverted light microscopy.

The percent hatch inhibition (% EHI) was calculated as:

$$\% \text{ egg hatch inhibition (\%EHI)} = \frac{\text{\# unhatched}}{\text{\# unhatched + \# larvae}} \times 100$$

The %EHI was plotted against log concentration. Extrapolation of the 50% EHI on the curve gave the half maximal inhibitory concentration (IC_{50}) of the test sample.

APPENDIX I: IR Data of Isolates

	Page
IR spectrum of friedelan-3one, DCS-P1	100
IR spectrum of friedelan-3β-ol, DCS-P2	101
IR spectrum of friedelan-3-one, DCS-E1	102
IR spectrum of friedelan-3β-ol, DCS-E2	103
IR spectrum of mixture of friedelan-3-one and friedelan-3β-ol, CPC-S1	104
IR spectrum of mixture of stigmasterol and β-sitosterol, DCS-E4	105
IR spectrum of DCS-E5	106
IR spectrum of DCS-E6	107
IR spectrum of DCS-E7	108
IR spectrum of DCS-E8	109
IR spectrum of DCS-E9	110
IR spectrum of DCS-E11	111

IR spectrum of friedelan-3one, DCS-P1

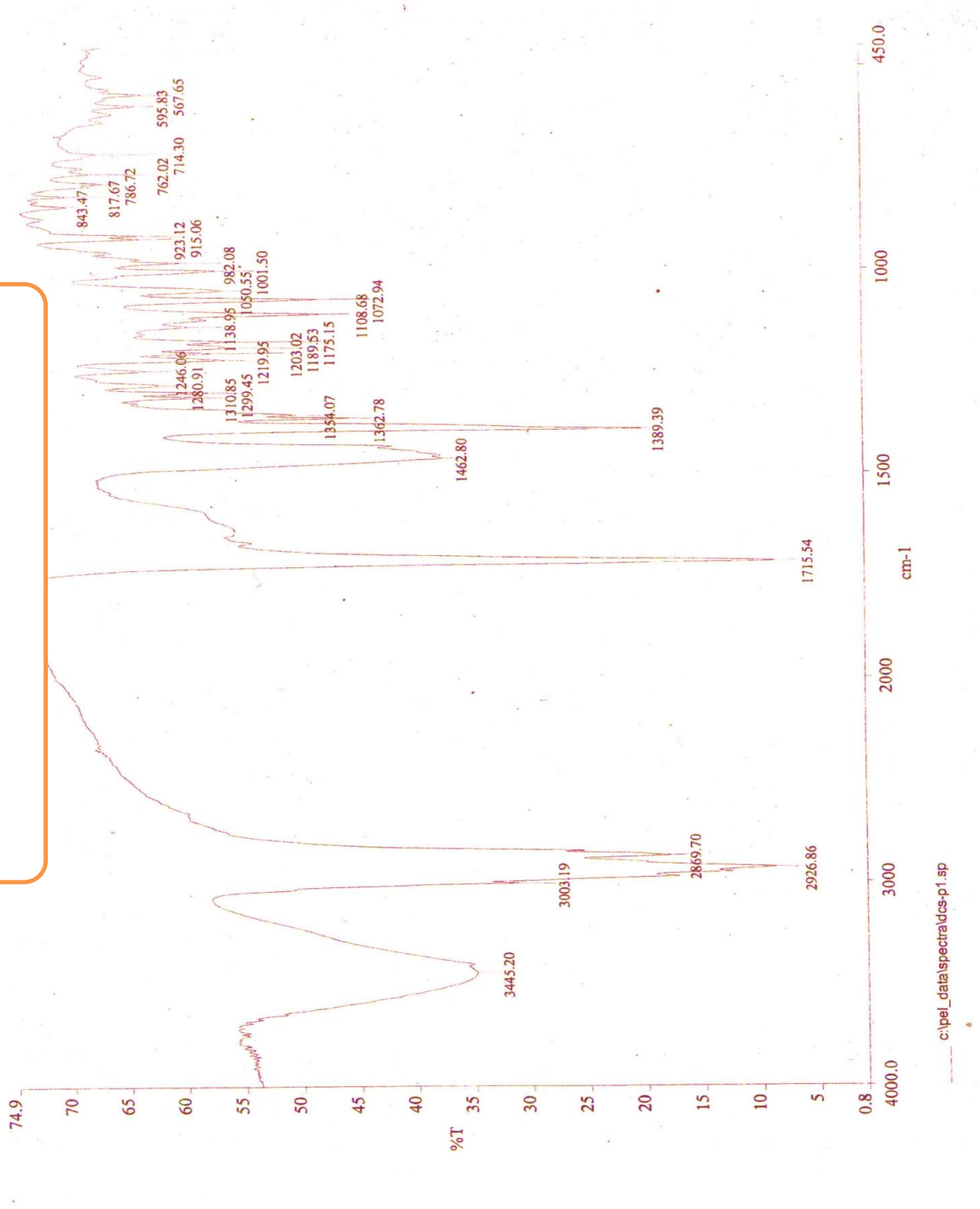

IR spectrum of friedelan-3β-ol, DCS-P2

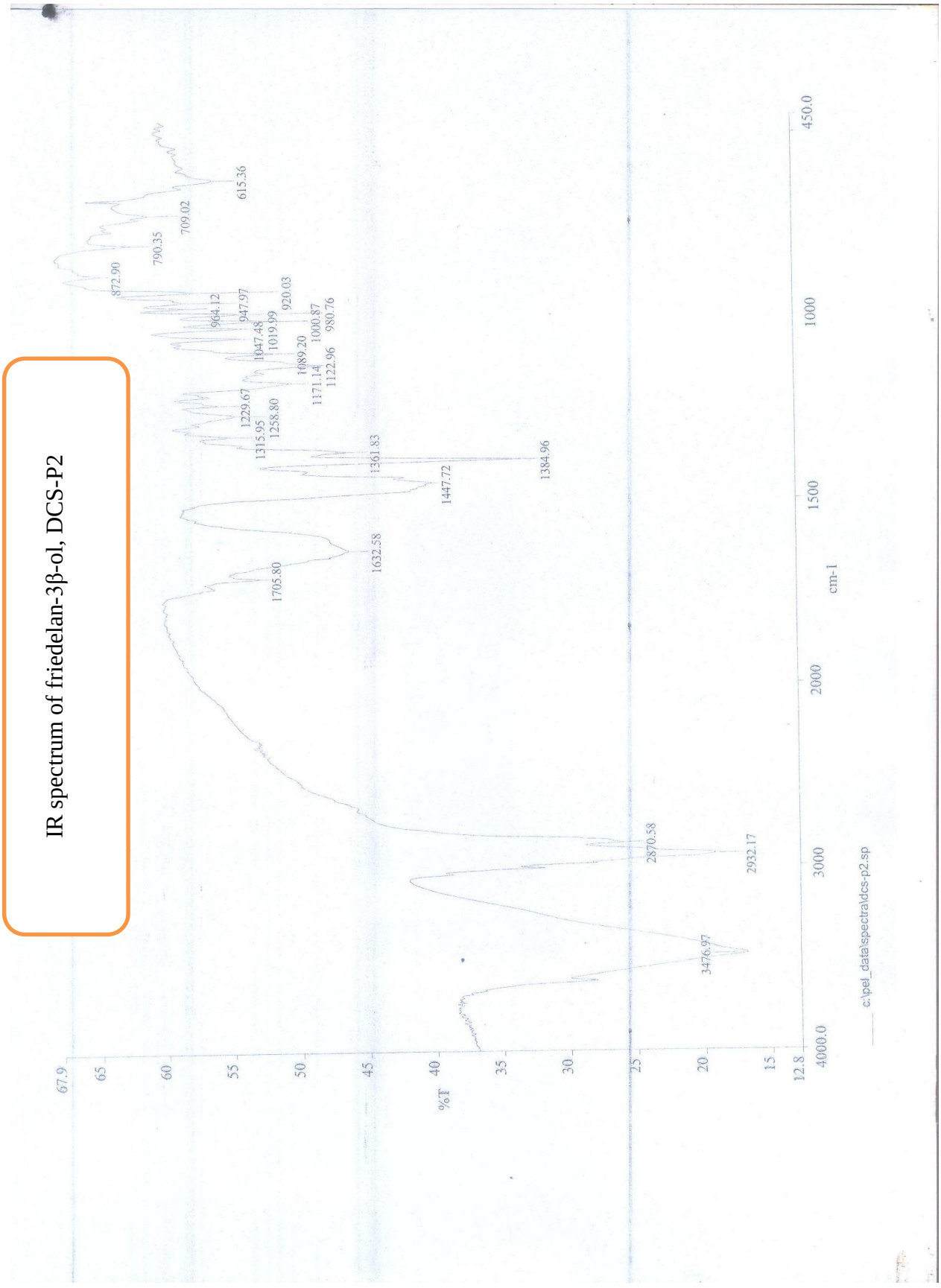

IR spectrum of friedelan-3-one, DCS-E1

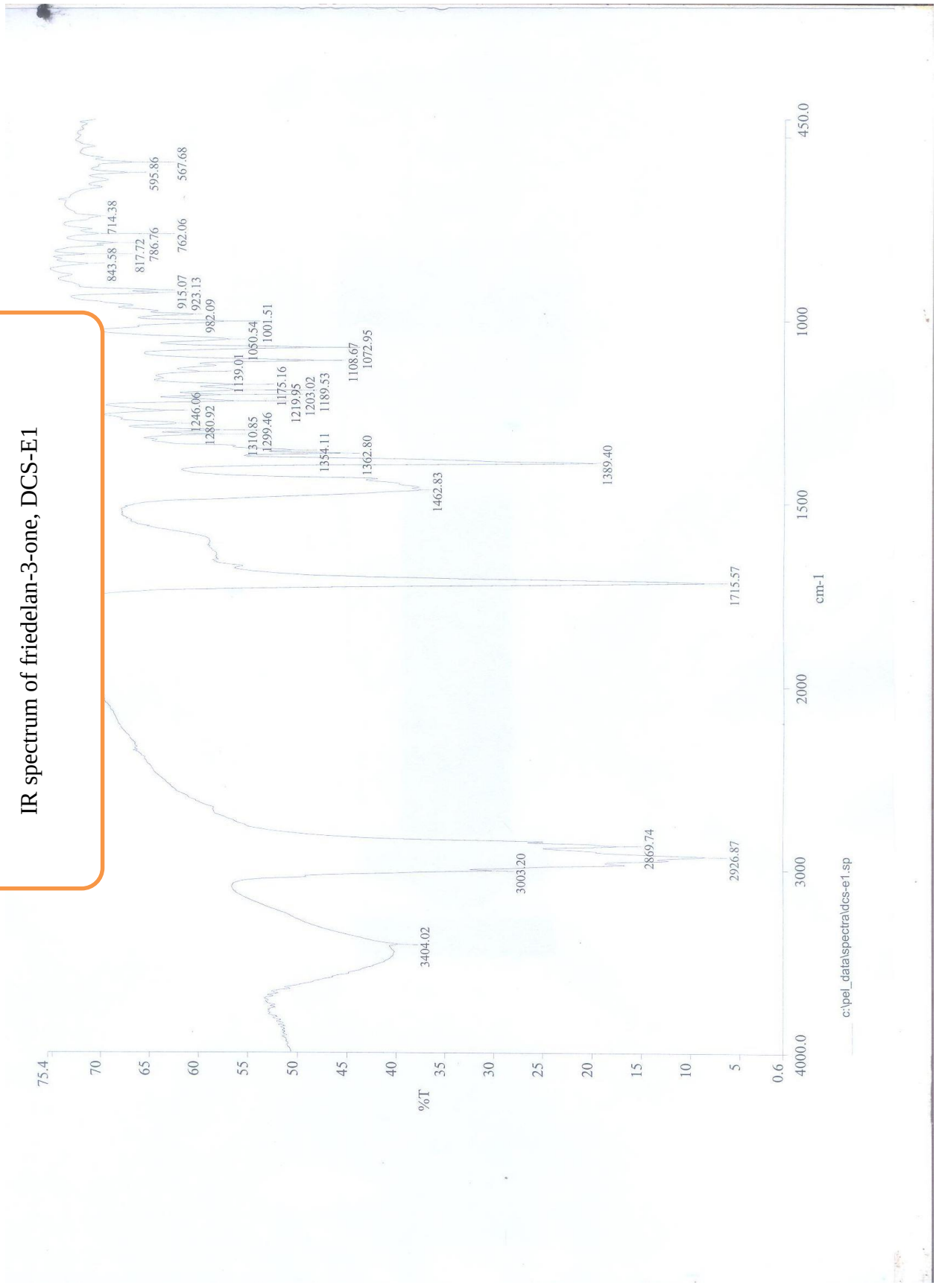

IR spectrum of friedelan-3β-ol, DCS-E2

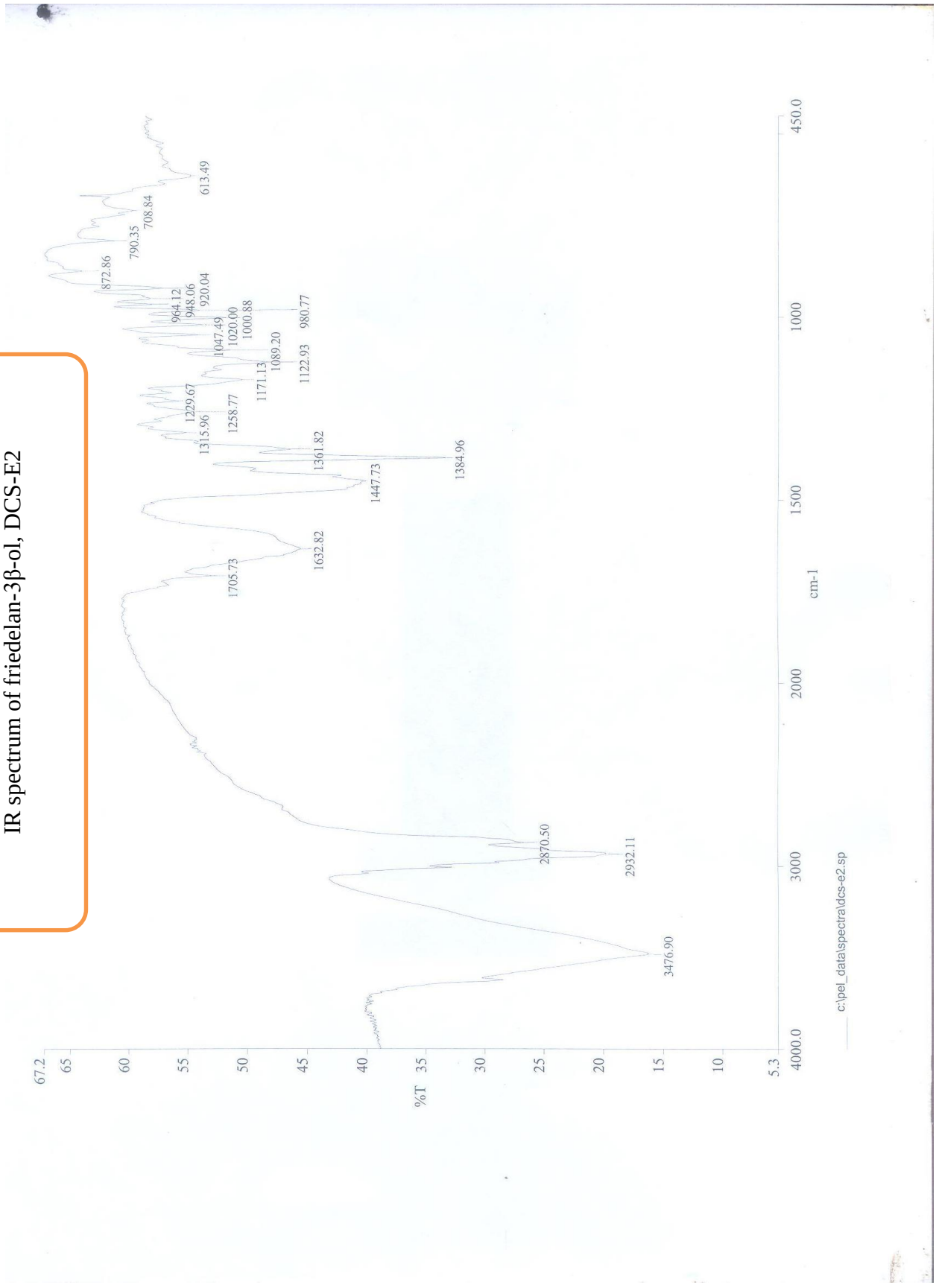

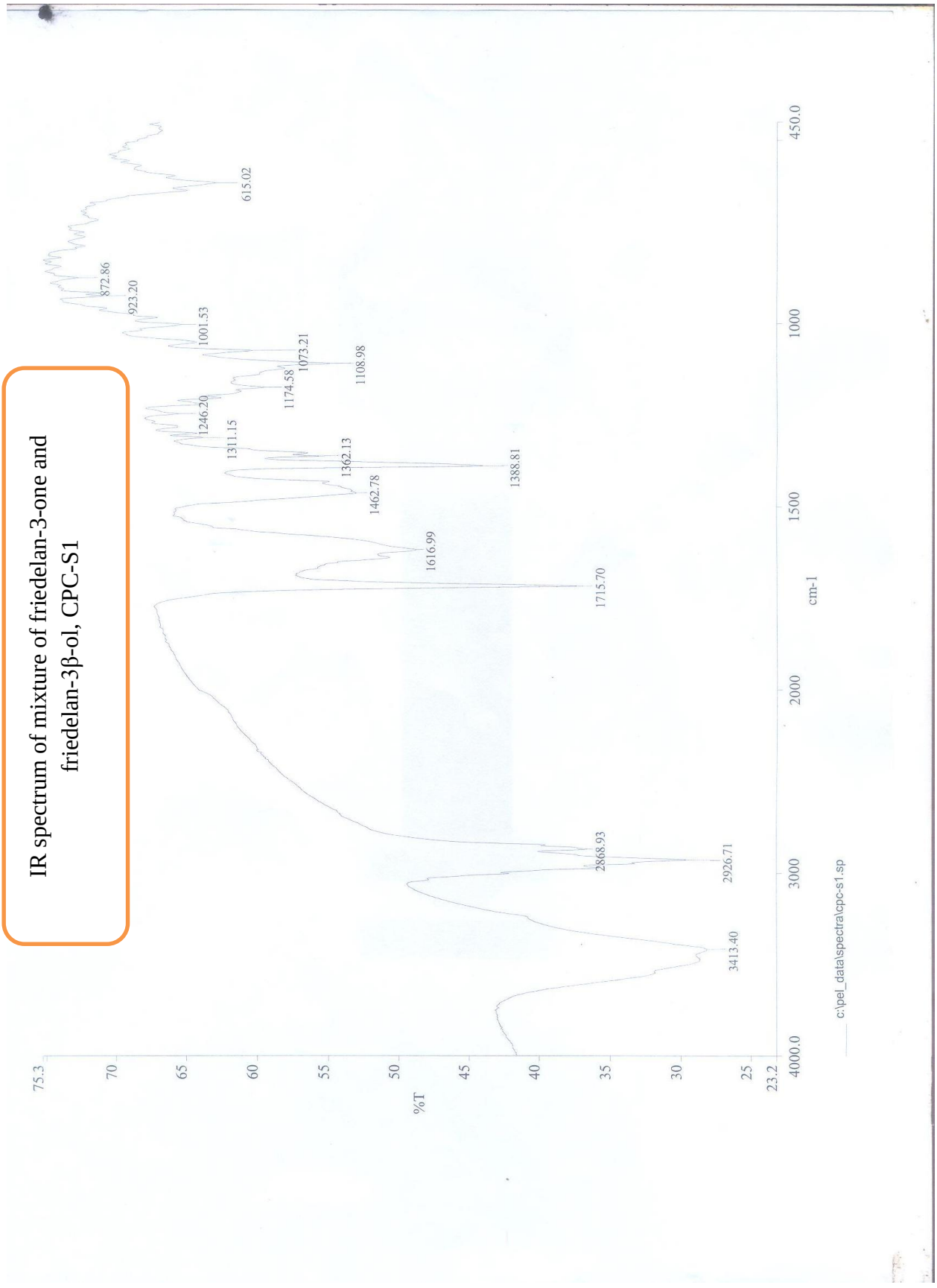

IR spectrum of mixture of friedelan-3-one and friedelan-3β-ol, CPC-S1

IR spectrum of mixture of stigmasterol and β-sitosterol, DCS-E4

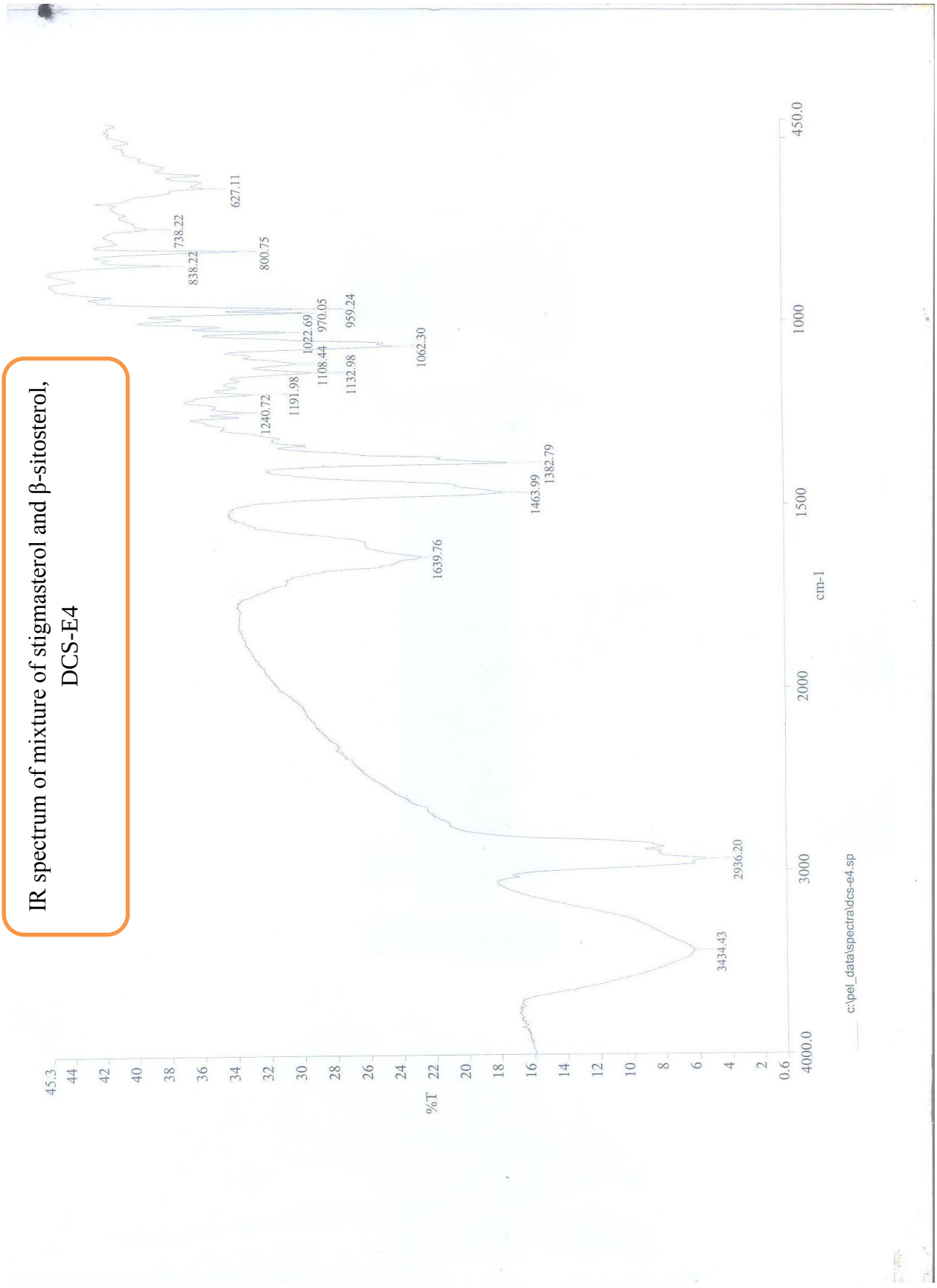

IR spectrum of DCS-E5

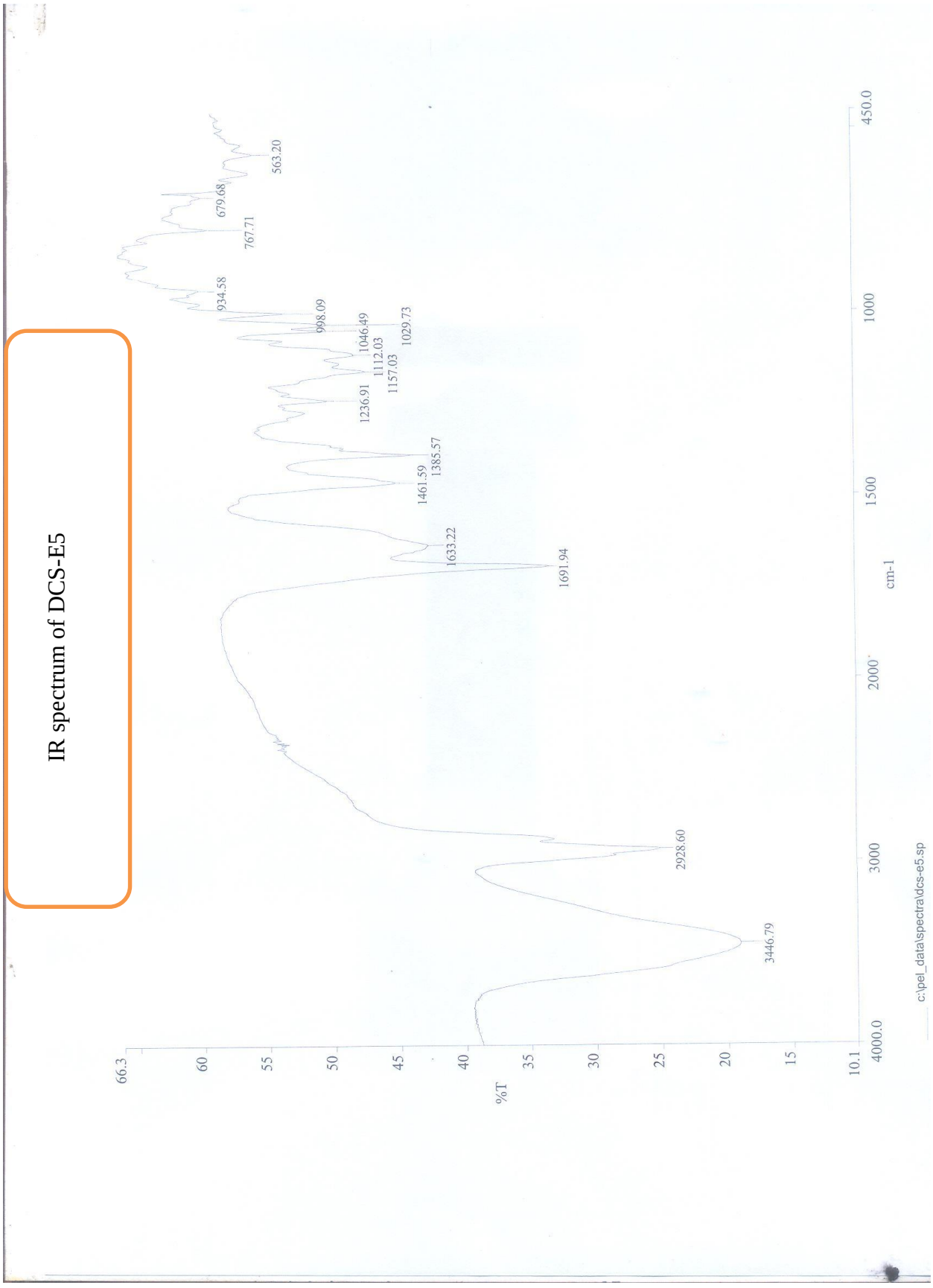

IR spectrum of DCS-E6, pomolic acid

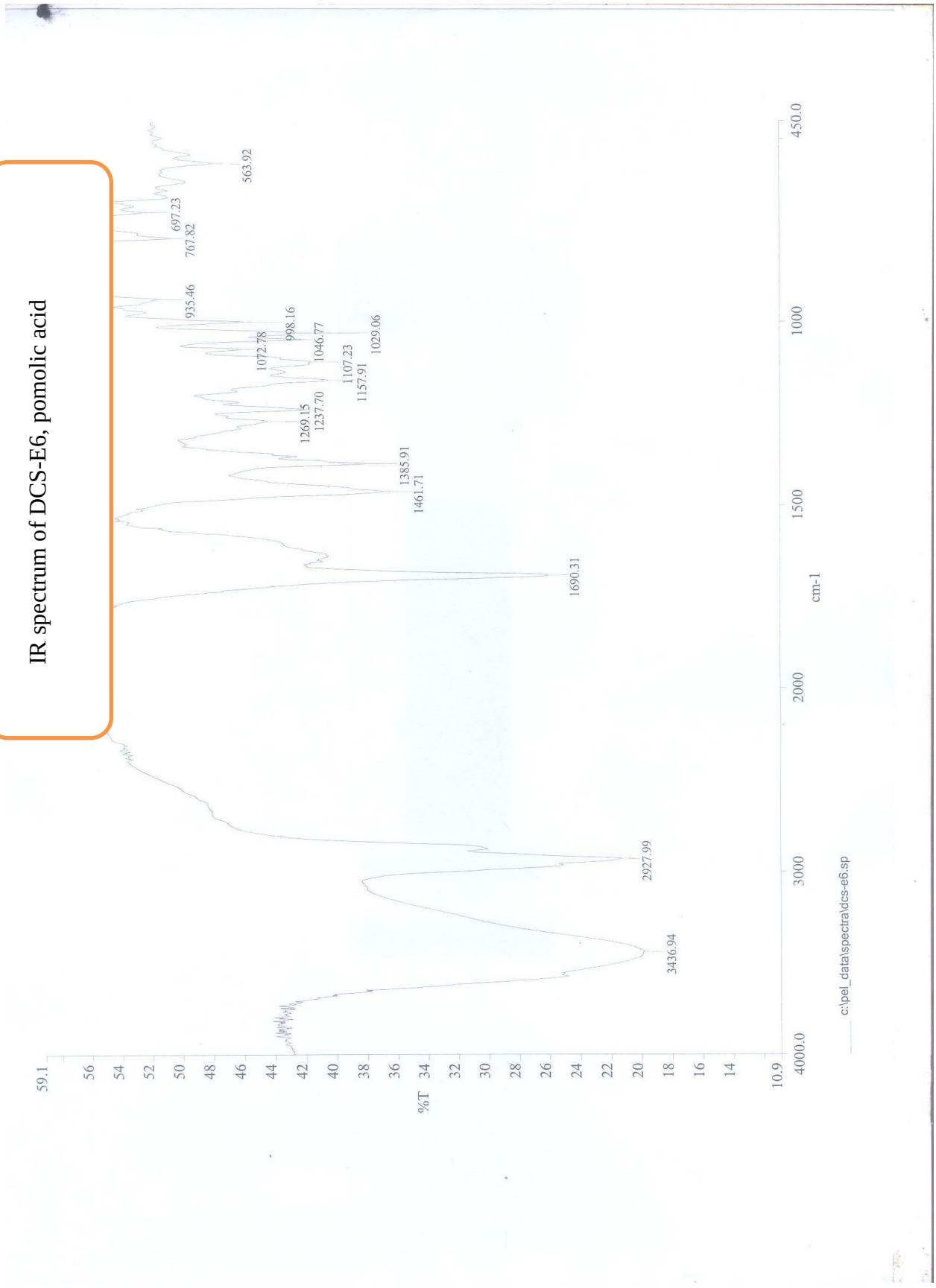

IR spectrum of DCS-E7, dichapetalin M.

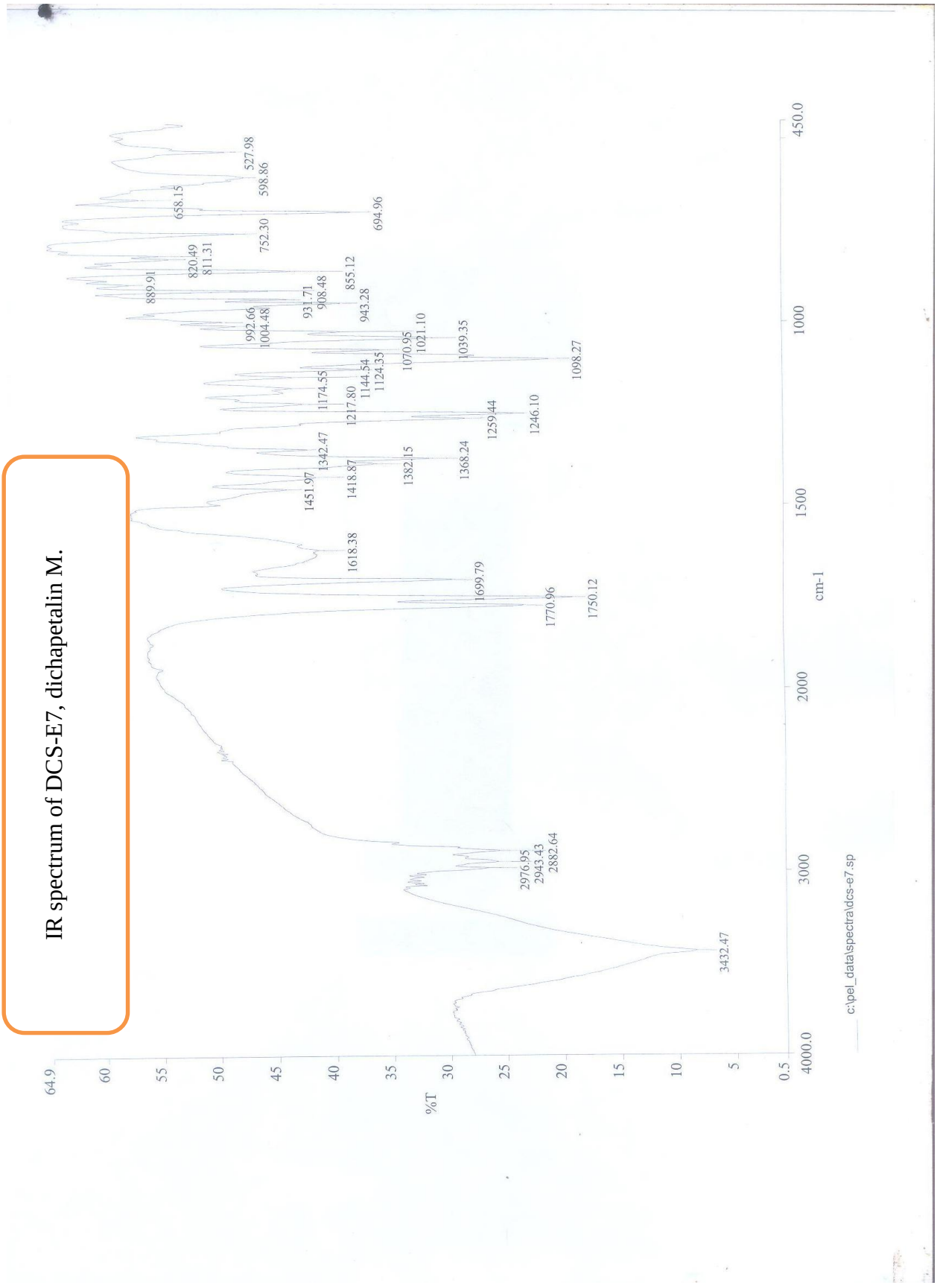

IR spectrum of DCS-E8, Maslinic acid

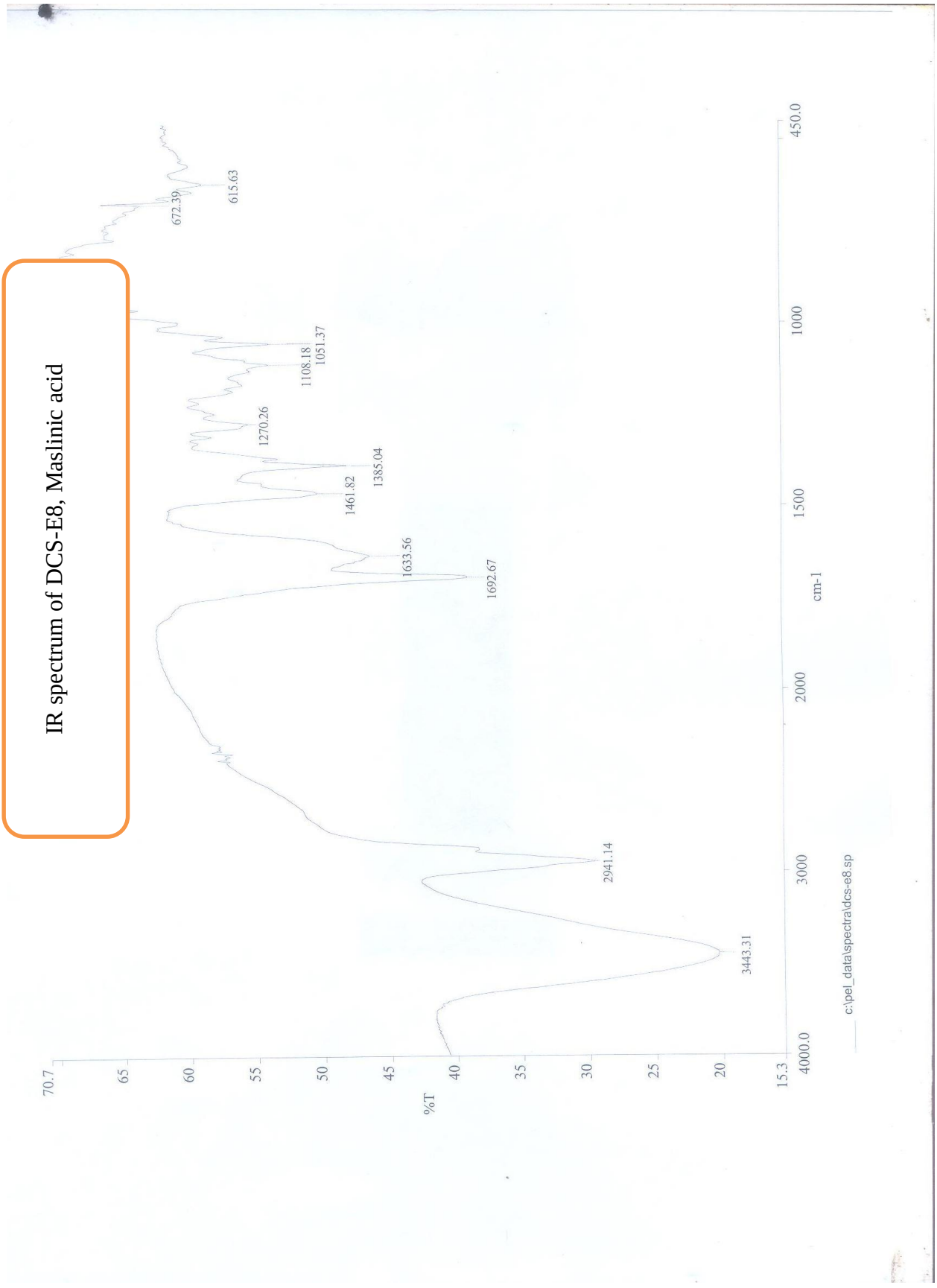

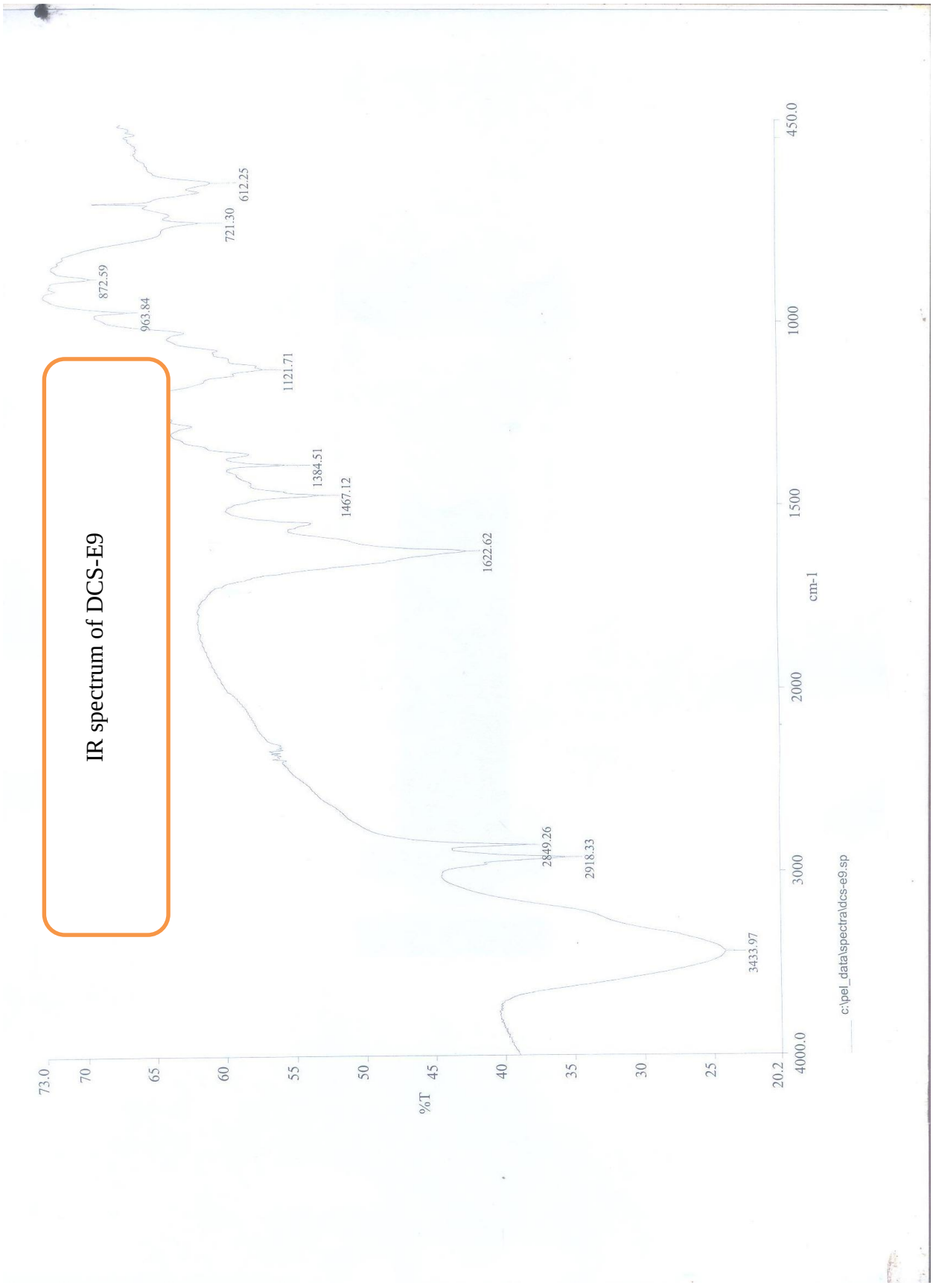

IR spectrum of DCS-E11

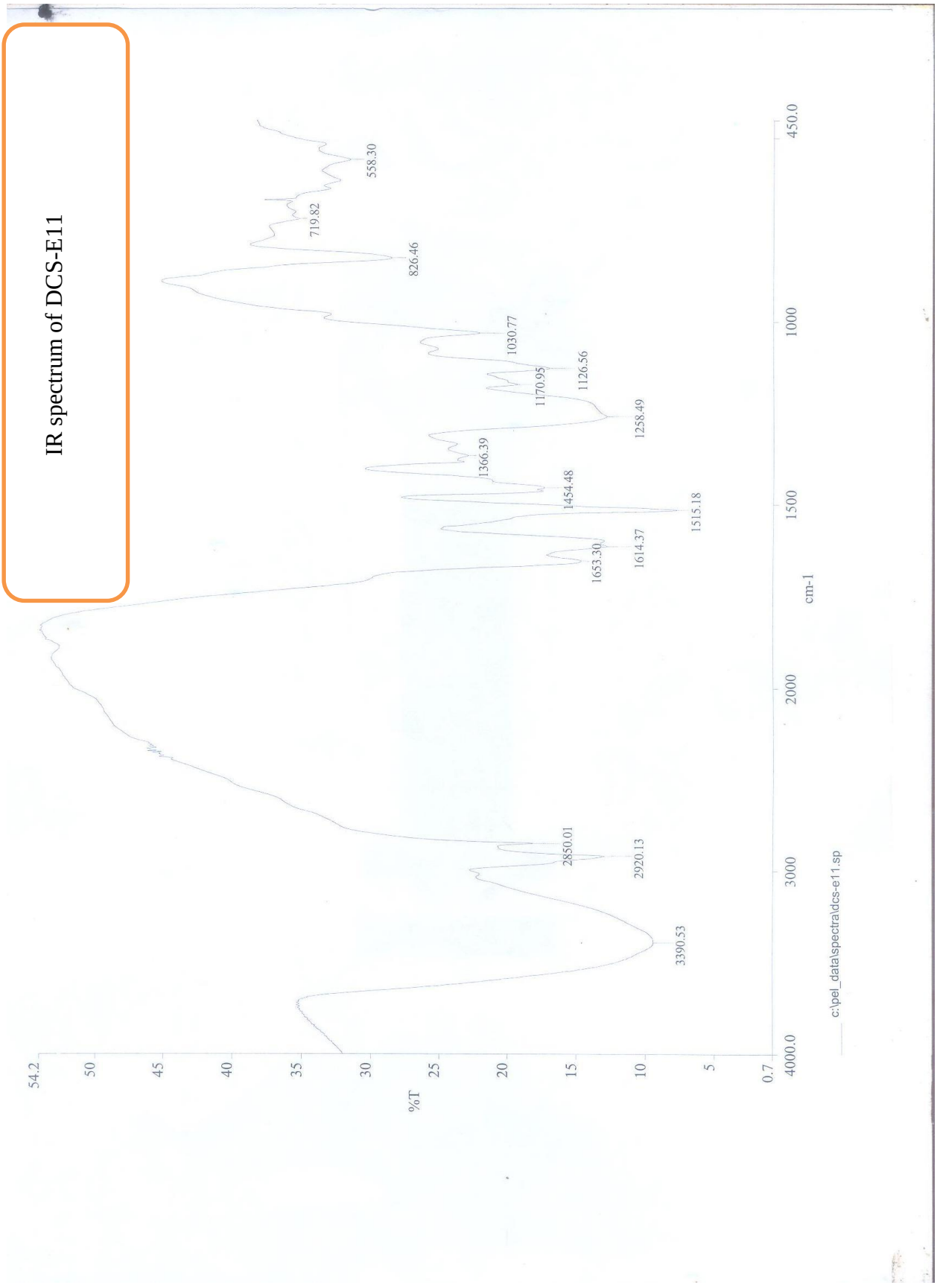

APPENDIX II: ^{1}H and ^{13}C NMR data of Isolates

	Page
^{13}C NMR data of DCS-E6, pomolic acid	113
^{1}H NMR data of DCS-E6, pomolic acid	114
^{1}H NMR data of DCS-E7, dichapetalin M	115
^{13}C NMR data of DCS-E7, dichapetalin M	116
Expanded ^{1}H NMR data of DCS-E7, dichapetalin M	117-120
^{13}C NMR data of DCS-E8, maslinic acid	121
^{1}H NMR data of DCS-E8, maslinic acid	122
Expanded ^{1}H NMR data of DCS-E8, maslinic acid	123-127

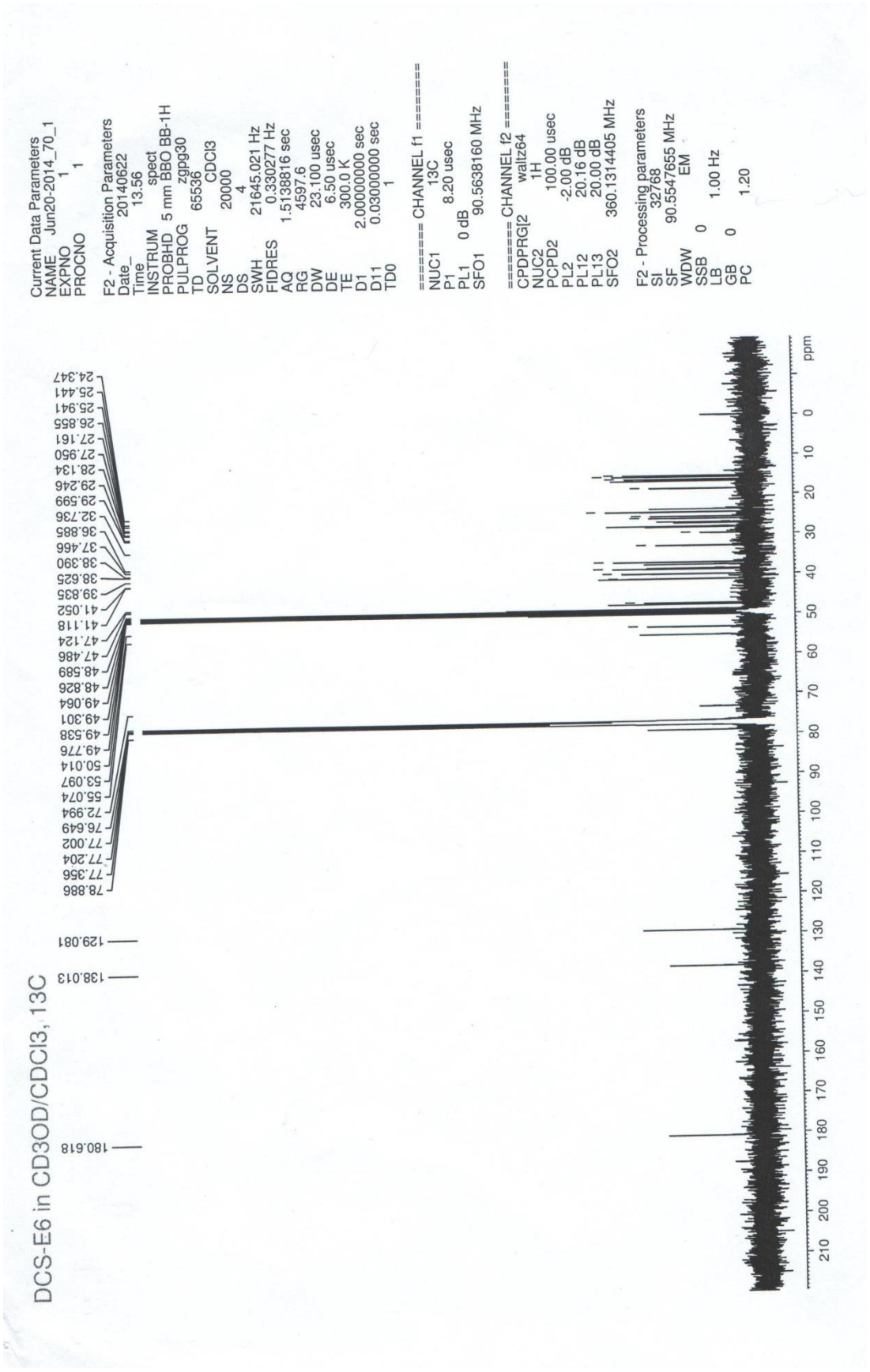

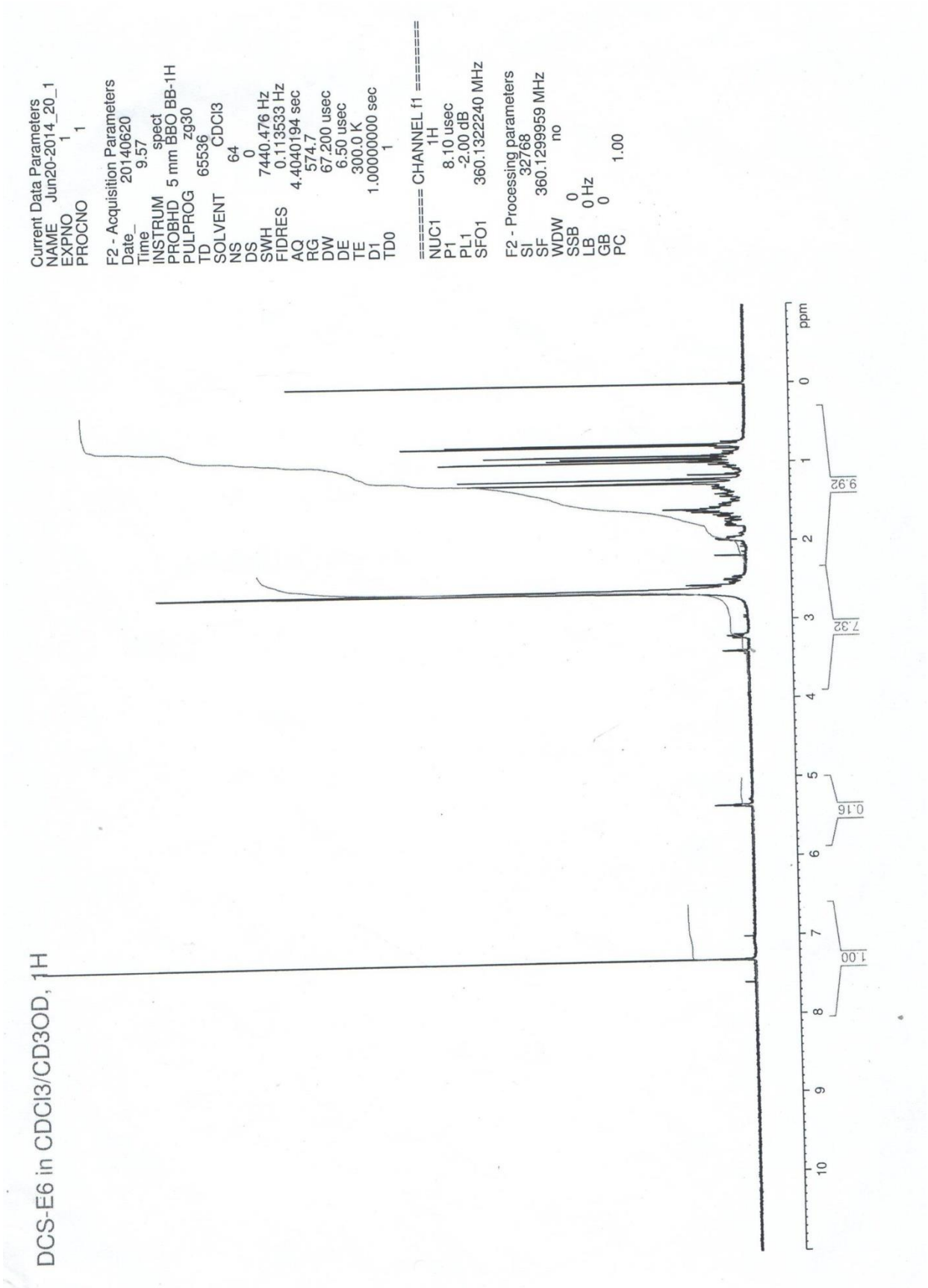

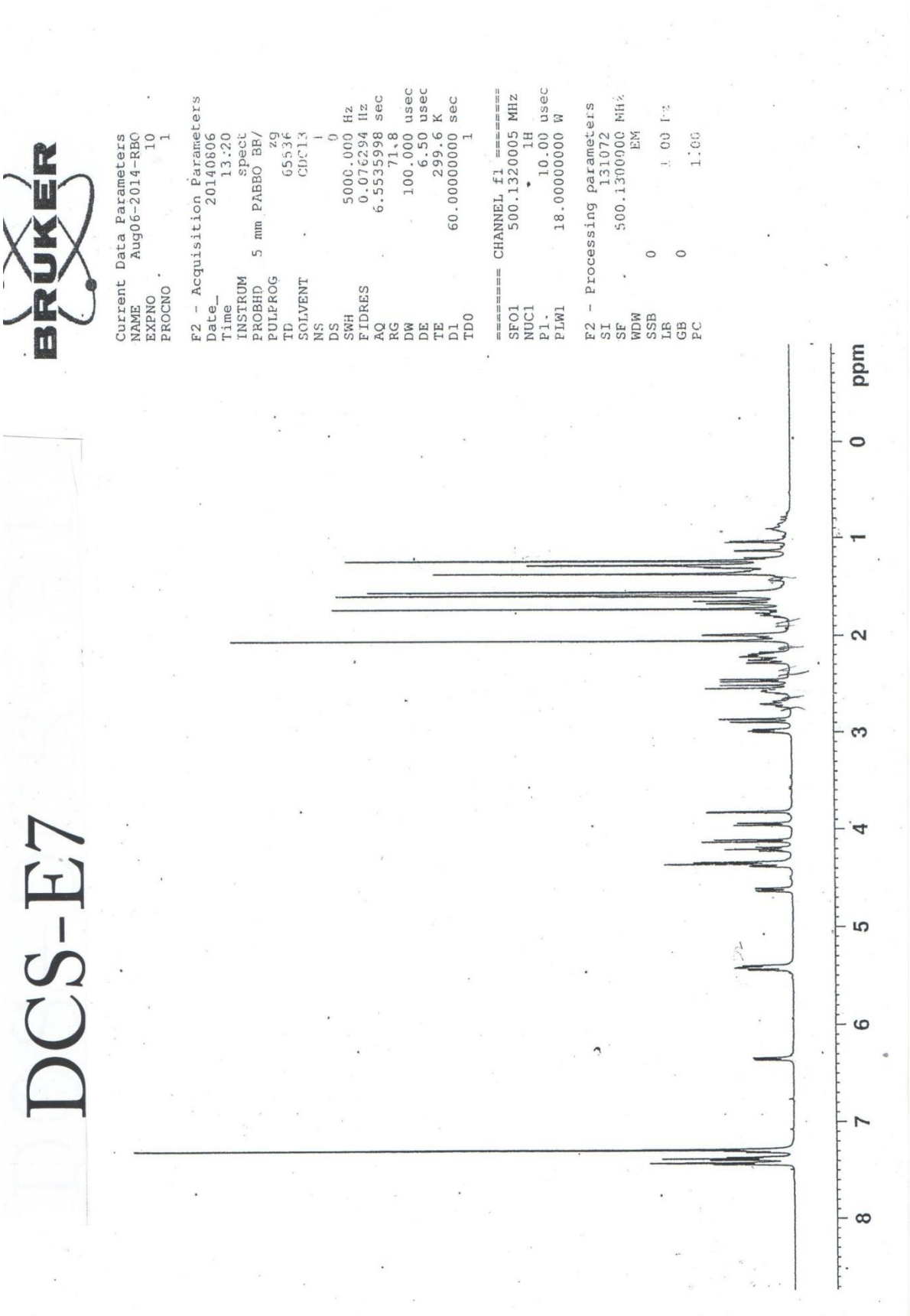

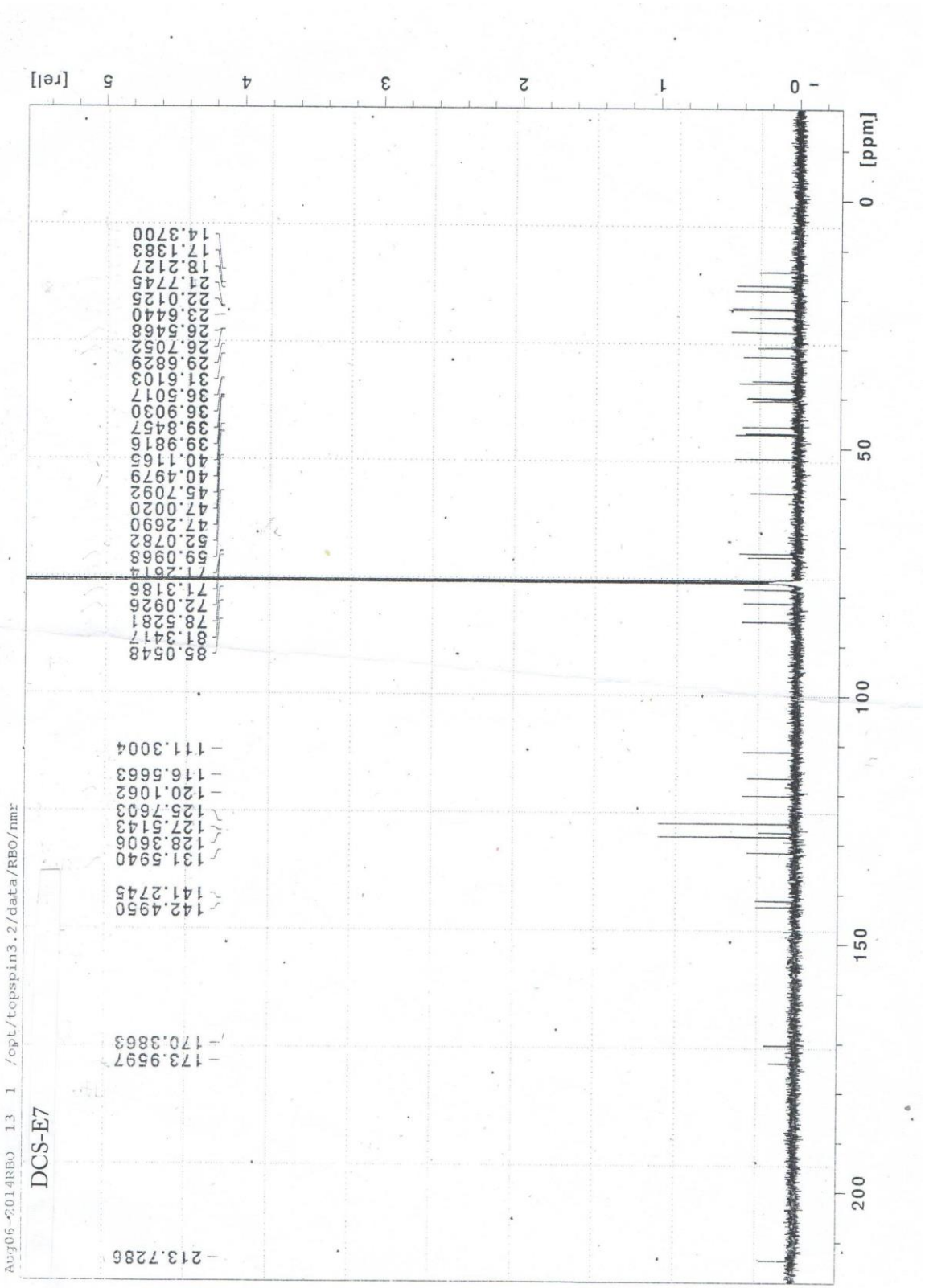

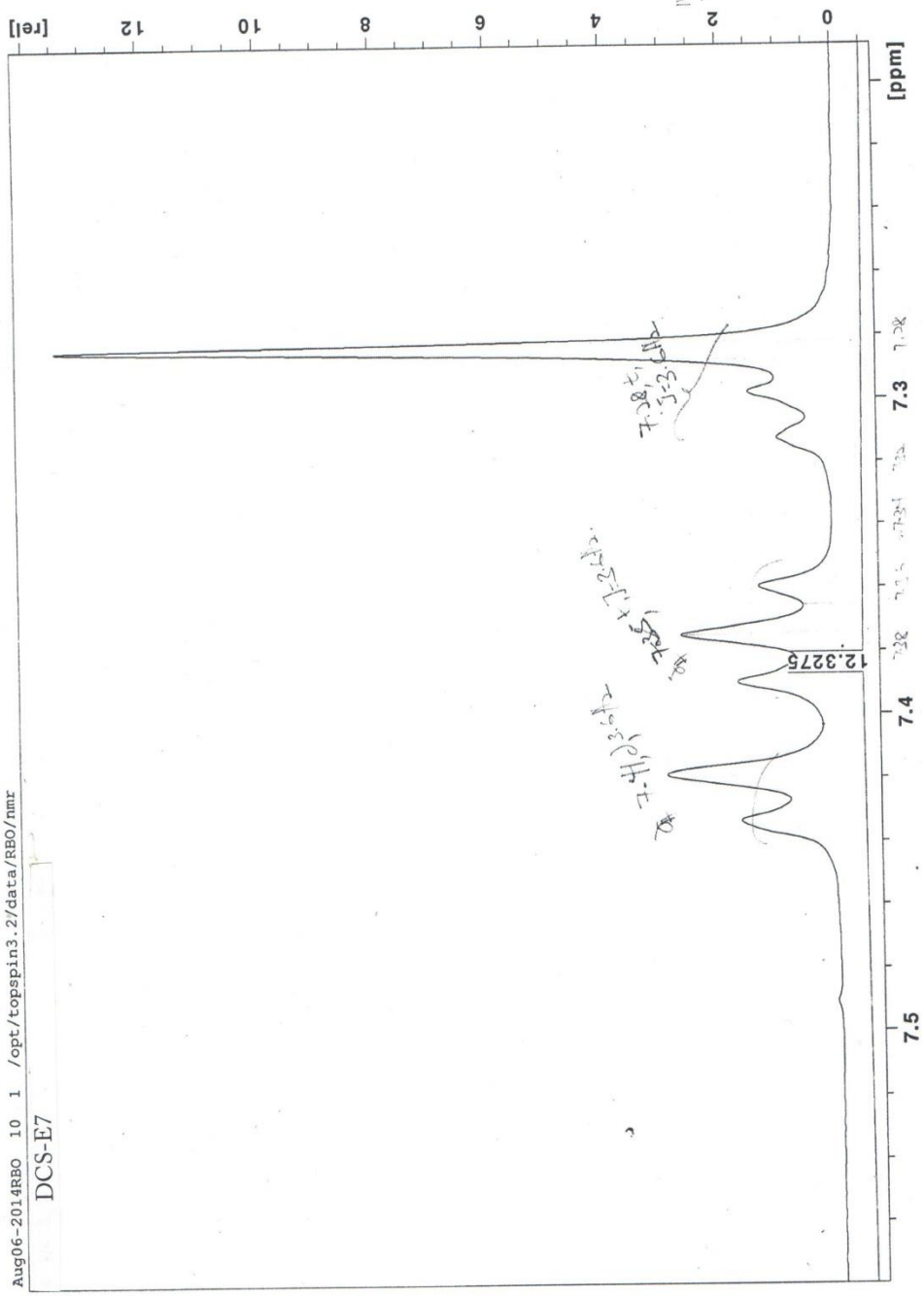

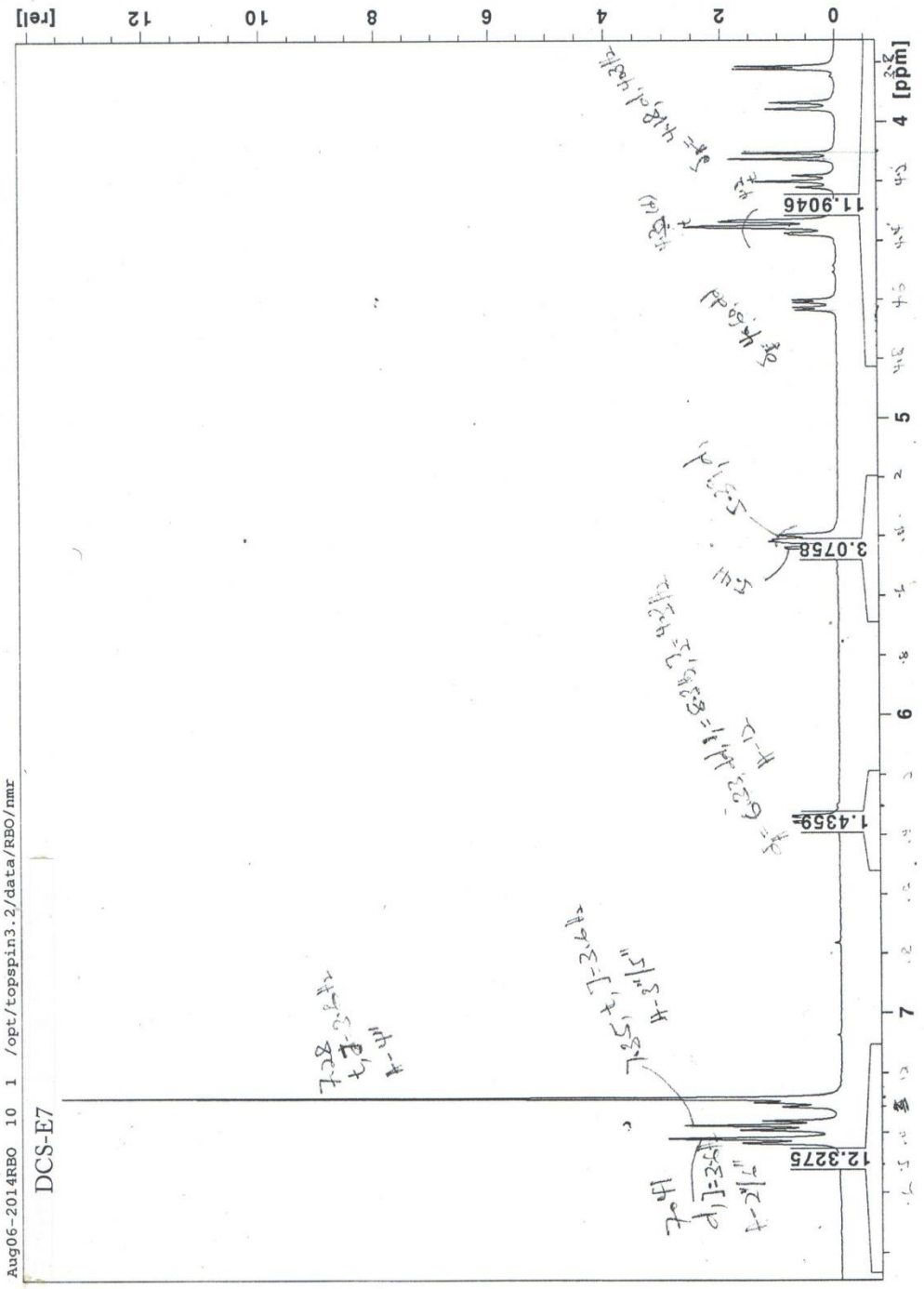

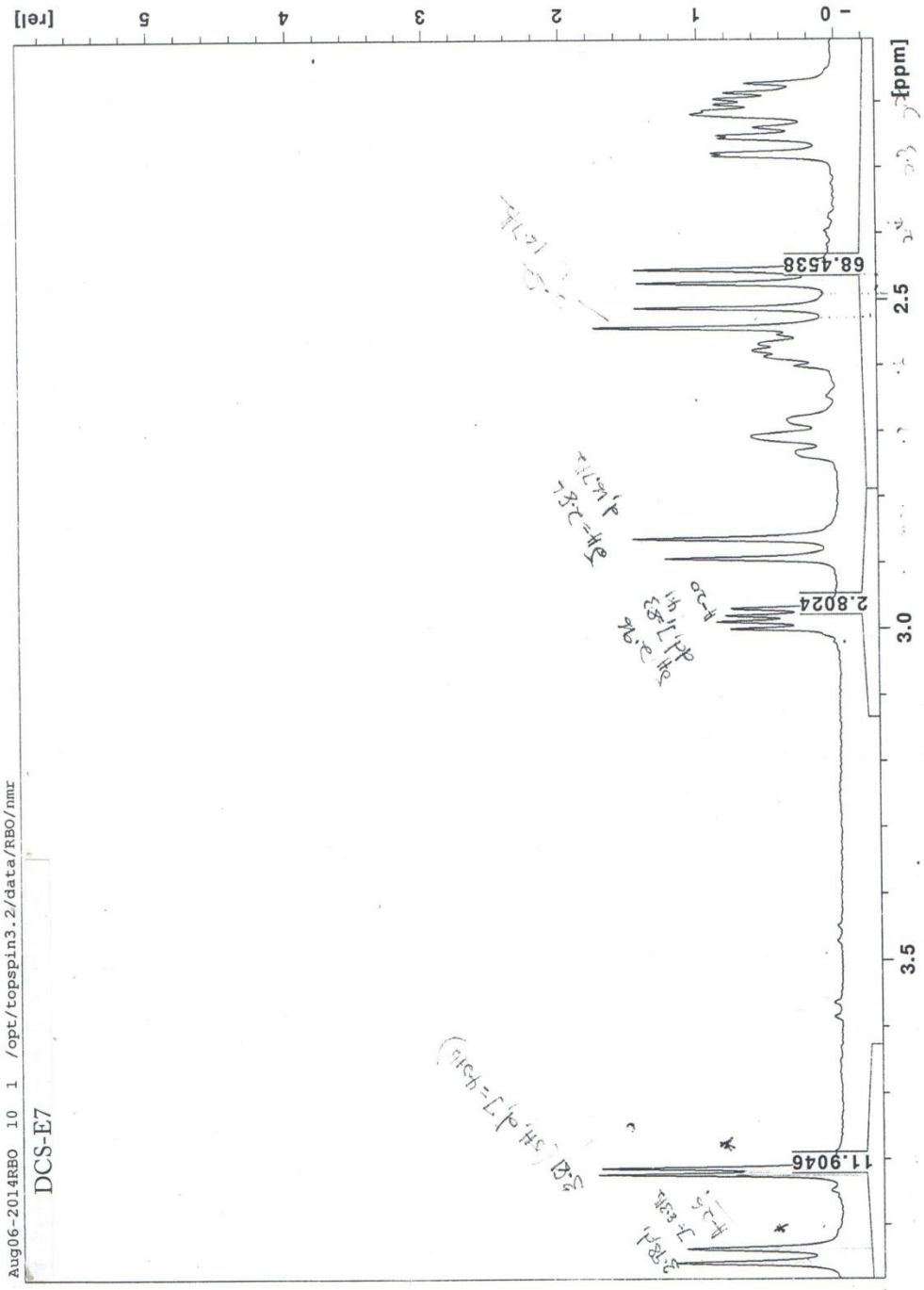

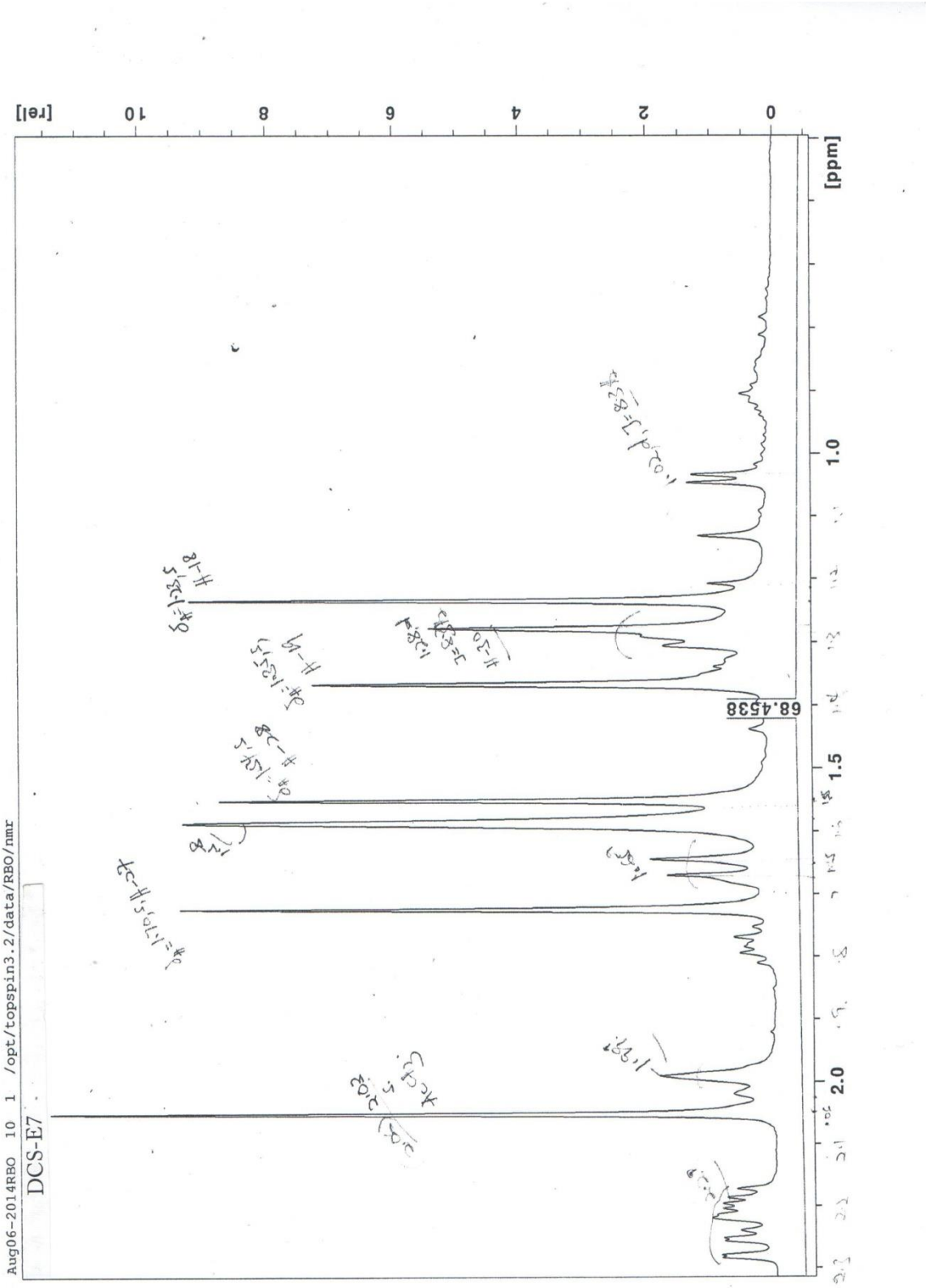

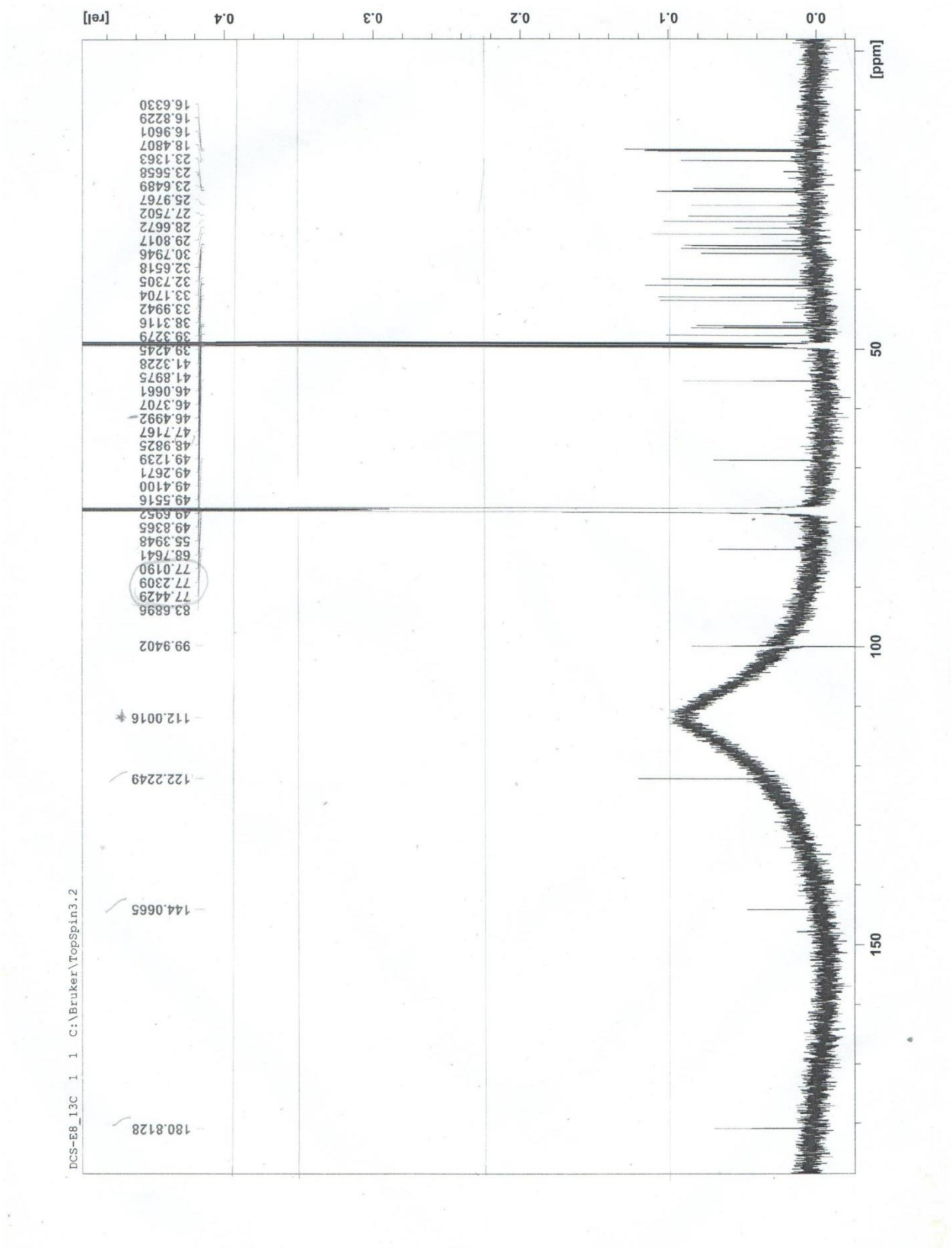

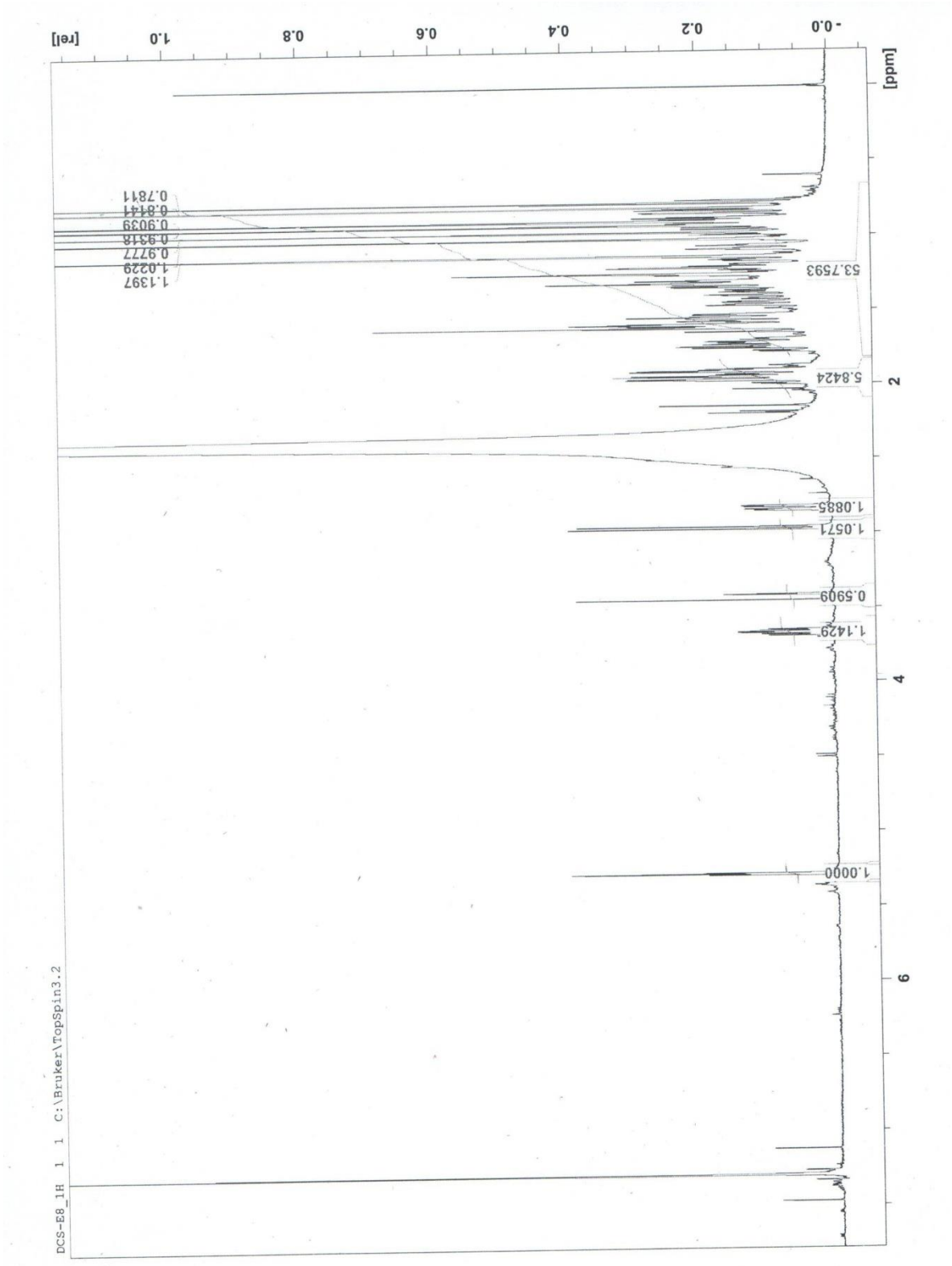

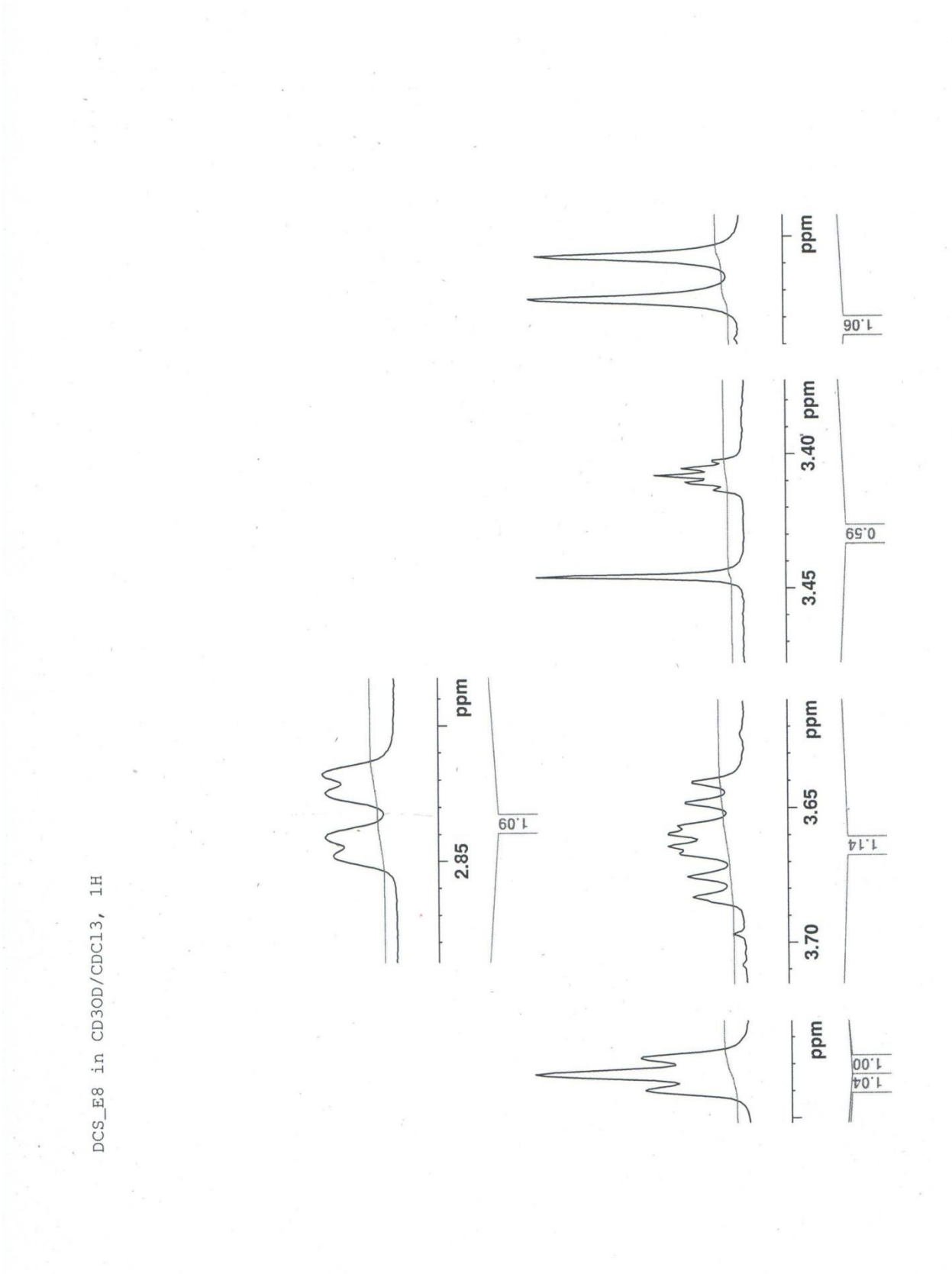

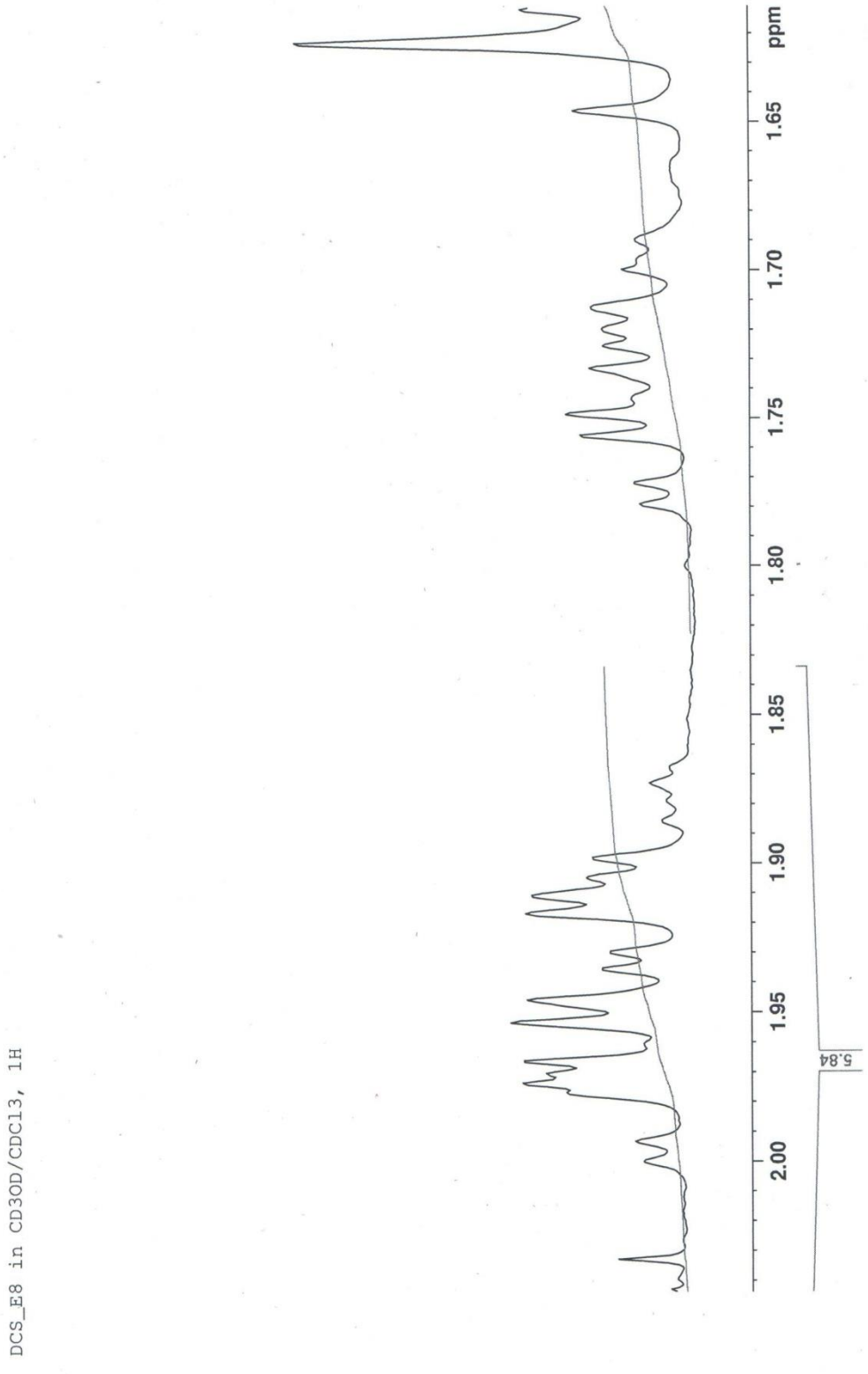

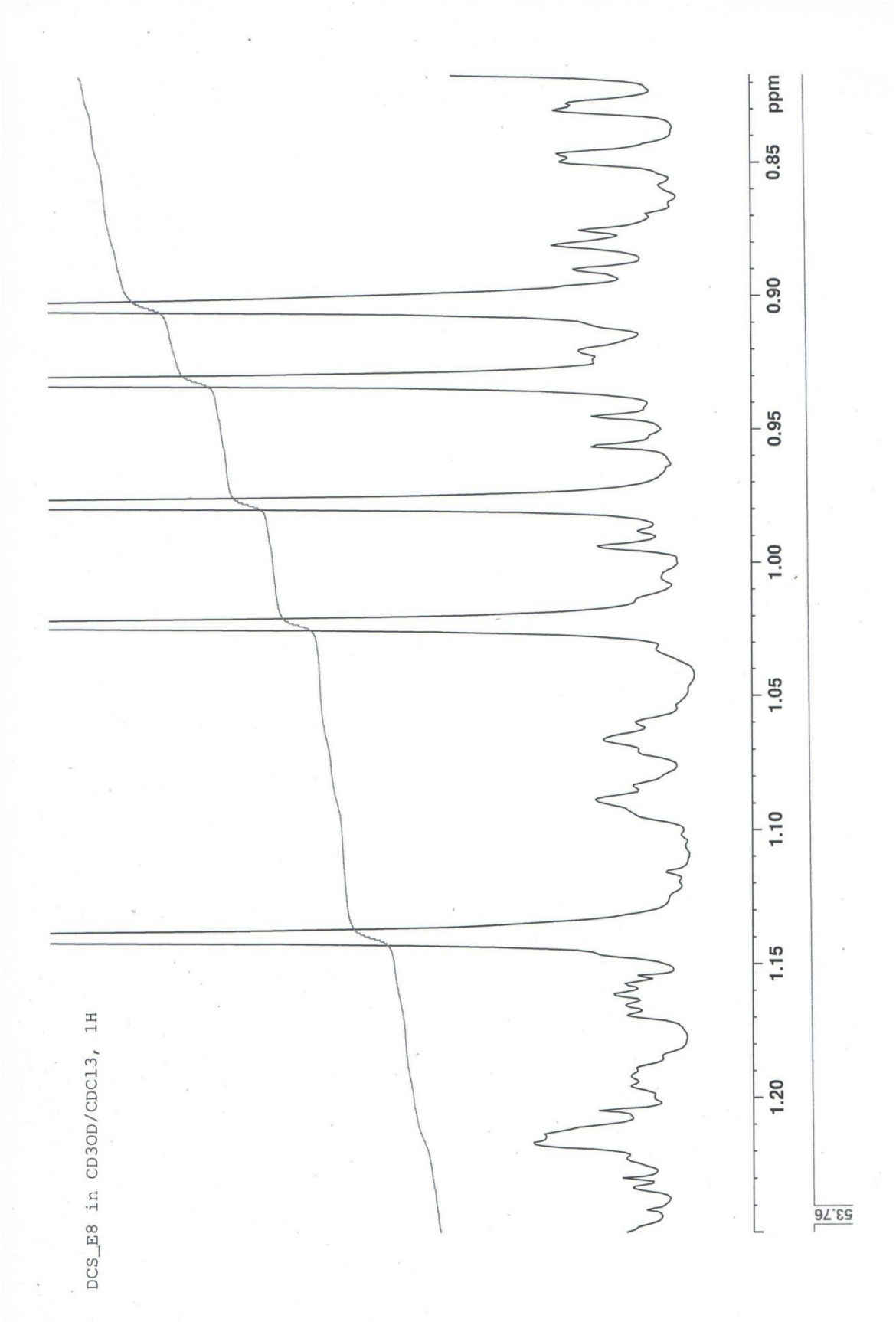

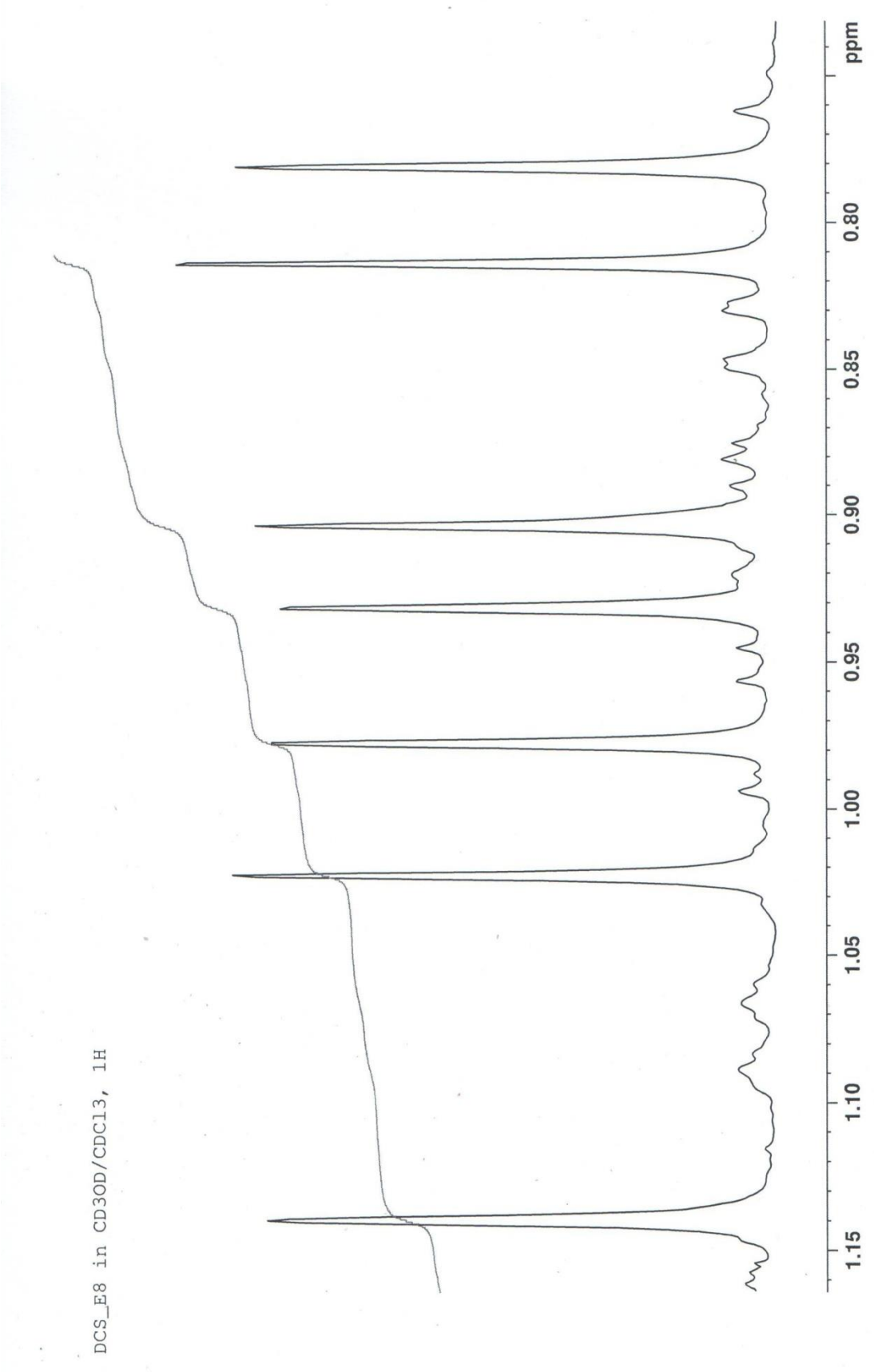

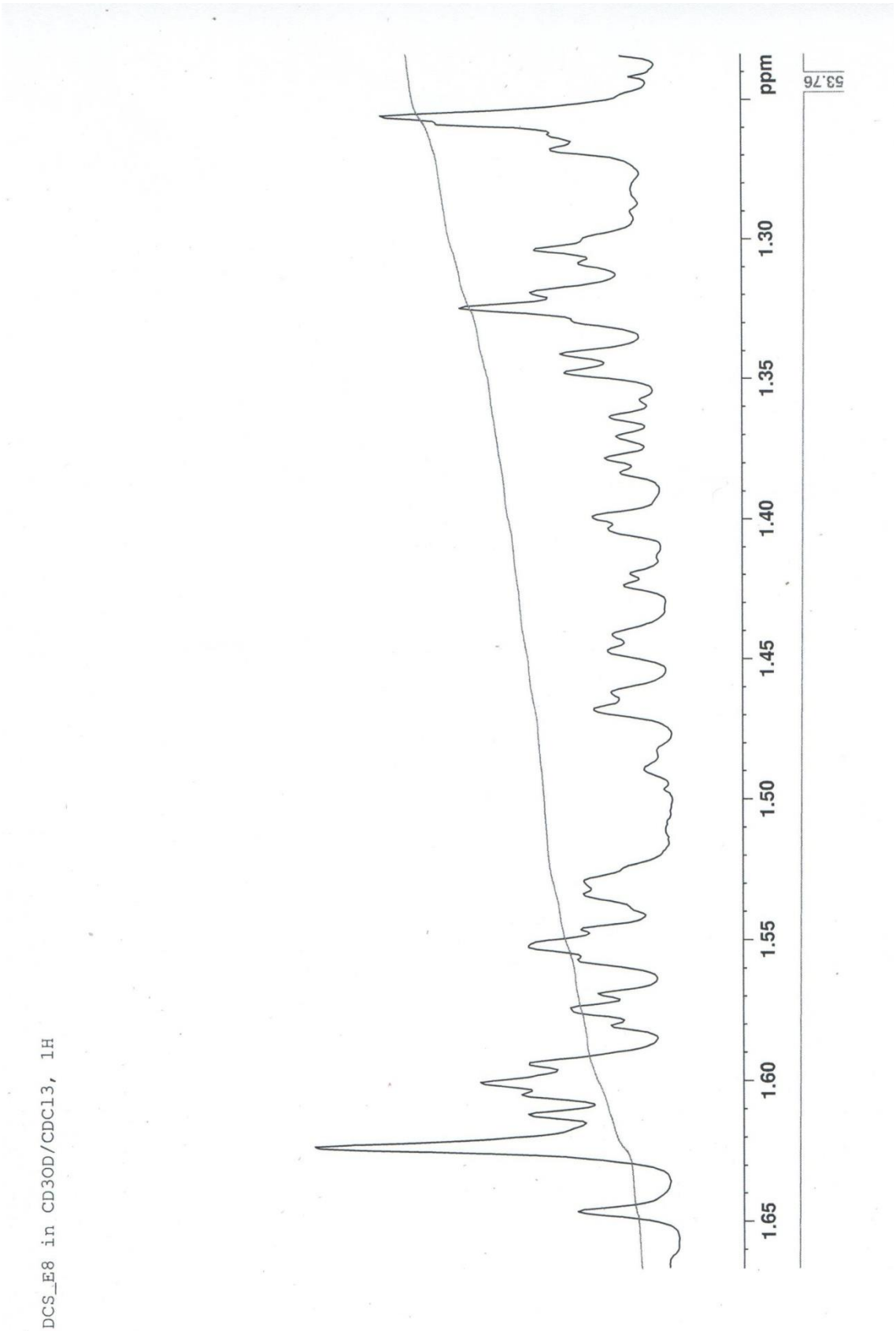

Appendix III: Ethical Clearance

NOGUCHI MEMORIAL INSTITUTE FOR MEDICAL RESEARCH
Established 1979
A Constituent of the College of Health Sciences
University of Ghana

INSTITUTIONAL REVIEW BOARD

Phone: +233-302-916438 (Direct)
+233-289-522574
Fax: +233-302-502182/513202
E-mail: nirb@noguchi.mimcom.org
Telex No: 2556 UGL GH

Post Office Box LG 581
Legon, Accra
Ghana

My Ref. No: DF.22
Your Ref. No:

28th March, 2014

ETHICAL CLEARANCE

FEDERALWIDE ASSURANCE FWA 00001824 **IRB 00001276**

NMIMR-IRB CPN 059/13-14 **IORG 0000908**

On 28th March, 2014, the Noguchi Memorial Institute for Medical Research (NMIMR) Institutional Review Board (IRB) conducted expedited review and approved your revised protocol titled:

TITLE OF PROTOCOL : **Investigation of some extracts and compounds from dichapetalum spieces as potential anti-schistosomal agents**

PRINCIPAL INVESTIGATOR : **Mary Anti Chama, PhD,**

CO-INVESTIGATORS : **Dr. Dorcas Osei-Safo**

Please note that a final review report must be submitted to the Board at the completion of the study. Your research records may be audited at any time during or after the implementation.

Any modification of this research project must be submitted to the IRB for review and approval prior to implementation.

Please report all serious adverse events related to this study to NMIMR-IRB within seven days verbally and fourteen days in writing.

This certificate is valid till 27th March, 2015. You are to submit annual reports for continuing review.

Signature of Chair: .....
Mrs. Chris Dadzie
(NMIMR – IRB, Chair)

cc: Professor Kwadwo Koram
Director, Noguchi Memorial Institute
for Medical Research, University of Ghana, Legon

References

1. Breteler F. J., (1973). The African *Dichapetalaceae*, XVII, A Taxonomical Revision IV, Wageningen, **3**, 23-25.
2. Prance G. T., (1972). Monograph of *Dichapetalaceae*. *Flora Neotropica* **10**, 1-84.
3. Poorter L, Bongers F, Kouame, Hawthrone W.D., (2004). Editors. Biodiversity of West African forests, an ecological atlas of woody plant species. CABI 2004, pg. 202
4. Gadella T. W. J., (1972). Cytological studies on some flowering plants collected in Africa. *Bulletin du Jardin Botanique National de Belgique*. **42,** 392-402
5. Irvine F.R., (1961). Woody Plants of Ghana. *Oxford University Press*, 266-269.
6. Lewis, W. H. and Elvin-Lewis M. P. F., (1977). Medical Botany, Plants affecting man's Health, *Wiley Interscience*, 234
7. O'Hagan, D., Perry, R., Lock, J. M., Meyer, J. J. M., Dasaradhi, L., Hamilton, J. T. G., Harper D. B., (1993). High levels of monofluoroacetate in *Dichapetalum braunii*. *Phytochemistry*, **33**, 1043-1045.
8. Hall, R. J., (1972). *D. barteri* as a potential rodenticide. *New Phytologist*, **71**, 855-871.
9. Addae-Mensah, I., Waibel, R., Asunka, S. A., Oppong, I. V., Achenbach, H., (1996). The Dichapetalins – A new class of triterpenoids. *Phytochemistry*, **43**(3), 649-656.
10. Achenbach, H., Asunka, S. A., Waibel, R., Addae-Mensah, I., Oppong, I. V., (1995). Dichapetalin A, A novel plant constituent from *Dichapetalum madagascariense*. *Natural Product Letters*, **7**, 93-100.
11. Weckert, E., Hümmer, K., Addae-Mensah, I., Waibel, R., Achenbach, H., (1996). The absolute configuration of Dichapetalin A. *Phytochemistry*, **43**, 657–660.

12. Chama M. A., (2007). Chemical Investigation of Two Ghanaian Medicinal Plants- *Dichapetalum madagascariense* and *Scoparia dulcis*, Ph.D (Chemistry), Thesis

13. Osei-Safo D., Chama M. A., Addae-Mensah I., Waibel R., Asomaning W. A. and Oppong I.V., (2008). Dichapetalin M from *Dichapetalum madagascariense*. *Phytochemistry* Letters **1**, 147-150.

14. Fang L., Ito A., Chai H-B, Mi Q., Jones W. P., Madulid D. R., Oliveros M. B., Gao Q., Orjala J., Farnsworth N. R., Soejarto D. D., Cordell G. A., Swanson S. M., Pezzuto J. M. and Kinghorn A.D., (2006). Cytotoxic constituents from the Stem Bark of *D. gelonioides* collected in the Philippines. *Journal of Natural Products.*, **69** (3), 332-337

15. Tuchinda P., Kornsakulkarn J., Pohmakotr M., Kongsaeree P., Prabpai S., Yoosook C., Kasisit J., Napaswad C., Sophasan S.and Reutrakul V., (2008). Dichapetalin-type triterpenoids and lignans from the aerial parts of *Phyllanthus acutissima*. *Journal of Natural Products*., **71** (4):655-663

16. Long C., Aussagues Y., Moliner N., Marcourt L., Vendier L., Samson A., Poughan V., Mutiso P. B. C., Auseil F., Sautel F., Arimando P. B., Massiot G., (2013). Dichapetalins from Dichapetalum species and their cytotoxic properties. *Phytochemistry* (2013). http://dx.doi.org/10.1016/j.phytochem.2013.03.023

17. Chama A. M., Dziwornu A. G., Waibel R., Osei-Safo D., Addae-Mensah I., Otchere J., Wilson M., (2015). Isolation, characterization and anthelminthic activities of a novel dichapetalin and other constituents of *Dichapetalum filicaule*. *Pharmaceutical Biology* (2015), 1-10. http://informahealthcare.com/phb

18. Jing S.-X, Luo S.-H, Li C.-H, Hua J., Wang Y.-L, Niu X.-M, Li X.-M, Liu Y., Huang C.-S, Wang Y. and Li S.-H., (2014). Biologically Active Dichapetalins from *Dichapetalum gelonioides*. *Journal of Natural Products*, **77**(4), 882-893

19. Gryseels B., Polman K., Clerinx J. and Kestens L. (2006). Human Schistosomiasis. *Lancet*, **368**, 1106-1118

20. Lengeler C., Utinger J. and Tanner M. (2002). *Bull World*. Health Organization, **80**(3), 235-242.

21. World Health Organization (2010). Working to Overcome the Global Impact of Neglected Tropical Diseases-First WHO report on Neglected Tropical Diseases, WHO Press: Geneve, **184**.

22. King C. H., Dickman K. and Tisch D. J., (2005). *Lancert*, **365**(9470), 1561-1569

23. Nsowah-Nuama N. N., Mensah G., Aryeetey M. E., Wayatsuma Y and Bentsil G., (2001). *American Journal of Tropical Medicine and Hygiene*, **65**(5), 484-490

24. Schmidt, T. J.; Khalid, S. A.; Ramanha, A. J.; Alves, T. M.; Biavatti, M. W.; Brun, R.; Da Costa, F. B.; de Castro, S. L.; Fenreira, V. F.; de Larcerda, M. V.; Largo J. H. G., Leon L. L., Lopes N. P., das Neves R. C., Niehues M., Scott M. J., Setzer W. N., and Tempone A. G., (2012). The Potential of Secondary Metabolites from plants as drugs or leads against Protozoan neglected diseases-Part II. *Curriculum of Medicinal Chemistry*, **19**, 2176-2228.

25. Ndjonka D.; Rapado L. N.; Silber A. M.; Liebau E.; and Wrenger C., (2013). Natural Products as a Source for Treating Neglected Parasitic Diseases. *International Journal of Molecular Sciences*, **14**, 3395-3439.

26. Marais J. C. S., (1943). "The Isolation of the toxic principle of "K cymonate" from "Gifblaar", *Dichapetalum cymosum"*. *Onderstepoort Journal of Veterinary Science and Animal Industry*, **18**, 203

27. Marais J. C. S., (1944). "Monofluoroacetic acid, the toxic principle of 'gifblaar' *Dichapetalum cymosum"*. *Onderstepoort Journal of Veterinary Science and animal Industry*, **20**, 67

28. Kim S. B., Kim Y. S., Kang O. H., Kwan D. Y., Choie J. G., Obounou B. W. O., Kewn J. H., Mun S. H. and Maroufath L. (2011). Evaluation of the Antimicrobial Activity of Seven Gabonese Medicinal Plants against Methicillin-Resistant *Staphylococcus aureus and Salmonela. Natural Product sciences*, **17**(1), 33-37.

29. Von Reis Altschul S., (1973). Drugs and Foods from Little-known Plants. Notes in Harvard University Herbaria; Harvard University Press: Cambridge, MA, 142

30. Breteler F. J., (1973). The African *Dichapetalaceae*, XVII, A Taxonomical Revision IV, Wageningen, 11

31. Watt J. M. and Breyer Brandwijk M. G., (1962). Medicinal and Poisonous Plants of Southern and Eastern Africa, *E & S Livingston Ltd*. Edinburg and London, 2nd Edition, 375-383.

32. Shrisha D. L., Raveesha K. A. and Nagabhusha S., (2011). Bioprospecting of selected medicinal plants for antibacterial activity against some pathogenic bacteria, *Journal of Medicinal Plants Research*, **5** (17), 4087-4093

33. Msami H. M., (1999). An outbreak of suspected poisoning of cattle by Dichapetalum sp. In Tanzania. *Tropical Animal Health and Production*, **31** (1), 71-74

34. Rabinovich M., (1928). The toxic properties of West African rats' bane. *Bulletin of the Imperial Institute*, **26**, 143-147

35. Murphy R. (2006). Nature's Materia Medica, *Lotus Health*, 700

36. Vickery B. and Vickery M. L., (1975). The synthesis and defluorination of monofluoroacetate from some Dichapetalum species. *Photochemistry*, **14**(2), 423-427

37. Ward P. F. V., Hall R. J. and Peters R. A., (1964). Fluorine fatty acids in the seeds of *D. toxicarium*, *Nature*, **201**, 611.

38. Kellerman T. S., Naude T. W., and Fourie N., (1996). The distribution, diagnosis and estimated economic impact of plants poisonings and mycotoxicosis in South Africa. Understerpoort *Journal of Vertinary Research*, **63**(2), 65-90.

39. Anon A., (1916). Hydrocyanic acid and two resins from *D. cymosum*. *Bulletin of the Imperial Institute*, London, 14

40. Dear R. E. A and Paltinson F. L. M., (1962). The Synthesis of Toxic Principles of *D. toxicarium*. *Journal of American Chemical Society*, **85**, 622-626

41. Meyer, M. O', Hagan D., (1992). Rare Fluorinated Natural Products, *Chemistry in Britain*, **28**(9), 785-788

42. Kalm E. R., (1945). Natural Occurrence of Fluoroacetic Acid, The Acid of New Rodenticide "1080", *Science*, **102**, 232

43. Omara F. and Sisodia C. S., (1990). Inhibition of Citric Acid Cycle. *Veterinary & Human Toxicology*, **32**, 429

44. Addae-Mensah, I., Adu-Kumi, S., Waibel, R., Asunka, S. A., Oppong, I. V., (2007). A novel D:A-friedooleanane triterpenoid and other constituents of the stem of *Dichapetalum barteri* Engl. ARKIVOK (Archives of Organic Chemistry) IX, 1-9

45. Gordaliza M., Garcia P.A., del Corral J. M., Castro M., A., and Gomez-Zurita M. A., (2004). "Podophyllotoxin: distribution, sources, applications and new cytotoxic derivatives", *Toxicology*, **44** (4), 441-459

46. Osei-Safo D., Chama M. A., Addae-Mensah I. and Waibel R., (2012). The Dichapetalins-Unique Cytotoxic Constituents from of the Dichapetalaceae, Phytochemicals as Nutraceuticals- Global Approaches to Their Role in Nutrition and Health, 245-254. Dr. Venketeshwer Rao (Ed.), ISBN: 978-953-51-0203-8. Intech, available from: http://www.intechopen.com/books/phytochemicals-as-nutraceuticals-global-approaches-to-their-role-in-nutrition-and-health/the-dichapetalins-unique-cytotoxic-constituents-of-the-Dichapetalaceae

47. Eloff J. N. and Grobberlaar N., (1969). Isolation and Characterization of N-methyl-L-Serine and N-methyl-L-Alanine, Novel Amino Acids from *D. cymosum*, *Phytochemistry*, **8**, 2201.

48. Van-der Werf M. J., de Vlas B. J., Brooker S., Looman C. W. N., Nagelkerke N. J. D., Habbenma J. D. F. and Engels D. (2003). *Acta Tropica*, **86**(2-3), 125-139

49. Knopp S., Person B., Ane S. M., Mohammed K. A., Ali S. M., Khamis I. S., Rabone M., Allan F., Gourras A., Blair K., Fenwich A., Utzinger J., Rollinson D., (2013). Elimination of Schistosomiasis Transmission in Zanzibar: Baseline findings before the onset of a Randomized intervention trial. *Neglected Tropical Disease*, 7(**10**), 24-74.

50. Fenwich A. and Savioli L., (2011). Schistosomiasis elimination. *The Lancet Infectious Diseases*, **11**(5), 346-347

51. Chimbari M. J., (2012). Enhancing Schistosomiasis Control Strategy for Zimbabwe: Building on past experiences. *Journal of Parasitology Research*, 2012, doi:10.1155/2012/353768

52. World Health Organization (2010). Working to Overcome the Global Impact of Neglected Tropical Diseases-First WHO report on Neglected Tropical Diseases, *WHO Press:* Geneve, **184**.

53. Bueding E. and Fisher J., (1966). Factors affecting the inhibition of phosphofructokinase activity of *Schistosoma mansoni* by trivalent organic antimonials, *Biochemical Pharmacology*, **15**,1197-1211

54. Cioli D., (1998). Chemotherapy of schistosomiasis: An update, *Parasitology Today*,**14**,418-422

55. Pica-Mattocia L. and Cioli D., (1985). Studies on the mode of action of oxamniquine and related schistosomicidal drugs. *American Journal of Tropical Medicine and Hygiene*, **34**, 112-118

56. Doenhoff M. J., Hagan P., Cioli D., Southgate V., Pica-Mattocia L., Batros S., Coles G., Tchuem T. C. H. U., Mbaye A., and Engels D., (2009). Praziquantel: Its use in control of schistosomiasis in sub-Saharan Africa and current research needs. *Parasitology*, **136**, 1825-1835

57. Jeziorski M. C. and Greenberg R. M., (2006). Voltage-gated calcium channel subunits from platyhelminths: Potential role in praziquantel action. *International Journal of Parasitology*, **36**, 625-632

58. Fallon P. G., Sturroch R. F., Niang A. C. and Doenhoff M. J., (1995). Short report: Diminished susceptibility to praziquantel in a Senegal isolates of *Schistosoma mansoni*. *American Journal of Tropical Medicine and Hygiene*, **53**, 61-63

59. Botros S. and Bennett J., (2007). Praziquantel Resistance. *Expert opinion on Drug Discovery*, **2**, 585-540

60. Couta F. F., Coelho P. M., Araojo N., Kusel J. R., Katz N. and Mattos A. C., (2010). Use of fluorescent probes as a useful tool to identify resistant *Schistosoma mansoni* isolates to praziquantel. *Parasitology*, **137**, 1791-1797

61. Ndamba J., Nyameza N., Makaza N., Anderson C. and Kaondera K. C., (1994). Traditional herbal remedies for the treatment of urinary schistosomiasis in Zimbabwe. *Journal of Ethnopharmacology*, **42**, 125-132

62. Molgaard P., Nielson S. B., Rasmussen D. E., Drummand R. B., Makaza N. and Andreassen J., (2001). Anthelmintic screening of Zimbabwean plants traditionally used against schistosomiasis. *Journal of Ethnopharmacology*, **77**, 257-264

63. Utinger J., Keiser J., Shusha X., Tannoer M. and Singer B. H., (2003). Combination chemotherapy of schistosomiasis in laboratory studies and clinical trials. *Antimicrobial Agents and Chemotherapy*, **47**, 1487-1495

64. Allam G., (2009). Immunomodulatory effects of circumin on murine Schistosoma mansoni. *Immunobiology*, **214**, 712-727

65. Cichewicz R. H. L., McKerrow J. H. and Nair M. G., (2002). Kwanzoquinones A-G and other constituents of *Hemerocallis fulva* "Kwanzo" roots and their activity against the human pathogenic trematode *Schistosoma mansoni*. *Tetrahedron*, **58**, 8597-8606

66. Cunha N. L., de Mendonoa Uchoa C. J., Cintra L. S., de Souza H. C., Peixoto J. A., Silva C. P., Malgalhaes L. G., Gimenez V. M. M., Groppo M., Rodrigues V., da Silva Filho A. A., e Silva M. L. A., Cunha W. R., Pauletti R. M. and Januario A. H., (2012). *In vitro* schistosomicidal activity of some Brazilian cerrado species and their isolated compounds. *Evidence-Based complement and Alternative Medicine*, 2012

67. Jisaka M., Kawanaka M., Sugiyama H., Takegawa K., Huffman M. A., Ohigashi H. and Koshimizu H., (1992). Antischistosomal activities of sesquiterpene lactones and steroid glucosides from *Vernonia amygdalina*, possibly used by wild chimpanzees against parasite-related diseases. *Bioscience. Biotechnology and Biochemistry*.,**56** (5), 845-846

68. Veras L. M., Guimaraes M. A., Campelo Y. D., Vieira M. M. and Nascimento C., (2012). Activity of epiisopiloturine against *Schistosoma mansoni*. *Curriculum of Medicinal Chemistry*, **19**, 2051-2058

69. De Moraes J., de Oliveira R. N., Costa J. P., Junior A. L. G., de Sousa D. P., Freitas R. M., Allegretti S. M. and Pinto P. L. S., (2014). Phytol, a diterpene alcohol from chlorophyll, as a drug against neglected tropical disease *schistosomiasis mansoni*. *Plos Neglected Tropical Diseases*, **8**, 2617

70. Moraes J., Nascimento C., Lopes P. O., Nakano E. and Yamaguchi L. F., (2011). *Schistosoma mansoni*: In vitro schistosomicidal activity of piplartine. *Experimental Parasitology*, **127**, 357-364

71. Silva P. N. M., Oliveira L. S. G., de Calvalho B. F. R., de Sausa P. D., Freitas R. M., Pinto P. L. S. and de Moraes J., (2014). Antischistosomal Activity of the Terpene Nerolidol. *Molecules*, **19**(3), 3793-3803

72. Magalhaes L.G., Kapadia, G.J., da Silva Tonuci L.R., Caixeta S.C., Parreira N.A. Rodrigues V. and da Silva Filho, A. A., (2008). *In vitro* schistosomicidal effects of some phloroglucinol derivatives from *Dryopteris* species against *Schistosoma mansoni* adult worms. *Parasitology Research*, **106**, 395–401.

73. Lima C.M., Freitas F.I., Morais L.C., Cavalcanti M.G., Silva L.F., Padilha R.J., Barbosa C.G., Santos F.A., Alves L.C. and Diniz M. D., (2011). Ultrastructural study on the morphological changes to male worms of *Schistosoma mansoni* after *in vitro* exposure to allicin. *Revista da Sociedade Brasileira de Medicina Tropical*

74. Queiroga C. L.; Silva G. F.; Dias P. C.; Possenti A. and De Caravlh J. E., (2000). Evaluation of the antiulcerogenic activities of friedelan-3β-ol and friedelin isolated from *Maytenus ilicifolia* (Celastraceae). *Journal of Ethnopharmacology*, **72**(3), 465-468.

75. Kamboj A. and Saluja A. K., (2011). Isolation of Stigmasterol and β-sitosterol from petroleum extract of aerial parts of *Ageratum conyzoides* (Asteraceae). *International Journal of Pharmacology and Pharmaceutical Sciences*, **3**(1), 242-244.

76. Igoli O. J. and Gray I. A., (2008). Friedelanone and other Triterpenoids from *Hymenocardia acida*. *International Journal of Physical Sciences*, **3**(6), 156-158

77. Dharmaratne H. R. and Marasinghe G. P., (2009). New methylethers of cordatolides from *Calophyllum cordato-oblongum* and their synthesis. *Natural Products Research*, **23**(10), 883-890.

78. Luiz Z. and Zhao R., (2011). Chemical Constituents from root bark of *Tripterygium hypoglaucum*, *China Journal of Chinese Materia Medica*, **36**(18), 2503-2506.

79. Howard D. M.; Ana M. L.; Shirley P. A.; Mercus L. B., (1987). Alkaloidal Insect Antifeedants from *Virola calophylla Warb*. *Journal of Agricultural and Food Chemistry*, **35**(5), 794-797.

80. The Wealth of India Raw Materials. New Delhi: Publications and Information Directorate, Council of Scientific and Industrial Research, **9**, 1948-1976

81. Huang K. C., (1993). The Pharmacology of Chinese Herbs, Tokyo: CRC Press

82. Sultana N., Ata A., (2008), Oleanolic acid and related derivatives as medicinally important compounds, *Journal of Enzyme Inhibition Medicinal Chemistry*, **23**, 739-756

83. Sha B. A., Qazi G. N. and Taneja S. C., (2009), Boswellic acids: A group of medicinally important compounds., *Natural Product Reports*, **26**, 72-89

84. Petroneli A., Pannitteri G. and Testa U., (2009), Triterpenoids as new Promising anticancer drugs, *Anti-Cancer drugs*, **20**, 880-892.

85. Antonisamy P., Duraipandiyan V. and Ignacimunthu S., (2011). Anti-inflammatory, analgesic, antipyretic effect of friedelin isolated from *Azima tetracantha* Lam. in mouse and rat models. *Journal of Pharmacy and Pharmacology*, **63**(8), 1070-1077

86. Kumara R., Meygappan A., Selvanmani P., Mukherjee J. and Jaisanka P., (2011). Lypoxygenase inhibitory activity of crude and bark extracts and isolated compounds from *Commiphora berryi*. *Journal of Ethnopharmacology*, **138**(1), 256-259

87. Ramesh N., Viswanathan M. B., Saraswathy A., Balakkrishna K., Brindh P., and Lakshmanapenmalsamy P., (2001). Phytochemical and antimicrobial studies on *Drynarai quercifolia. Fitoterapia.* **72**(8), 934-936

88. Wang D., Xia M.; and Cui Z., (2006). New triterpenoids isolated from the root bark of *Ulmus pumila* L. *Chemical and Pharmaceutical Bulletin (Tokyo*). **54**(6), 775-778

89. Lin R. J., Chen C. Y. and Lo W. L. (2008). Cytotoxic activity of *Ipomoea cairica*. *Natural Product Research*, **22**(9), 747-753.

90. Li S., Chem R. Y. and Yu D. Q., (2007). Study on chemical constituents of *Myricaria paniculata* I. *China Journal of Chinese Materia Medica*, **32**(5), 403-406

91. Yang H. H., Son J. K., Jung B., Zhong M. and Kim. J. R., (2011). Epifriedelanol from the root bark of *Ulmus davidiana* inhibits cellular senescence in human primary cells. *Planta Medica*, **77**(5), 441-449

92. Liby K. T., Yore M. M. and Spom M. B., (2007). Triterpenoids and rexinoids as multifunctional agents for the prevention and treatment of cancer. *Nature Review Cancer***,** **7**, 357-369.

93. Laszczyk M. N., (2009). Pentacyclic triterpenes of lupane, oleanane and ursane group as tools in cancer therapy. *Planta Medica*.**75**, 1549-1560

94. Flores-Sanchèz I. J., Ortega-Lopèz J., Montes-Horcasitas M. D. C. and Ramos-Valdivia A. C., (2002), Biosynthesis of sterols and Triterpenes in Cell Suspension Cultures of *Uncaria tomentosa*, *Plant Cell Physiology*, **43**(12), 1502-1509

95. Clouse D. S., (2002), Arabidopsis Mutants Reveal Multiple Roles for Sterols in Plant development, *Plant Cell*, **14**(9), 1995-2000.

96. Garima M.; Saurabh S. and Nagori B. P., (2010). Pharmacological and Therapeutic Activity of *Cissus quadrangularis*: An Overview. *International Journal of Pharmacological Technology Research*, **2**(2), 1298-1310.

97. Chandler R. F.; Hooper S. N. and Ismail H. A., (1979). Antihypercholesterolemic Studies with Sterols: β-sitosterol and Stigmasterol. *Journal of Pharmaceutical Sciences*, **68**, 245-247.

98. Tzong-Huei L., Shin- Hun J., and Chang-Yi W., (2005). Triterpene acids from the leaves of *Planchonella duclitan* (Blanco) Bakhuizan. *Journal of the Chinese Chemical Society*, **52**, 1275-1280

99. Wu XD., He J., Li XY., Dang LB., Gang X., Gao X., Song LD., Li Y., Peng LY., and Zhao QS., (2013). Triterpenoids and steroids with Cytotoxic Activity from *Emmenopterys henryi*. *Planta Medica*, **79**, 1356-1361.

100. Fermandes J., Weinlich R., Castillo R. O., Kaplana M. A. C., Amarante-Mendes G. P and Gattass C. R., (2005). Pomolic acid triggers mitochondria dependent apoptotic cell death in leukemia cell line. *Cancer letters*, **219**, 49-55.

101. Yoshida M., Fuchigami M., and Nagao T.T., (2005). Anti-proliferative constituents form umbelliferase plants VII. Active terpenes and rosmarinic acid from *Centella asisatica*. *Biological & Pharmaceutical Bulletin*, **28**, 173-175.

102. Kuang WX., Li HW., Wang QH., Yang BY., Wang ZB., and Xia YG., (2011). Triterpenes form the roots of *Sanguisorba tenuifolia* var. Alba. *Molecules*, **16**, 4642-4651.

103. Banno N., Akihisa T., and Tokuda H., (2004). Triterpene Acids from the Leaves of *Perilla frutescens* and their Anti-inflammatory and Antitumor-promoting Effects. *Bioscience & Biotechnology of Biochemistry*, **68**(1), 85-90.

104. Estrada O., Alvarado-Castillo C., and Fernadez A. Z., (2009). Pomolic acid isolated from the Leaves of *Licania pitteiri* Inhibits ADP-and Epinephrine-Induced Platelet Aggregation and has Hypotensive Effects on Rats. *Current Bioactive Compounds*, **5**, 219-225.

105. Martinez A., Rivas F., Perojil A., Parra A., Garcia-GranadosA., and Fernandez-Vivas A., (2013). Biotransformation of oleanolic and maslinic acids by *Rhizomucor miehei*. *Phytochemistry*, **94**, 229-237.

106. Lozana-Mena G., Sanchez-Gonzalez M., Juan M. E., and Planas J. M., (2014). Maslinic Acid, a Natural Phytoalexin-Type Triterpene from Olives- A Promising Nutraceutical? *Molecules*, **19**, 11538-11559

107. Rufino-Palomares E. E., Reyes-Zurita F. J., Lupianez J. J., and Cascante M., (2009). Maslinic acid, a natural triterpene from *Olea europaea* L., induces apoptosis in HT29 human colon-cancer cells via the mitochondrial apoptotic pathway. *Cancer letters*, **273**, 44-54.

108. Kotze A. C., Coleman G. T., Mai A. and McCarthy J. S. (2005). Field evaluation of anthelmintic drug sensitivity using in vitro egg hatch and larval motility assays with *Necatar americanus* recovered from human clinical isolates. *International Journal of Parasitology*, **35**(4), 445-453.

109. Moraes J. D., Almeida A. A., Brito M. R., Marques T. H and Lina T. C., (2013). Anthelmintic activity of the natural compound (+)-limonene against *Schistosoma mansoni*. *Planta Medica*, **79**, 253-258.